JOHANNES GUTENBERG UNIVERSITÄT MAINZ

Oligodeoxynucleotide-Polypeptide Block Copolymers

Dissertation

zur Erlangung des Grades

„Doktor der Naturwissenschaften“

im Promotionsfach Chemie

am Fachbereich Chemie, Pharmazie und Geowissenschaften

der Johannes Gutenberg-Universität in Mainz.

Sabine Flügel

geboren in Fulda

Mainz 2010

Die vorliegende Arbeit wurde im Zeitraum von Januar 2007 bis März 2010 am Institut für Physikalische Chemie der Johannes Gutenberg-Universität Mainz angefertigt.

Dekan:

1. Berichterstatter:

2. Berichterstatter:

Tag der mündlichen Prüfung: 16. April 2010

To my family

Don’t curse the darkness

-light a candle.

Chinese proverb

Contents

1 Motivation

One major challenge in Polymer Science today is the design of well-defined, tailor-made materials. During the last few decades macromolecular research provided great advances in the precise synthesis of functional materials. The development in "living" polymerization techniques[1] enhanced the control of properties such as architecture, chain length and distribution, block copolymer composition and end-group functionalization. Living polymerization techniques became an important tool for the synthesis of biomedical relevant polymer conjugates, because they result in reduced polymer heterogeneity and typically provide an easy polymer end-group functionalization. The control of endgroup chemistry is demanded for post polymerization modifications e.g. with biological active compounds. Despite the remarkable advances in polymer synthesis, the produced polymers are still polydisperse in nature. For biomedical applications, this inherent property is a major issue. The inherent size distribution of the polymer may result in less defined structure-property relationships, which has to be considered in understanding the basic correlations between chemical nature of the polymer and its biological response[2].

Recent approaches in polymer design are modeled on the sophistication of Mother Nature. Biopolymers, like DNA and proteins, are exactly defined both in functionality and size. In other words, biopolymers are characterized by a well defined monomer sequence and they are typically monodisperse. Additionally, nature uses a wide variety of weak interactions to provide controlled self-assembly, biorecognition, specific catalysis, efficient energy harvesting and high-strength materials[3]. In comparison, polymer self-assembly is usually based on simple dispersion forces, and therefore, rather simple.[4] The combination of biologic and synthetic compounds has led to a new class of hybrid biomaterials that should overcome the limitations of the single components. For example, synthesis of polymer-protein hybrid materials is attractive for supramolecular assemblies with an intrinsic biologically active property. Additionally, the polymer-protein conjugation provides an opportunity to the area of biomedical research in enhancing and stabilizing protein therapeutics by the synthetic polymer. The same applies for the conjugation of oligodeoxynucleotides (abbreviated oligonucleotide or ODN), short single stranded DNAs, to macromolecules.

The concept of this work is based on an approach being even one step ahead. The limitations of macromolecular building blocks (polydispersity and limited control in precise location of functional groups) are overcome by utilizing natural building blocks like oligonucleotides, peptides and proteins. These building blocks are used to create well-defined monodisperse block copolymers with defined functionalities. On the one hand, the development of solid-phase synthesis of oligonucleotides provides an excellent tool to design short functionalized DNA building blocks. On the other hand, the field of genetic engineering makes it possibile to create monodisperse and perfectly defined polypeptides in means of sequence and functionality. The challenge of this work was the development of a synthetic approach for the coupling of oligonucleotides to polypeptides. The post synthetic conjugation involves the reaction of two macromolecules: the oligonucleotide and the polypeptide. One difficulty arising from this approach is the reduced accessibility of functional groups on macromolecules in comparison to small molecules, which usually leads to a decrease in conversion. Therefore, the reaction conditions have to be chosen carefully, and optimized to yield high coupling efficiencies. The coupling reactions itself have to be chosen orthogonal to obtain specific conjugations. Additionally, the isolation of a coupling product from a mixture of macromolecular reactants may be difficult. Questions arising in this context are:

- *Does genetic engineering yield perfectly end-group functionalized polypeptides?*
- *Is it possible to get efficient end-group coupling of ODN and polypeptide blocks?*
- *Which endgroups can be used?*
- *Is the coupling specific to yield monodisperse block copolymers?*
- *How can the conjugates be purified? How can the monodispersity be demonstrated?*

Besides the development of a synthetic approach, the application of the ODN-polypeptide conjugates in supramolecular self-assembly was envisioned. The questions arising in this context are:

- *Are the synthesized ODN-Polypeptide block copolymers utilizable in DNA self-assembly?*
- *Can they form stable molecular assemblies? How does the peptide block influence the hybridization?*
- *Do DNA self-assemblies like four-arm junctions form in the presence of a covalently linked peptide block? Is the hybridization in this case quantitative?*
- *Can DNA junctions be designed that are stable at room temperature?*

The synthesis of ODN-polypeptide-ODN triblock copolymers provides the opportunity for a variety of self-assembled structures by DNA hybridization. In Figure 1.1 the formation of a dendritic network is pictured. The network building blocks are the ODN-polypeptide-ODN triblock copolymers. The oligonucleotide sequences of the different building blocks (P1-P7) are designed to form four-arm DNA junctions, which are acting as crosslinks between the polypeptide blocks. The stability of the network depends only on the stability of the four arm junction itself and its hybridized double strands. The network formation is performed sequentially comparable to a dendrimer synthesis. First, the building blocks P1-P4 are hybridized and in a second "generation" P5-P7 are added.

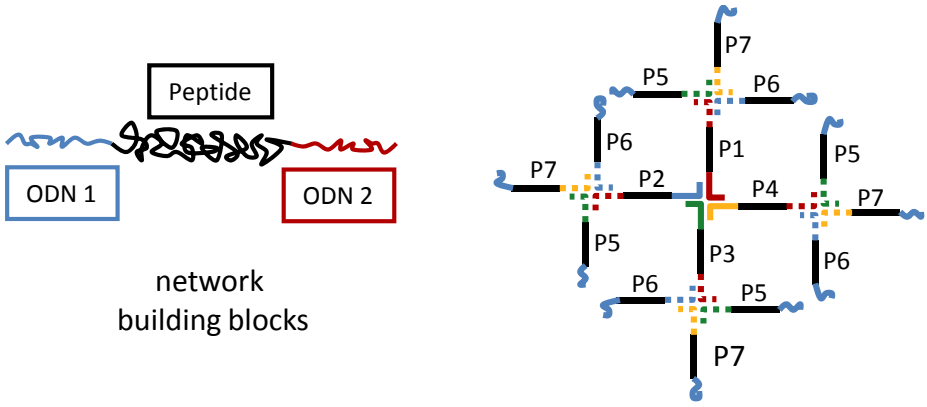

Figure 1.1 Scheme of ODN-peptide-ODN network building blocks and their self-assembly into dendritic networks.

These networks are envisioned to provide control over the network topology, the mesh size and the functionality. The topology can be altered by incorporating dangling ends or loops. The mesh size can be varied by choosing peptides of different length. It is well-defined due to the monodispersity of the building blocks. The variation of the functionality involves the altering of the junction points, e.g. four-arm junction vs. three-arm junction, and the properties of the peptide block chosen. The peptide block may carry defined functional groups to induce e.g. pH sensitivity of the network. In this work presented the polypeptide blocks are chosen to be Elastin-like Polypeptides (ELPs), which exhibit a lower critical solution temperature (LCST) behavior. Hence, prepared networks should be temperature sensitive.

This approach is motivated by the classical but still controversial problem of equilibrium swelling of polymer gels in a good solvent. The question that has not yet been solved is concerned with the length scale on which the system begins to deform upon swelling.[5] The classical Flory-Rehner theory[6, 7] considers the strand size, the length between two cross linking points, to be the determining length scale (global connectivity). This approach

disregards any local fluctuation effects. Other approaches e.g. from de Gennes[8] assumed that the swelling is controlled by the local connectivity of the strands. The problem of any experimental studies and their theoretical interpretation is typically the network topology. The local structure of polymer gels is undefined due to statistical crosslinking, entanglements, polydispersity of the polymer chains and different functionalities of the crosslinking point. Therefore, the need of well-defined networks is given to provide a tool for basic studies on gel swelling.

Many answers have been found during the course of this work, but on the other hand, lots of new unanswered questions have been raised. Chapter 2 provides basic information on the fundamental research fields involved in this work. The characteristics of DNA and the Elastin-like Polypeptides (ELP) are discussed as well as the opportunities in bioconjugation and the used characterization methods. In Chapter 3, the design of stable four-arm junctions is demonstrated to yield the basis for further DNA self-assembly experiments. Chapter 4 presents the genetic engineering of end-group functionalized ELPs, their expression and characterization. Finally, in Chapter 5, two synthesis approaches to ODN-ELP conjugates are discussed. A detailed study on the ODN functionalization by linkers and small molecules is included, providing the basis for an optimized coupling protocol. Additionally, the characterization of the obtained ODN-ELPs and their self-assembly behavior is analyzed in this chapter. Chapter 6 presents the results for the synthesis of ODN-ELP-ODN triblock copolymers and their hybridization behavior. Results and arising opportunities are summarized in the final Chapter 7.

2 Background

2.1 DNA

In 1871, Johann Friedrich Miescher, a physician and biologist, reported the extraction of a phosphate rich compound from the nuclei of white blood cells and called it "nuclein"[9]. He isolated the first sample of today's called deoxyribonucleic acid (DNA). In 1943, first evidences were found that DNA carries the genetic information and plays a key role in genetic transformation[10]. Finally, in 1953 the double helical structure was revealed by Watson, Crick, Franklin and Gosling based on x-ray diffraction measurements[11, 12]. Not only the fields of molecular biology and genetics are based on these observations. Also, the development of DNA nanotechnology in the 1980s relys on the principle of Watson-Crick base pairing. The following sections provide an insight into the basic properties of DNA, its synthesis and its use in nanotechnology.

2.1.1 Structure

DNA is a biopolymer[13, 14]. Its monomers are the so-called nucleotides. Nucleotides of DNA are composed of a 2-deoxyribose unit, a nucleobase and one phosphate group. Four different nucleobases occur naturally. They are bound to ribose units via a glycosidic bound, which is β-configurated in natural nucleic acids. The nucleobases can be derived from two basic chemical structures (Figure 2.1). Cytosine (C) and thymine (T) are based on the pyrimidine structure, a heterocyclic aromatic compound. For adenine (A) and guanine (G) the pyrimidine ring is additionally connected to an imidazole ring called the purine structure. The phosphate groups link the sugar units by phospordiester bonds at the 3′ and the 5′ position of the sugars. This asymmetric connection gives a direction to each single strand of DNA. The 5′ end is terminated by a phosphate group and the 3′ end carries a hydroxyl group. The natural synthesis of DNA is performed by DNA-polymerases from the 5′ end to the 3′ end. The chemical synthesis of short DNA strands proceeds from the 3′-end to the 5′-end.

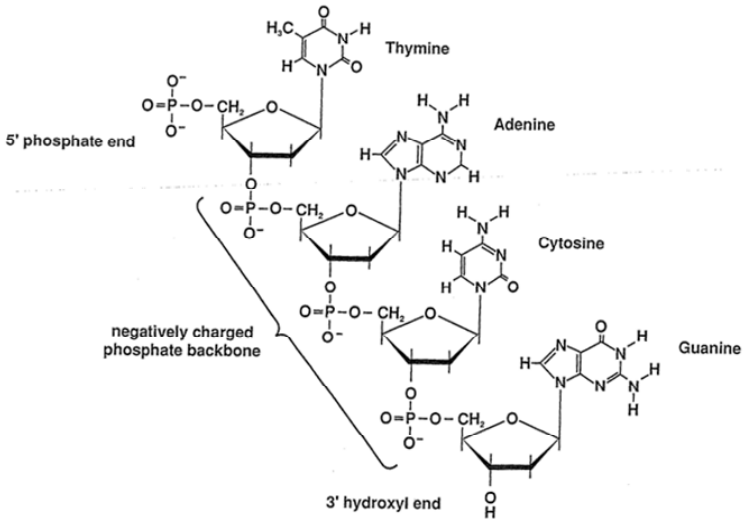

Figure 2.1 Structure of a single strand of DNA[15]. The chain is composed of the four different building blocks of DNA: the bases thymine, adenine, cytosine and guanine.

When two strands align in an antiparallel manner, they form a double helix (Figure 2.2). Each base of one strand pairs with a base from the other strand by the formation of hydrogen bonds. Base pairing is highly structure selective: a purine base pairs with a pyrimidine base. Adenine and thymine form a base pair with two hydrogen bonds. Cytosine and guanine pairs are stabilized by three hydrogen bonds. This arrangement is called complementary base pairing (Watson-Crick pairing). It allows a prediction of the complementary strand for any given base sequence. This molecular recognition is used in DNA nanotechnology to assemble well-defined DNA structures.

The double helix formation is additionally stabilized by base stacking, a hydrophobic interaction based on Van der Waals forces. The aromatic rings of the bases are oriented parallely, which enables the π-orbitals of the adjacent bases to interact with each other. Typically the binding energy of hydrogen bonds is 3-7kcal/mol, but the structural arrangement of DNA limits the stabilization of DNA by hydrogen bonds to 2-3 kcal/mol[15] only. Base stacking is sequence specific and stabilized by a binding energy between -6.57 to -14.59 kcal/mol[16]. The largest contribution yields the stacking of (GC)•(CG) pairs with -14.59 kcal/mol, which explains the increased stability of DNA with a high GC content.

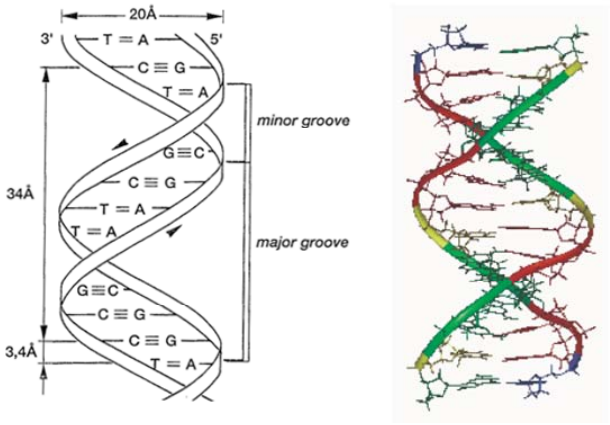

Figure 2.2 The structure of the B-double helix based on the Watson-Crick model[17, 18].

Table 2.1 summarizes the basic properties of the B-DNA double helix, the classical Watson-Crick model. Besides the B-DNA, other structures (A-, C-, D-, or Z-DNA) are known. The transition from B-DNA to A-DNA for example is induced by the conversion of the C2'endo conformation of the sugar to a C3'-endo pucker. Furthermore, structures based on alternative base pairing (Hoogsteen or wobble base pairs) or mismatch base pairing was found. The non-Watson-Crick pairing usually results in a thermodynamic destabilization of the double helix.

Table 2.1 Physical properties[15] of the B- and A-configurated double helix. The values put in parentheses apply for DNA under physiological conditions. Other values are obtained from X-Ray diffration

parameter	B-DNA	A-DNA
helix sense	right	right
residue per turn	10 (10.5)	11
axial rise	3.4 Å	2.55 Å
base pair tilt	-6°	20°
diameter of helix	20 Å	23 Å
rotation per residue	36° (34.3°)	33°
glycosidic bond configuration	anti	anti
sugar pucker	C2' endo	C3' endo
intrastrand phosphate-phosphate distance	7 Å	5.9 Å

The thermodynamic stability of a DNA duplex can be analyzed experimentally by measuring the melting profile by UV absorption (see Chapter 2.4.2). In theory, a model is used that takes the nearest-neighbor interaction[19] of the bases into account. This way it is possible to estimate the melting temperature of oligodeoxynucleotide (ODN), short single stranded DNA, duplexes. Several software packages, for example the mfold web server[20] or

the oligoanalyzer (IDT, Integrated DNA technologies)[21], use this theory to predict DNA folding (secondary structure formation) and hybridization.

In vivo the denaturation is not heat-induced. The strands are separated by enzymes, the helicases. The strand separation is part of many important biological processes like translation, transformation, recombination and replication. The latter is the basis for biological inheritance. Each strand serves as template for the synthesis of its complementary strand in DNA replication. The complementary nature of DNA also protects the encoded base sequences. If single bases are damaged in one strand, the second strand will serve as template for the repair mechanism. The helical nature of the DNA protects the genetic information as well. The formed hydrogen bonds, the base stacking interactions and the hydration of the helix stabilize and chemically insulate the bases from the environment. Biological DNA is synthesized by polymerase enzymes. They extend an already existing strand paired with a template strand. This process has been applied to the amplification of DNA in vitro. The so-called polymerase chain reaction (PCR)[22] is an important tool in molecular biology especially for DNA cloning, sequencing and genetic fingerprints. Large DNA fragments are amplified by PCR. The synthesis of oligonucleotides (short, single stranded DNA, ODNs) can also be performed chemically. The next section gives an introduction into the solid-phase synthesis of oligonucleotides.

2.1.2 Chemical Synthesis

Today oligonucleotides up to 200 bases are chemically synthesized based on the principles of solid phase peptide synthesis established in 1963 by R. Merrifield.[23, 24] The oligonucleotide synthesis starts with the first nucleoside at the 3' end, which is attached to the solid support (controlled pore glass, CPG) with a base labile linker, and proceeds to the 5' end of the oligonucleotide.

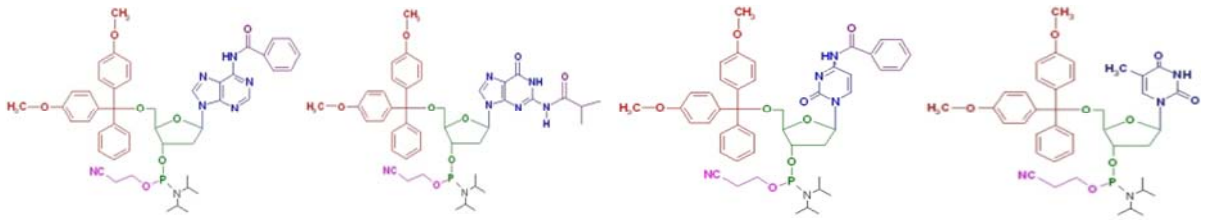

adenosine phosphoramidite | guanosine phosphoramidite | cytosine phosphoramidite | thymidine phosphoramidite

Figure 2.3 Phosphoramidite monomers for the chemical synthesis of oligonucleotides[25]

The monomers are phosphoramidite nucleosides (Figure 2.3). The 3′- hydroxyl group carries the reactive phosphoramidite functionality. The 5′OH group is protected with an acid labile dimethoxytrityl group which is cleaved off during the synthesis process. The exocyclic amino residues of the nucleobases are blocked by acyl groups (benzoyl for A and C bases, isobutyryl for G bases).

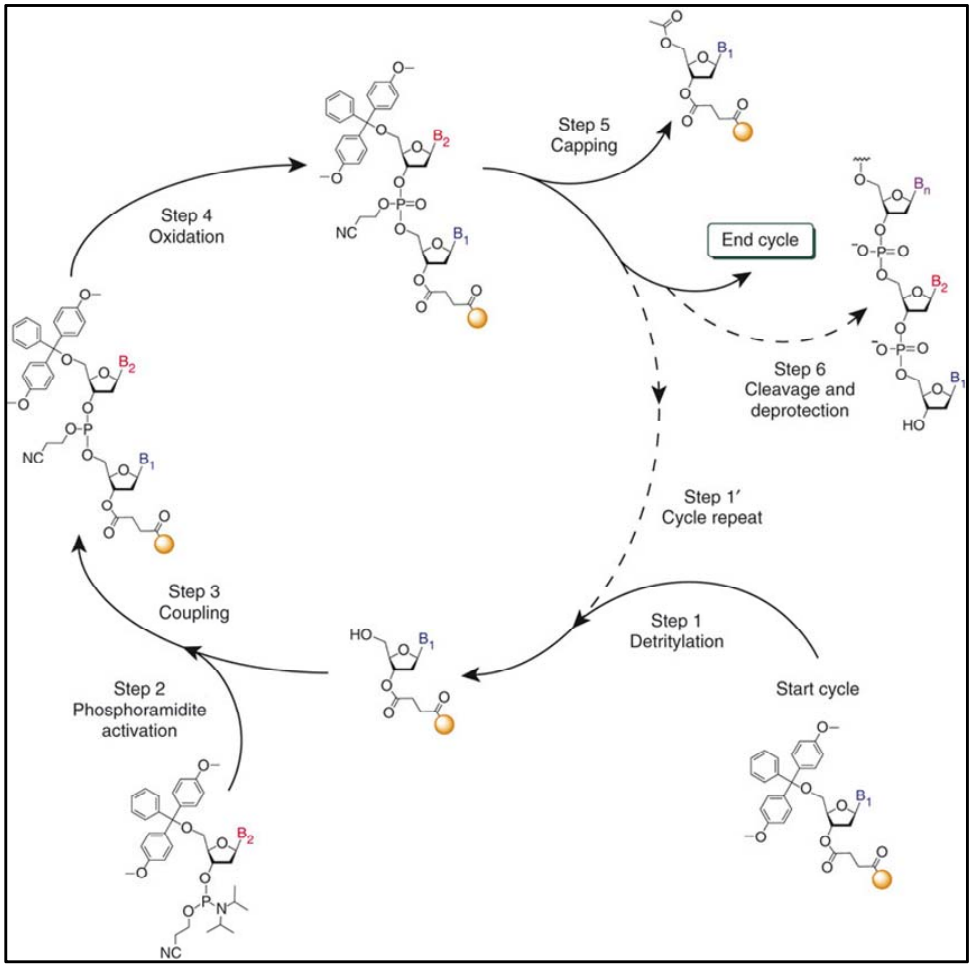

Figure 2.4 Phosphoramidite synthesis cycle[26]. Step 1: the first base (B1) bound to the solid support is detritylated by trichloroacetic acid. Step 2: Addition of a phosphoramidite activated base (B_2). Step 3: Tetrazol catalyzed coupling reaction. Step 4: Oxidation of the phosphite triester to a phosphoric triester by iodine. Step 5: Capping of unreacted 5′OH groups by acetylation. Step 6: Cleavage and Deprotection of the final oligonucleotide by aminolysis.

The synthetic cycle of oligonucleotides by phosphoramidite chemistry is shown step by step in Figure 2.4. The first step is the cleavage of the dimethoxytrityl (DMT) protecting group by trichloroacetic acid (detritylation). The free 5′OH group of the solid support bound nucleoside reacts in a tetrazol catalyzed condensation with the next phosphoramidite activated monomer (step 2 and 3). The fourth step is the oxidation of the formed phosphite triester to a stable phosphoric triester in presence of iodine. In the last step unreacted 5′OH groups are capped by acetylation to suppress any coupling failure (step 5). The steps of the cycle are repeated until the desired oligonucleotide sequence is built up. Then the

oligonucleotide is cleaved off the solid support by the addition of concentrated ammonium hydroxide solution (step 6).

The coupling steps in the oligonucleotide synthesis do not reach 100% conversion. The so-called coupling efficiency largely influences the yield of the targeted oligonucleotide.[27] In Figure 2.5 the synthetic yield Y estimated for three different coupling efficiencies c_{eff} is plotted against the number n of bases in the oligonucleotide. The theoretical yield Y is given under the assumption that the efficiency will be constant for each nucleotide:

$$Y = (c_{eff})^{n-1} \qquad (2.1)$$

The plot in figure 2.5 demonstrates how crucial the yield depends on the coupling efficiency especially for longer oligonucleotides. For example, a good coupling efficiency of 0.990 yields less than 60% of the desired oligonucleotide with 60 bases. More than 40% are failure sequences shorter than 60 bases.

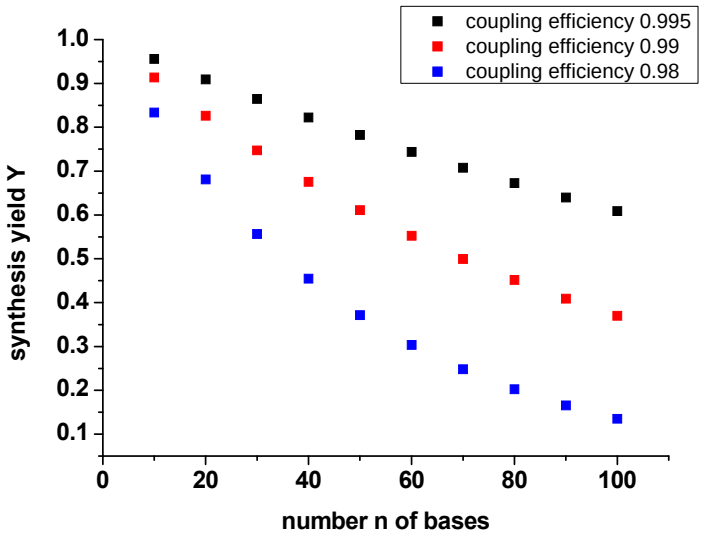

Figure 2.5 Relationship between the coupling efficiency and the synthesis yield Y for different oligonucleotide lengths (number n of bases).

The standard purification of synthetic oligonucleotides is the "DMT-on" HPLC (Chapter 2.4.3). For a complete separation of the failure sequences purification by gel electrophoresis is needed. The oligonucleotide is analyzed by denaturating polyacrylamide gel electrophoresis (Chapter 2.4.1) in this case. The desired oligonucleotide band is cut from the gel and extracted.[27, 28]

The chemical synthesis also allows the modification of the oligonucleotides in a wide variety. The sequences can be modified at the 5'-, 3'-end or internally.[29] Besides modified

bases, the incorporation of spacer molecules like short PEO spacers is possible. Oligonucleotides may also be modified by the attachment of fluorescent dyes or quencher molecules. The use of phosphorthioate bases provides an increased resistance to degradation. Additionally, the functionalization of oligonucleotides by thiol, amine and biotin linkers is widely employed. Important for this work are the modification of oligonucleotides at the 5'-end with C6 amino-, C6 thiol- and the Acrydite™ (IDT)-linker (Figure 2.6). Furthermore, oligonucleotides synthesized with a succinimidyl linker at the 5'-end (5'-Carboxy (C10) modifier, Glen research[30]) were applied for the synthesis of ODN-ELP conjugates (Chapter 5.4). This linker introduces an activated ester functionality, which has to be utilized for further modification prior to the cleavage of the solid support.

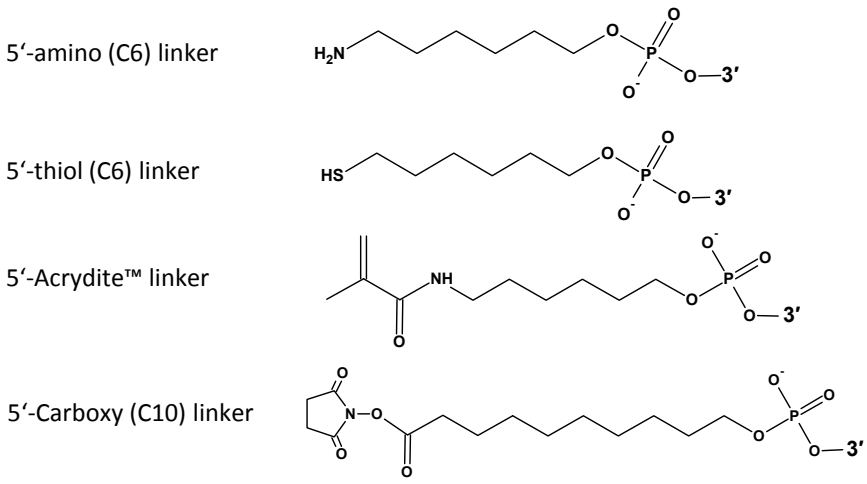

Figure 2.6 Different oligonucleotide linker modifications. All linkers are attached at the 5'-end of the oligonucleotide.[29, 30]

The chemical oligonucleotide synthesis made it possible to create oligonucleotides with a designed base sequence. Based on this possibility, the formation of designed nanostructures evolved. The following chapter discusses the first controlled assembly of DNA: the DNA four-arm junction.

2.1.3 DNA four-arm junctions

One key element in homologous genetic recombination is the so called Holliday junction. Robin Holliday[31] proposed this mobile four-arm DNA junction in 1964 to explain the exchange of genetic information between two similar DNA strands. An important feature of the mobile junction is the ability to perform branch point migration (Figure 2.7A). This process enables the strands to exchange base pairs. The mobility of the junction is caused by a twofold sequence symmetry at the branching point. The sequence symmetry makes the junction unstable. The symmetry has to be minimized to construct a stable immobile

junction. This concept was first employed by Prof Seeman et al. [32] in the early 80s to construct a stable four-arm junction (Figure 2.7B). The following chapter highlights the main designing criteria for immobile stable four-arm junctions.

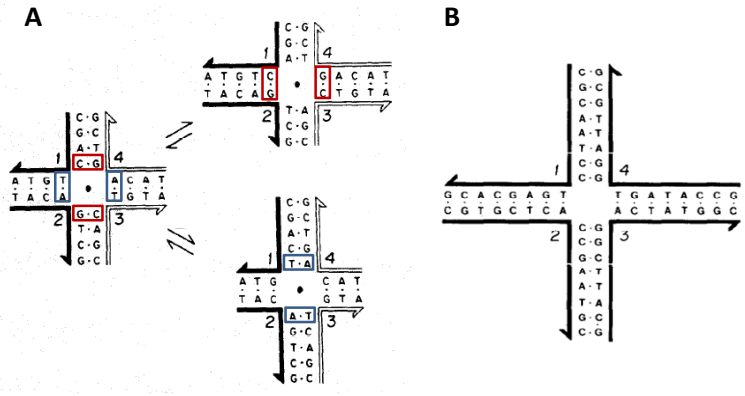

Figure 2.7 A) Branchpoint migration of the Holliday junction. B) Immobile junction designed by Seeman.[32]

2.1.4 Junction Design

The key feature of immobile junctions is the unique base pairing of each arm. The designing rules are based on two assumptions:

- Watson-Crick pairing is the optimal form of base association.
- Individual strands will maximize their Watson-Crick base pairing in the hybridization process.

To ensure a unique base pairing pattern, the strands can be visualized as series of overlapping sequences, called "criton", of the length N_c. For example, a strand with 16 bases is composed of thirteen critons of the length four. For the design of a non-migratory junction the following rules must be obeyed: first, the critons forming the junction have to be unique throughout all strands. Second, the complementary to any criton that forms a bend (the linkage between two bases that pair to different strands) must not be present in any strand. Third, self-complementary critons are prohibited. Fourth, the same base pair can only adjoin the junction point twice. The first three rules ensure the unique base pairing. The last rule takes into account that the Watson-Crick pairing is disturbed at the junction point and guarantees therefore specific base pairing. The rules have been implemented in the SEQUIN computer program written by N. Seeman[33, 34]. The program uses a sequence-symmetry minimization algorithm that enables the design of branched nucleic acid structures with a maximized control over the secondary structure.

The SEQUIN program was used in this work to design stable four-arm DNA junction with 23 base pairs per arm. Three individual junctions were constructed in parallel to ensure a minimized interaction between each junction. The criton length N_c was chosen to be smaller than five. A few additional criteria applied for the sequence design. Triplets of one base were prohibited (e.g. AAA, TTT). Base sequences consisting of a series of large bases (G or A) or of small bases (C, T) longer than 5 bases were not permitted. The latter two criteria were only followed, if the basic rules were obeyed.

2.1.5 Junction Geometry

The geometry of four-arm DNA junctions has been studied extensively. First experiments were done by comparative gel electrophoresis of immobile junctions[35-37]. This analysis compares the gel mobility of junctions differing in arm length. The mobility is determined by the overall geometry and shape of the junction. The method provides information on the inter-helical angles. The different studies show that the junction adopts a planar extended cruciform structure in absence of divalent ions (Figure 2.8). This geometry minimizes the strong repulsion forces of the phosphate groups at the intersection of the strands. The forces are screened by increased salt concentration especially divalent cations. The junction forms a stacked X structure with a more compacted geometry under these conditions. Each forming duplex consists of an exchanging strand on the inside, that crosses over, and of a non-exchanging on the outside. The outside strands can be arranged parallel or anti-parallel.

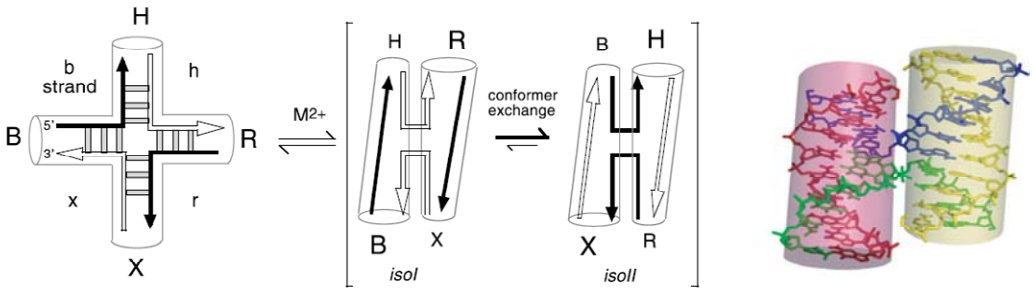

Figure 2.8 Schematic of the ion-induced folding of a four-way DNA junction into two possible conformers (*isoI* and *isoII*). The junction consists of four DNA strands (b, h, r and x) that associate to form the helical arms (B, H, R and X). The unmodified junction is extended in the absence of metal ions. On the addition of metal ions the junctions forms a stacked X-structure by pairwise coaxial stacking of the helical arms. [38, 39]

The gel mobility experiments as well as FRET measurements verify the antiparallel alignment as the major geometry[38, 40, 41]. The strands can change partners depending on their sequence. All derived structural features have been confirmed by NMR studies[42, 43] and crystallography[44]. Two excellent reviews on more structural details of helical DNA

junctions have been published by D.M.J. Lilley[39, 45], who has been working in this field since the early 1980s.

2.1.6 Controlled self-assembly of DNA

The formation of a stable DNA junction was the pioneer work of DNA self-assembly more than 25 years ago. Since then, DNA nanotechnology is a continuously expanding research field. Nanotechnology in general is based on two principal methods: the top-down and the bottom-up approach. DNA self-assembly is part of the bottom-up approach, which uses molecular recognition to assemble molecules into superstructures[46]. DNA plays a key role in nanotechnology because of the well-known double helical parameters, its stiffness and its specific Watson-Crick pairing. The formation of the DNA four-arm junction was followed by the construction of a cube-like structure (Figure 2.9A) by N. Seeman et al.[47] in 1991. The edges of the cube are double helices. The cube consists of six cyclic interconnected single strands. The next step in DNA self-assembly was the design of well-structured arrays, which was possible by the introduction of the DNA double-crossover (DX) motif.[48] This stiff building block shown in figure 2.9B contains two parallel double helices connected to each other by strand exchange. In the late nineties the addition of sticky ends to the DX motif made the formation of two-dimensional arrays possible (Figure 2.9B). [49]

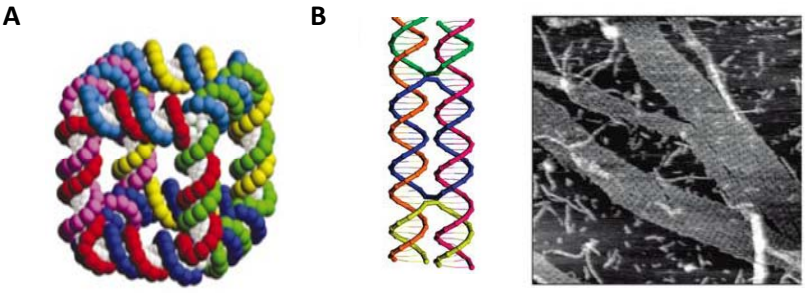

Figure 2.9 Early DNA self-assembly[50] A) Model of a DNA cube. B) Schematic of a double crossover (DX) tile and AFM picture of 2D DNA lattices.

A revolution in DNA technology took place in 2006, when P.W.K. Rothemund reported the formation of complex DNA structures like the star or the smiley shown in Figure 2.10A.[51] The scaffold in the so-called DNA origami technique is a single-stranded virus. It is put into place by hundreds of short staple strands, which form repeating DX patterns. At the beginning, this method allowed the formation of large, two-dimensional DNA structures. Three years later, it was brought to the third dimension by H. Yan.[52] He constructed a three-dimensional cage of tetrahedron geometry (Figure 2.10B). A further step was achieved by W. Shih and H. Dietz[53] in the formation of bend DNA structures (Figure 2.10C). The

controlled insertion and deletion of bases causes the designed DNA bundles to twist and bend.

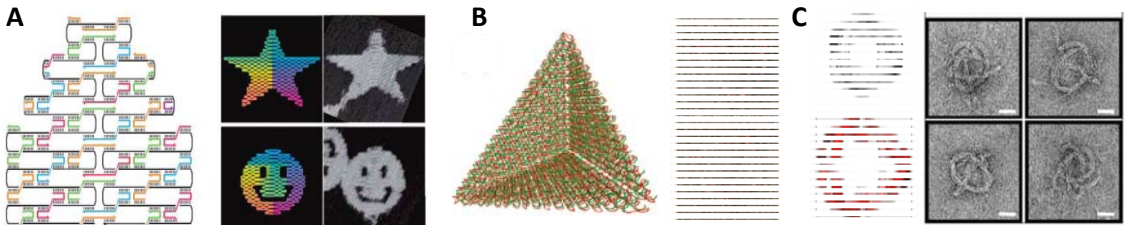

Figure 2.10 Recent DNA nanoarchitectures: A) DNA Origami[50] B) DNA tetrahedron container[52] C) DNA folded into twisted and curved shapes[53].

The fast developing field of DNA nanotechnology is a powerful tool for controlled structure formation, but still some questions have to be answered. The self-assembly of DNA is still not fully understood, and the dependence of the error rate on the annealing process for example is still under investigation.[50] This is especially important for the field of DNA computation or the self-assembly of DNA in vivo, which will be a future step in DNA nanotechnology.

2.2 Elastin-like Polypeptides (ELPs)

2.2.1 Elastin

Elastin is the main protein responsible for the elastic properties of vertebrate tissues. It consists of alternating hydrophobic and crosslinking domains. The hydrophobic domains are dominated by hydrophobic amino acids, such as proline, valine, alanine and leucine. The crosslinking domains contain lysyl residues combined with proline-rich regions or polyalanine domains. The elastogenesis[54], the biological synthesis of elastin, involves the synthesis of a soluble precursor protein: tropoelastin. It binds to galactolectin after its translation to prevent the intracellular aggregation. After the excretion of the tropoelastin-galactolectin complex in the extracellular space the tropoelastin is released locally and aligned at the microfibrillar scaffold. Most lysyl residues are then deaminated and oxidized by the lysyl oxidase to allysine. The crosslinks of the elastin network are formed by the reaction of the allysines and unmodified lysine to desmosine or isodesmosine linkages. The elastin network is organized in filaments that form large bundles.[55]

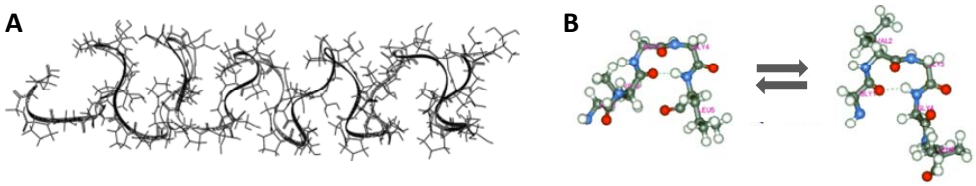

Figure 2.11 Structure model for elastin elasticity. A) β-spiral model by Urry B) model of sliding β-turns proposed by Tamburro et al.[56]

Two structural models for the elastin elasticity are in discussion. Based on extensive studies on synthetic Poly(ValProGlyValGly), Urry proposed the β-spiral model[57] (Figure 2.11A). He suggests a helical arrangement of type II β-spirals per pentameric peptide unit. The ProGly unit is positioned at the corner of the bend and a hydrogen bond connects the carbonyl group of the first valine with the amino residue of the fourth valine. The dipeptide segments of VG, suspended between the β-turns, exhibit large amplitude librations. The decrease of these librations upon extension results in a large decrease in entropy of the segments explaining the rubber elasticity of elastin. At variance of the classical theory of rubber elasticity this model assumes fixed, end-to-end chain lengths. Molecular dynamics simulations assuming freely fluctuating ends resulted in a loss of the helical β-spiral structure[58]. A second model has been provided by Tamburro et al.[59] (Figure 2.11B), which involves the formation of non-recurring, isolated type II β-turns for the (GlyXGlyGlyX) repeat units of the elastin sequence. The XGly or GlyGly segments build up the corners. The first and fourth glycine or the second and fifth X residue are connected via hydrogen bonds.

Due to the absence of proline residues, the resulting β-turns can dynamically slide along the chain. The polypeptide can therefore freely fluctuate and obtains high intrinsic entropy, which is decreased upon extension. The elastin entropy is increased by water, which facilitates the conformational mobility of the polypeptide segments. Both models have the presence of type II β-turns in common, but their dynamic interpretations are different. Molecular simulations[58, 60, 61] performed in the group of V. Daggett have indicated that the hydration of the hydrophobic residues largely contributes to the gain in entropy. Upon the collapse of the polypeptide the hydration waters are released and the entropy of the solvent increases significantly.

Biopolymers based on the repeat unit sequences of Elastin have been synthesized by solution and solid phase chemistry as well as by genetic engineering. The following section highlights the synthesis of monodisperse, well-defined Elastin-like polypeptides (ELPs), which are derived from the hydrophobic repeat unit of the mammalian tropoelastin, by recombinant genetic engineering.

2.2.2 Genetic Engineering of ELPs

Genetically encoded synthesis of polypeptides provides precise control of the peptide sequences, their chain length and the stereochemistry. In general, genetic engineering[62] involves three molecular biology steps. First, a plasmid called the vector is linearized by digestion with a restriction enzyme and, an insert that encodes the desired peptide sequence is ligated into the vector. Second, the recombinant plasmid is transformed into competent bacteria cells. Third, the cells are cultivated and the replication of the cells produces many copies of the recombinant plasmid.

The genetic engineering of the ELPs used for this work is based on the strategy reported by D.E. Meyer and A. Chilkoti [63]. The approach called recursive directional ligation (RDL) is a stepwise oligomerization of a DNA monomer to yield an oligomeric library from the monomer to the oligomer of the desired length. Elastin-like Polypeptides are based on a repetitive pentapeptide motif (Val-Pro-Gly-Xaa-Gly). Xaa is a guest residue that can be any amino acid except proline. The first step of the RDL procedure (Figure 2.12) involves the insertion of a synthetic monomer gene (encoding a defined number of the polypeptide repeat units) into a plasmid cloning vector. The gene is designed to contain two different restriction sites (RE1 and RE2) on each end of the coding sequence. The prepared plasmid containing the synthetic oligonucleotide is subjected to two different digestions. One digestion involves the linearization of the vector with the enzyme 1. In the second digestion

an insert is produced by the cleavage of the plasmid with enzyme 1 and enzyme 2. The purified insert is then ligated into the linearized vector. The product contains two repeats of the original gene connected head-to-tail. The RE1 and RE2 restriction sites are conserved at the end of the gene enabling the new plasmid to be used in future rounds of RDL. Additional rounds proceed identically employing products from the previous rounds as starting material.

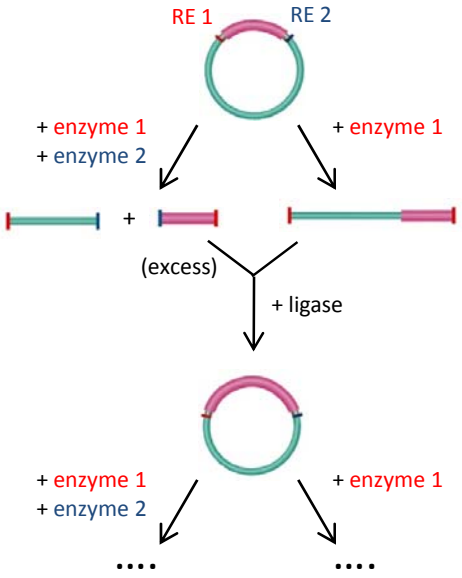

Figure 2.12 The molecular biology steps of the recursive directional ligation (RDL) method. The cloning vector carries two restrictions sites (RE1, RE2) at each end of the coding sequence (pink). An insert of the coding sequence is prepared by the digestion of the vector with enzyme 1 and enzyme 2. This insert (in excess) is ligated into the vector that has been linearized by the digestion with enzyme 1. Additional rounds of RDL proceed identically with the cloning vector of the previous round.

One disadvantage of this method is the occurrence of multiple insertions. The resulting plasmid contains sometimes double or triple inserts. A new variation of the original RDL method was developed by J. McDaniel (unpublished) to control the insert size. The scheme of the modified RDL method is shown in Figure 2.13. It involves the incorporation of a third restriction site, which is positioned in the middle of the plasmid sequence. The digestion of an aliquot of the plasmid is performed by the incubation with enzyme 1 and enyzme 3. The second digestion uses the restriction enzymes 2 and 3. Both digestion products contain the encoding insert and carry compatible cohesive ends. The ligation of these two products results in a dimerization of the gene. This method ensures the defined formation of dimeric inserts.

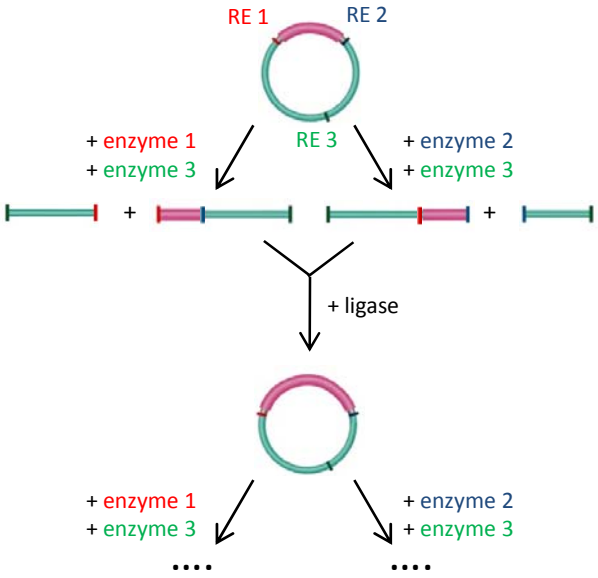

Figure 2.13 The molecular biology steps of the modified RDL method. The cloning vector carries three restrictions sites (RE1, RE2, RE3). RE1 and RE2 are positioned at each end of the coding sequence (pink). RE3 is located in the vector backbone. One aliquot of the vector is digested with enzyme 1 and enzyme 3. A second aliquot is digested with enzyme 2 and enzyme 3. In a third step the digestion products carrying the coding sequence are ligated yielding a new vector with a double insert. Additional rounds of RDL proceed identically with the cloning vector of the previous round.

The results of the oligomerization steps are usually monitored by agarose gel electrophoresis (Chapter 2.4.1) the encoded sequences are confirmed by DNA sequencing. For the expression of an oligomeric gene derived by RDL, it is usually first excised from the cloning vector and ligated into an expression vector. Some vectors can be employed as cloning and as expression vector. Details on the used vectors and restriction sites for the synthesis of the ELPs used in this work are given in Chapter 4.1.

ELPs are produced in high yield in *Escheria coli* and are rapidly purified by the so-called inverse transition cycling (ITC)[64] exploiting their inverse phase transition. ELPs composed of the pentapeptide motif (Val-Pro-Gly-Xaa-Gly) are thermally responsive biopolymers. They are soluble in aqueous solution below their transition temperature (T_t.). Above their T_t they aggregate rapidly. The transition behavior is discussed in detail in the next Chapter 2.2.3. The ITC purification (Figure 2.14) uses this aggregation to separate the overexpressed Elastin-like polypeptide from other contaminating biomolecules in the cell lysate. The ELP is aggregated by an increase in temperature and/or ionic strength. The aggregated protein is separated from the soluble contaminants by centrifugation above its T_t. It is then resolubilized in cold buffer below its T_t and centrifuged again to separate any insoluble matter. This cycle of aggregation and resolubilization can be repeated several

times to obtain high purity grade ELP. The reported yields of expressed ELP are in the range of 100-200mg per liter of cultured media.[65]

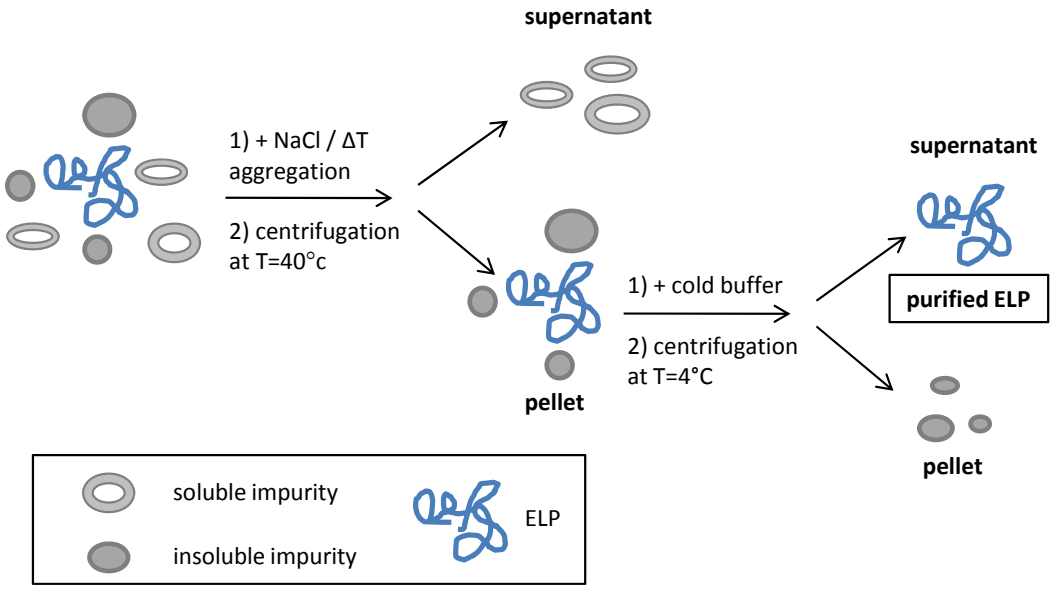

Figure 2.14. Illustration of the inverse transition cycling (ITC) method for the purification of ELPs. The ELP mixture is incubated at elevated temperatures or/and with the addition of NaCl. The ELP aggregates under these conditions. After centrifugation at elevated temperatures (T=40°C) the supernatant containing the soluble impurities is separated from the pellet. The pellet is resuspended in cold buffer and centrifuged again at T=4°C to remove any insoluble matter. The supernatant contains the purified ELP.

2.2.3 Thermosensitivity of ELPs

The inverse temperature phase transition is the most interesting feature of ELPs.[66, 67] As described above, ELPs are highly soluble below their lowest critical solution temperature (LCST) or transition temperature T_t. If the temperature is raised above the T_t, they undergo a sharp phase transition within a range of 2°C resulting in the aggregation of the polypeptide. This phase transition can be determined by measuring the turbidity profile as a function of temperature. The measurements are usually performed by monitoring the optical density at 350nm. The transition temperature depends on the ELP sequence, the chain length, the peptide concentration and the ionic strength of the solvent. The transition temperature decreases with increasing peptide length, increasing peptide concentration and with increasing salt concentration[68]. The hydrophobicity of the guest residue also modulates the T_t. A hydrophilic guest residue increases the T_t.[69] Figure 2.15 shows the turbidity profile and the corresponding hydrodynamic radius R_H (measured by dynamic light scattering) for an ELP diblock copolymer.[70] The blocks of the ELP copolymer differ in their guest residue composition. One block contains a more hydrophilic guest residues resulting in a higher T_t. The second block with a hydrophobic guest residue has a lower T_t. This block composition enables the ELPs to self-assemble into spherical micelles (Figure 2.15). The more

hydrophobic block aggregates in the range of T=40°C resulting in the formation of spherical micelles (R_H = 32 nm). The turbidity profile shows in this range a slight increase in optical density (OD). The second transition of the more hydrophilic block at T=50°C induces the complete aggregation demonstrated by the high OD value. The measurement highlights the narrow transition range of the polypeptide aggregation.

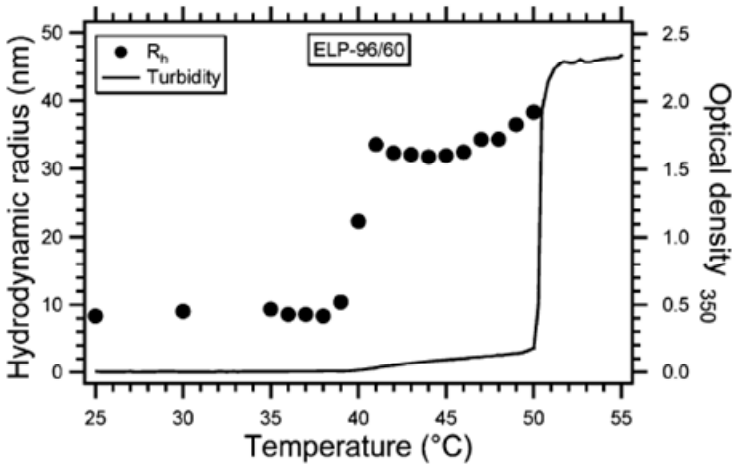

Figure 2.15 Hydrodynamic radius and turbidity profile of an ELP diblock copolymer ELP-96/60 versus temperature[70].

The thermal behavior of the ELPs synthesized in this work is discussed in Chapter 4.3. The inverse transition behavior of the ELPs makes them interesting for applications in drug delivery, tissue engineering and protein purification highlighted in the next section.

2.2.4 Applications of ELPs

The LCST behavior of ELPs is exploited in many different biomedical and biotechnical applications.[71] The purification of fusion proteins incorporating an ELP tag was successfully demonstrated for various recombinant proteins. The purification is based on the ITC technique described above. The target protein is recovered by the enzymatic cleavage of the ELP tag.

The precise structure control provided by the genetically encoded synthesis of ELPs is important for many biomedical applications.[72] The polypeptide sequence can be tuned to control the type, number and location of any reactive sites. It also provides a tool for the altering of the LCST behavior of the ELPs by changing the guest residue composition or its molecular weight. The molecular weight is a key parameter that controls the half-life of a substance in vivo and its degradation in the body. In general, ELPs are non-toxic, biodegradable and they show good pharmacokinetics. ELPs with an transition in the range

of 37°C-42°C were used in hyperthermia treatments. Recently, ELPs were employed as drug carriers. For example, ELPs conjugated to Doxorubicin, a hydrophobic anticancer drug, via an acid-labile hydrazone bond were investigated in respect to their pharmacokinetics and their biodistribution within the tumor.[65]

Elastin-like Polypeptides were also tested as injectable tissue-engineered biomaterials for cartilage repair. The chosen polypeptides need to exhibit a transition temperature at 37°C, the body temperature. The gel precursor is liquid and injectable at room temperature. Exposed to the body temperature, the ELPs aggregate and form a gel like material. Gels based on ELPs promoted the chondrogenesis (biosynthesis of cartilage) in vitro.[73]

The surface modification of biomedical devices has become an important research field. The surfaces of implants for example are primarily in contact with body fluids, cells and tissues. Their biocompatibility and an enhanced cell adhesion depend on their surface properties. Elastin-like Polypeptides have been designed for biosensing surfaces. The polypeptides carrying an affinity tag for a target protein are conjugated to ssDNA that binds to a DNA functionalized solid support.[74]

Concluding, recombinant peptide-based biopolymers like ELPs show a high potential in biomedical applications. They combine important biological functions such as biocompatibility, elasticity and cellular adhesion with precisely tailor made functions.

2.3 Bioconjugation

The conjugation of biomolecules and their crosslinking is manifold. Depending on the functional groups different coupling strategies are possible. Simple acylation reactions by carbodiimide activation[75] are utilized as well as click chemistry[76] or the native ligation.[77] An overview of the common techniques and coupling reactions is provided in the book "Bioconjugate Techniques" by T. Hermanson.[78] The following sections discusses the relevant conjugation chemistries used in the course of this work.

2.3.1 Conjugation by activated ester chemistry

The conjugation of reagents containing an activated ester residue to primary or secondary amines is one of the most common methods in the field of bioconjugation. Most reactive esters employed today are N-hydroxysucciminide (NHS) activated esters. The activation of a carboxylate by NHS is performed in the presence of a carbodiimide and in nonaqueous conditions to avoid hydrolysis. The activation by NHS can also be done in situ to react a carboxylate containing molecule with an amino compound. In this case the transformation into an activated ester is performed in the presence of EDC, a water soluble carbodiimide.

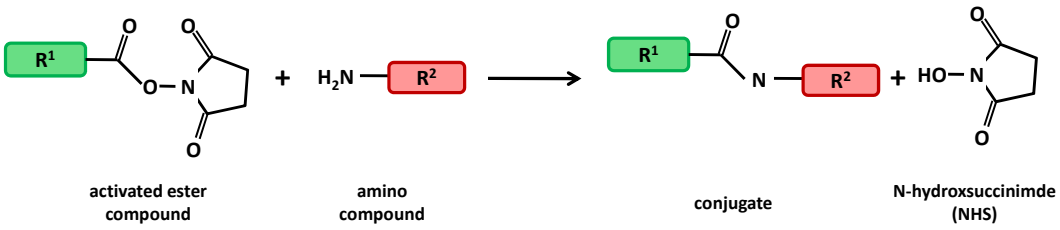

Figure 2.16 Scheme of the reaction between an NHS ester activated derivative and an amine compound resulting in the formation of an amide bond and the release of NHS.

The NHS ester activated reagent is attacked by amine nucleophiles forming a stable amide bond. The leaving group is the NHS. The reaction of NHS ester with thiol or hydroxyl nucleophiles yields unstable thioesters or ester linkages that hydrolyze in aqueous solution. One disadvantage of the NHS ester chemistry is the hydrolysis of the active compound in aqueous solution. The half-life of an NHS ester is typically 4-5h at 0°C and pH=7.[79] The hydrolysis rate increases with increasing pH. It can be monitored by measuring the absorption of the NHS leaving group at 260nm. Usually a high excess of the activated ester reagent and a high concentration of target molecule are used to minimize the hydrolysis and to maximize the modification yield.

Most NHS activated reagents are water-insoluble and have to be dissolved in organic solvent before the conjugation reaction. Their water soluble analogues are the N-

hydroxysulfosuccinimide (sulfo-NHS) esters that show the same reactivity and specifity, like the NHS ester.

The conjugation reactions with NHS reagents should be performed in amine free buffers like phosphate buffers. The pH should be in the range of 7.0-7.5 to minimize the hydrolysis rate and to promote the unprotonated state of the amine that is the nucleophilic species. The NHS ester chemistry was employed in this work for the modification of amino oligonucleotides by heterobifunctional linkers (Chapter 5.2) and in the synthesis of ELP-ODN conjugates (Chapter 5.4).

2.3.2 Conjugation by thiol addition

Free thiol groups are able to form thioether linkages by Michael-type addition reactions.[80] The most common sulfhydryl reactive functional group is the maleimide moiety, a maleic acid imide. The double bond of maleimides can undergo an alkylation reaction with sulfhydryl groups forming a stable thioether bond. The maleimide functionality is often part of heterobifunctional crosslinking agents used for the conjugation of cysteine containing proteins. The reaction of thiol groups with maleimides is specific in the pH range of 6.5-7.5.[78] At neutral pH the reaction of sulfhydryl groups proceeds 1000x faster than the addition reaction of amines. High pH values are therefore not advisable to avoid any cross reaction with amino groups. At pH values >8.5 the amine addition is favored.

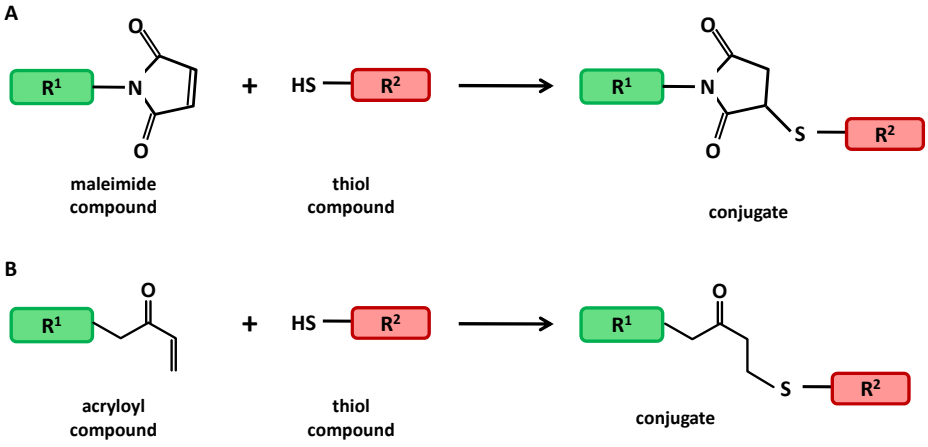

Figure 2.17 A)Reaction scheme of the Michael-type addition of thiol containing compounds to maleimide derivatives. B) Reaction scheme of the Michael-type addition of thiol containing compounds to acryloyl derivatives.

The maleimide group may hydrolyze to a maleamic acid derivate that is unreactive towards sulfhydryl moieties. Comparable to the hydrolysis of NHS ester, the rate increases with increasing pH. Some crosslinking agents provide an increased stability to maleimide hydrolysis because of steric hindrance. For example, the heterobifunctional linker SMCC

(Succinimidyl 4-[*N*-maleimidomethyl]cyclohexane-1-carboxylate, see Figure 5.4) contains a cyclohexane ring that connects the NHS reactive group and the maleimide moiety. It shows a decreased hydrolysis rate compared to the linker MBS (m-Maleimidobenzoyl-N-hydroxysuccinimide ester) that carries a phenyl ring. Besides maleimide groups, the addition of thiol containing compounds can also occur with derivatives of acrylic acid. The acryloyl compounds form as well a stable thioether bond, but the reaction usually proceeds at a slower rate.

The thiol containing compounds are usually incubated with reducing agent prior to the coupling reaction. Thiol containing reducing agents like dithiothreitol (DTT), 2-mercaptoehylamine or 2-mercaptoethanol have to be removed before the addition of the maleimide compound. The removal of non-thiol containing reducing agents like tris(2-caroxyethyl)phosphine (TCEP) is reported to be unnecessary[78], but studies on conjugation reactions performed in the presence of TCEP showed a major decrease in yield[81, 82]. Thus, the removal of reducing agents is advisable in all cases. Difficulties encountered in the complete removal of the reducing agents are disscused in Chapter 6.3.

2.3.3 Oligonucleotide conjugates

Many different research areas are interested in the synthesis of well defined oligonucleotide (ODN) conjugates. The research of oligonucleotide based therapeutics has been intensified since the modulation of specific genes by synthetic oligonucleotides had been observed.[83] The need for oligonucleotide conjugates arises due to several reasons.[84] Naked oligonucleotides show a poor cellular uptake and are not stable in the intracellular fluid. They usually bind to a target non-specifically and have a low binding affinity. The covalent conjugation of oligonucleotides to synthetic peptides, biocompatible polymers or proteins is one strategy to surpass these failures. The synthetic strategies for the design of oligonucleotide-peptide conjugates (POCs), also called peptide-oligonucleotides (POs) or oligonucleotide-peptide conjugates (OPCs) are reviewed in various articles.[84-86] Their application ranges from therapeutics, artificial enzymes to models for structural and mechanistic studies.

Besides the biomedical application oligonucleotide conjugates are also of interest in biosensing application. ODN-Protein conjugates have been employed successfully in hybridization assays[78] or FRET measurements[87] (fluoresence resonance energy transfer). A new strategy for the conjugation of ODNs to proteins employing click chemistry was reported by Distefano et al.[88] in 2007. The synthesized conjugates were used to create

protein nanostructures by DNA self-assembly. The design of ODN-ELP[74] conjugates was reported in relation with protein surface functionalization. The conjugates were used to capture recombinant target proteins from solution.

The conjugation of DNA with synthetic polymers has been applied in different research fields. For example, in the field of bioanalytics ODN-Polyacrylamide conjugates were used for single-nucleotide polymorphism genotyping by capillary electrophoresis. The biomedical application of ODN-Polymer conjugates targets gene delivery[89]. Especially antisense therapy, which uses oligomeric antisense DNA to block the expression of specific proteins by the hybridization with targeted mRNA sequences, applies polymer conjugation for an increased cellular uptake and the protection against enzymatic hydrolysis. Park et al.[90] prepared DNA-b-PLGA (poly(D,L-lactic-co-glycolic acid)) block copolymers that form micelles in aqueous solution with the PLGA segments as hydrophobic core and the ODNs as the corona. Tests in vitro demonstrated that the spherical micelles exhibit an increased cellular uptake. Similar results were obtained for DNA-b-PEO block copolymers electrostatically complexed with PEI (polyethylenimine) or PLL (poly(L-lysine)) showing an increases stability against deoxyribonuclease.[91, 92] The formation of micellar structures was also observed in the case of DNA-b-PPO block copolymers, which were synthesized by attaching a phosphoramidite activated PPO block in the last step of the solid-phase synthesis.[93] The formed micelles were used as templates for organic reactions.

In 2004, S. Craig started a more fundamental approach to reversible polymers employing self-complementary oligonucleotides linked with a PEO spacer.[94] These ODN-PEO-ODN triblock copolymers were synthesized completely on a solid support, applying phosphoramidite chemistry. After the standard solid phase synthesis of the first ODN the PEO spacer was attached and the second ODN block was synthesized again using step by step synthesis on the solid support. The study investigated the thermodynamics of association of the resulting polymeric strutures formed by DNA hybridization.

2.4 Characterization Methods

The following sections provides a short introduction into the characterization methods used. Gel electrophoresis and UV/VIS absorption measurements are two essential tools in DNA and peptide research. The analysis and purification of biomolecules by High-performance liquid chromatography (HPLC) is also well established. Finally, the characterization by dynamic light scattering (DLS), that reveals information about the uniformity and the hydrodynamic properties, is discussed.

2.4.1 Gel Electrophoresis

Gel electrophoresis is today the major analytical tool for the characterization of biomacromolecules like DNA and proteins. The electrophoretic separation of proteins was first studied by A. Tiselius[95] in the early 1930s, who received the noble prize in 1948 for his contribution to the electrophoretic separation of proteins and especially for the discovery of the complex nature of serum proteins. The first characterization of DNA by gel electrophoresis was published in 1967 by H. V. Thorne.[96] Since then, electrophoresis has become a standard technique in biochemistry. Depending on the analyte, various methods are applied. Small DNA fragments (<500bp) can be analyzed by polyacrylamide gel electrophoresis (PAGE).[97] Larger DNA fragments are usually separated in agarose gel electrophoresis.[98] For the molecular weight estimation of peptides and proteins the sodium dodecyl sulfate (SDS)-PAGE analysis[99] is used. Before the different electrophoretic methods used in this work are discussed, a brief introduction on the theoretical basics of electrophoresis[100-102] is given.

Electrophoresis is based on the separation of charged particles by applying an external electric field. Two different forces act on the charged particle: the accelerating force F_e and the friction force F_f. F_e is proportional to the effective charge q of the particle and the electric field E.

$$F_e = q \cdot E \qquad (2.2)$$

The friction force F_f retards the migration of the charged particles proportional to their velocity v and the friction coefficient f.

$$F_f = f \cdot v \qquad (2.3)$$

The ion reaches a steady state velocity, where the frictional force and the accelerating forces are equal. The velocity of the particle can be expressed as:

$$v = \frac{q}{f}E = \mu \cdot E \qquad (2.4)$$

The electrophoretic mobility μ of the particle is proportional to its charge q and inverse proportional to its friction coefficient f, which can be estimated for spherical particles by Stokes' law:

$$f = 6\pi\eta R_H \qquad (2.5)$$

A larger hydrodynamic radius, therefore, results in a lower electrophoretic mobility. The frictional forces in gel electrophoresis also depend on the viscosity of the medium and the pore size of the gel matrix.

Two additional forces derived in the Debye-Hückel theory[103] have to be considered in dilute solution. The migration of the particles is retarded in an electric field by the relaxation force, because the ion cloud of the ion is moving slower than the central ion. The retardation force also decreases the velocity of the charged particle, because the central ion is surrounded by counter-charged ions. These two forces cause the decrease in migration with increasing ion strength. Therefore, samples are desalted prior to the electrophoretic separation to obtain comparable results.

In the case of acids and bases the dissociation degree determines the effective mobility. This is important for the analysis of peptide and proteins, which are weak acids or bases. The separation can be optimized by adjusting the pH value of the puffer system. In general the specific conductivity of a solution depends on the effective mobilities of all ions in the system. Hence, the electrophoretic separation can be optimized by choosing different buffer systems. Additionally, it has to be taken into account that the applied voltage produces heat, which is released through the walls of the system. For example, the so called "smiling effect" occurs, if the center of the gel is hotter then the outside. The samples in the middle therefore run faster than the ones applied on the outside lanes. The heat dissipation can be increased by using thin gels and an effective cooling system.

Today mainly two compounds are applied as gel matrices[102]: polyacrylamide and agarose. The polyacrylamide gels are formed by the polymerization of acrylamide with the cross linker N,N'-methylenbisacrylamide. Depending on the crosslinker to monomer ratio, pore sizes between 100-1000Å can be achieved. The gels are optically clear and electrically

neutral, which prevents the electroendosmostic effect. Agarose is a natural polysaccharide, which needs to be dissolved by heating. Upon cooling the molecules organize themselves into double helices, which aggregate into thick and interconnected rods. The aggregation results in the formation of large pores (500-5000Å) depending on the agarose concentration. Important for the application of agarose is its melting temperature and its degree of electroendosmosis. Electroendosmosis refers to the migration of solvent in an electric field due to charges present on the gel matrix. The degree of electroendosmosis m_r depends on the amount of polar residues of the agarose. A m_r value of 0.25 corresponds to a highly charged agarose and a value of 0.00 would refer to an electroendosmotic free agarose.[100]

For this work the agarose gel electrophoresis was applied in a native manner to characterize the hybridization of ODN-ELP conjugates (Chapter 5) and to analyze the molecular cloning experiments (Chapter 4). It was also used to observe the migration behavior of surface functionalized gold nanoparticles (Chapter 6). The experimental conditions are described in Chapter 8.6.4.

For the analysis of oligonucleotides and their conjugates the DNA polyacrylamide gel electrophoresis (DNA-PAGE) was performed either under denaturating conditions or under native conditions. The native DNA-PAGE was mainly used to characterizes the formation of DNA four-arm junctions (Chapter 3). The denaturating DNA-PAGE was the method of choice for the characterization of the modification and conjugation of oligonucleotides (Chapter 5). In all cases a vertical slab gel was freshly prepared. The gel preparation and the electrophoresis conditions are described in Chapter 8.6.3. The gels resolved samples in the range of 10-300 bases (20-200bp). DNA gels are stained with fluorescent dyes that bind electrostatically or by intercalation to the nucleotides. The fluorescent signal obtain from the gel picture can be used to estimate the amount of DNA. Usually the gel picture is transformed into intensity profiles of the different sample lanes by standard software, e.g. ScionImage (Scion Corporation). The DNA quantification is in this case only an estimation. The binding of the fluoresence dye is strongly depended on the staining conditions. The fluoresence signal depends on the concentration of dye, the concentration of DNA and the ionic strength[104]. Especially in the case of single stranded DNA the dye binding was demonstrated to be sequence specific[105]. In this work the quantification by gel intensities was used to evalute the yield of conjugation reactions. All quantifications are estimations due to the inconsistency of the determination.

The SDS-PAGE[99] was applied for the characterization of Elastin-like polypeptides (Chapter 4.2) and their conjugates (Chapter 5.4). For this method the anionic detergent SDS is added in excess to the sample and the running buffer. The SDS covers the peptide charge and forms micelles with a constant negative charge per mass unit: 1.4g SDS per 1g protein. Hence, the separation in SDS-PAGE is simply due to the molecular size. The samples for SDS-PAGE are usually denatured by heating (destruction of secondary structures) and the addition of reducing agent (cleavage of disulfide bridges). Due to the constant mass to charge ratio a separation only determined by molecular size is achieved. For all SDS-PAGE measurements precast pore gradient (4-20% or 10-20%) gels were used. Pore gradient gels have a larger resolution range. For example 16% gels have a resolution of 8-80kDa. A gradient gel of 10-20% resolves proteins in the range of 20-200kDa. Further specifications and conditions can be found in chapter 8.6.5.

2.4.2 UV/Vis Absorption Spectroscopy

In UV/Vis absorption[100] measurements a sample is exposed to light ranging from 200-740nm in wavelength (UV/Vis range). Depending on the wavelength the light excites valence electrons from a lower occupied orbital into a higher energy orbital. The absorbed energy depends on the type of electronic transition that occurs. In the UV range n-π* and π-π* transitions are observed. The measurements are usually performed by using a standard spectrophotometer.

The measured absorbance A of a sample is directly proportional to the sample concentration c and the path length d. The relationship of these variables is stated in the Beer's Law (2.6), which is valid for dilute solutions and for the absorption of monochromatic radiation.

$$A = log \frac{I_0(\lambda)}{I(\lambda)} = \varepsilon \cdot c \cdot d \qquad (2.6)$$

I_0 and I correspond to the intensities measured before and after the sample at the given wavelength λ. The molar extinction coefficient ε is an intrinsic property of the sample. The linear relationship between the absorption and the concentration of a species makes the UV absorption spectroscopy an important tool in the concentration determination of DNA and peptides.

Peptides containing aromatic amino acids, for example tryptophan and tyrosine, are detected at 280nm, which corresponds to the π-π* transitions of the aromatic side chains.[100] The absorption of different peptides varies strongly depending on the amount of aromatic residues. Non-aromatic peptides can be analyzed by observing the π-π* transition of the

peptide bonds with its absorption maximum at 190nm. A disadvantage is the potential absorbance of the buffer and other components at this wavelength.

The DNA concentration is usually measured by observing the absorption at 260nm. It is often referred to the optical density instead of the absorption. The optical density (OD) value of a sample is defined as the absorption of 1ml sample in a cuevette with 1cm path length at a given wavelength (for DNA 260nm). The concentration of the sample can be calculated by applying Beer's law. The needed extinction coefficient is a unique property of every oligonucleotide sequences due to the increased absorption of purine bases in comparison to pyrimidine bases. The extinction coefficient can be calculated by taking the single extinction coefficient ($\varepsilon_{individual}$) of every base[106] and by considering the nearest neighbor interactions (ε_{NN})[27, 107]. The latter account for the base order and include the base stacking. The extinction coefficient is then given by the expression:

$$\varepsilon_{260} = \sum_1^{n-1}(\varepsilon_{NN}) - \sum_2^{n-1}(\varepsilon_{individual}) \qquad (2.7)$$

For convienience, the DNA concentration is often approximated by assuming a concentration of 37 µg/ml at an OD value of 1 for single stranded DNA or 47 µg/ml for double stranded DNA. A comparison of the nearest neighbor calculations and the approximation can be found in the publication of M.J. Cavaluzzi and P.N. Borer [108].

UV absorption measurements can also be used to monitor the melting profile of DNA[15, 109]. DNA melting refers to the denaturation of double stranded DNA into two single strands. The denaturation involves the overcoming of the base stacking energies and the breaking of the hydrogen bonds. The DNA absorption is increasing with temperature due to the unstacking of the bases. Single stranded (ss)DNA shows an increased absorbance of 40% in comparison to double stranded DNA.[110] This characteristic increase of absorption is also called the hypochromic effect. The plot of the absorption at 260nm versus the temperature is called the UV melting curve. The melting temperature T_m of DNA is defined as the temperature, at which the fraction X_{ds} of double stranded DNA equals the fraction X_{ss} of single strands. The melting temperatures measured in the course of this work were analyzed by using the following approach[110]. Figure 2.18 shows a typical melting profile. The lower $A_L(T)$ and upper $A_U(T)$ limit of the absorption can be fitted by linear regression of the pre- and posttransition region. The fraction X_{ss} of broken base pairs corresponds to:

$$X_{ss} = \frac{A(T) - A_L(T)}{A_U(T) - A_L(T)} \qquad (2.8)$$

This method assumes a two state model. Two strands are either hybridized or they are not. The single strand adopts a random-coil structure in solution. The denaturation is therefore a helix-coil transition. DNA is also being denaturated by the treatment with strong acids or bases. At pH>12 or pH<2 the bases are ionized and the hydrogen bonds are disrupted. Acid treatment leads to the cleavage of the glycosidic band resulting in depyrimidation and depurination.

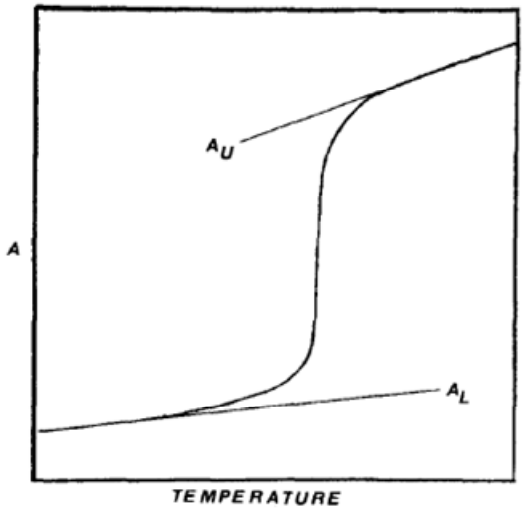

Figure 2.18 A typical melting profil of a short DNA. The absorption measured at 260nm is plotted versus the temperature. The linear functions A_u and A_L indicate the post- and pretransition linear regions.

Since 2005 the so-called DNAMelt web server[111] provides the possibility to simulate the melting behavior in solution of one or two nucleic acids. It calculates the melting temperature as well as the free energy, enthalpy, entropy and the heat capacity of the system. Additionally, the UV absorption profile can be simulated. The prediction for DNA junctions like the earlier discussed four arm junction is not reliable. The determined melting temperatures are much higher than the experimental values, because no structural constrains are taken into account.

2.4.3 High-performance liquid chromatography (HPLC)

The basic principle in chromatography involves the interaction of an analyte, dissolved in a mobile phase, with a stationary phase. Depending on the polarity of the analyte, the used mobile phase and the nature of the stationary phase, the analyte is retarded and elutes at a specific retention time. High-performance liquid chromatography (HPLC)[100] is a separation technique based on liquid column chromatography. The sample is transported in a mobile phase over the stationary phase by applying high pressure. HPLC can be performed in the normal phase mode (NP) with a polar column material and a non-polar

eluent. The separation for this method is based on adsorption. The NP method is not applicable to biomacromolecules due to the non-aqueous eluent. Therefore, the HPLC measurements of biomacromolecules are performed in the reverse-phase mode (RP). In RP-HPLC, a non-polar stationary phase[112], often alkyl modified silica, and a polar, aqueous eluent are utilized. The retention of the analyte depends on its hydrophobicity. The RP-HPLC is an important method for the purification of synthetic oligonucleotides. It is usually employed after the solid phase synthesis in the "DMT-on" mode[113]. The dimethoxytrityl (DMT) protecting group is not cleaved from the oligonucleotide in the last step of the synthesis. Its hydrophobicity is used to separate the desired product from shorter failure sequences, which do not carry the trityl group. RP-HPLC separation yields oligonucleotides with a purity greater than 95%.[114]

The separation of fully deprotected oligonucleotides ("trityl off") is achieved by using ion-pair reversed phase chromatography (IP-RP-HPLC).[115] In this method amphiphilic ions, ion pair (IP) reagents, are added to the mobile phase to increase the retention of the ionic sample. The retention theory in ion pair chromatography can be divided into two categories: the stoichiometric and non-stoichiometric theories[116]. The stoichiometric theories are base on the direct interaction of the IP reagent with the analyte. These theoretical models proposed the formation of a stoichiometric ion-pair complex of the analyte and the ion pair reagent either in the mobile phase (ion-pair model) or at the stationary phase (dynamic ion exchange model). The non-stoichiometric theories suggest the adsorption of the IP reagent at the stationary phase creating an electrostatic surface potential. The analyte interacts with the created electric field. The lack of understanding the retention process completely results in a difficult development of separation conditions for complex analytes.[117] Numerous variables have to be considered. The mobile phase, for example, can be adjusted by varying the ionic strength, the pH, the addition of organic solvent as well as by the type of ion pair and its concentration.

The IP-RP-HPLC method used for this work (Chapter 5.2.4) is based on the work of M.Gilar et al.[115] The described conditions were altered to achieve the separation based on the oligonucleotide end group. All separations were performed with gradient elution and with triethylammonium acetate (TEAA) as ion pair reagent. The complete conditions are described in Chapter 8.3.4.

2.4.4 Dynamic Light Scattering

Light scattering[118, 119] is an important method for the characterization of polymers. Depending on the scattering method, dynamic or static light scattering, different properties are determined. Static light scattering (SLS) gives information on the weight average of the molar mass M_w, the second virial coefficient A_2 and the z-average of the squared radius of gyration $\langle R_g^2 \rangle_z$. Dynamic light scattering (DLS) is used to measure the diffusion coefficient, which allows the determination of the hydrodynamic radius R_H. Both methods are performed with the same instrumental setup. A scheme of a standard single angle light scattering setup is shown in Figure 2.19.

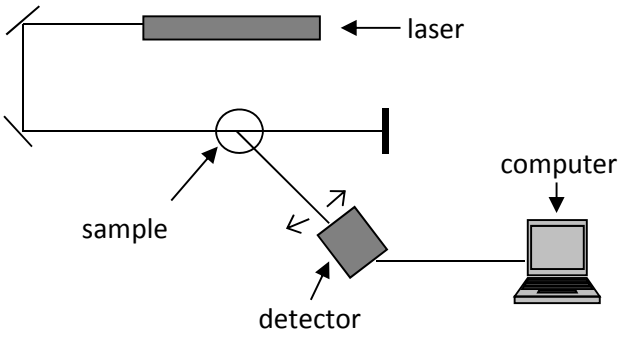

Figure 2.19 Standard single angle light scattering setup. The laser is focused on the sample by optical lenses and mirrors. The scattered light is monitored by the detector (photo multiplier or avalanche photo diode) which is positioned on a goniometer arm. The detected signal is processed and stored on-line.

In this work only dynamic light scattering measurements were used to characterize Elastin-like polypeptides (Chapter 4.4) and ODN-ELP diblock copolymers (Chapter 5.4.5). Therefore a short introduction on the basic DLS theory follows.

Dynamic light scattering (DLS) measurements record the fluctuations in the scattering intensity at a constant angle due to interparticle interference. The fluctuations are caused by Brownian motion of the scattering particles. The measured intensity fluctuations can be described by an intensity-time correlation function $g_2(t)$ (2.9).

$$g_2(q,\tau) = \frac{\langle I(q,t)I(q,t+\tau)\rangle}{\langle I(q,t)\rangle^2} \qquad (2.9)$$

with I(q,t): intensity at time t I(q,t+τ): intensity at time t+τ

This correlation function describes the interaction of two particles at time t=t and at t=t+τ with the correlation time τ. The function $g_2(t)$ decays exponentially with time, because the particles diffuse away from each other and their correlation decreases (Figure 2.20).

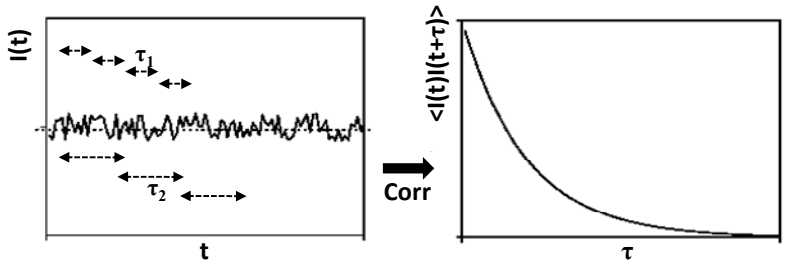

Figure 2.20 Principle of dynamic light scattering[119]. The left-hand picture shows the detected intensity fluctuations. The intensity autocorrelation function is calculated for various correlation times τ and plotted in the right-hand picture.

The diffusion coefficient can be determined by converting the intensity autocorrelation function into the amplitude autocorrelation function $g_1(t)$ (2.10) with the help of the Siegert relation.

$$g_1(q,\tau) = \exp(-Dq^2\tau) = \sqrt{\frac{<I(q,t)I(q,t+\tau)>}{\langle I(q,t)\rangle^2} - 1} \qquad (2.10)$$

The Brownian statistics derive a correlation function, decaying single exponentially, for small monodisperse particles in solution, which corresponds to the amplitude autocorrelation function $g_1(t)$. Hence, the diffusion coefficient can be calculated for monodisperse samples by the simple relationship 2.10. In the case of polydisperse samples a multi exponential decay is usually observed due to their size distribution. The amplitude autocorrelation function has to be analyzed by the cumulant analysis[118] (2.11) to account for the superposition of the single exponential decays of the polydisperse sample.

$$\ln g_1(t) = -\Gamma t + \frac{\mu_2}{2}\Gamma^2 t^2 - \frac{\mu_3}{6}\Gamma^3 t^3 + \cdots \qquad (2.11)$$

with μ_i: i-th cumulant

The first cumulant μ_1 determines the q-dependent, apparent diffusion coefficient $D_{app}(q)$. The second cumulant μ_2 yields information on the polydispersity of the sample. For monodisperse samples μ_2 is smaller than 0.05.

The hydrodynamic radius R_H may be calculated from the diffusion coefficient D_z using the Stokes-Einstein relation:

$$R_H = \frac{kT}{6\pi\eta D_Z} \qquad (2.12)$$

with k: Boltzmann constant T: Temperature η: viscosity

If measurements performed at different angles or temperatures are compared, they have to be normalized in respect to the angle, the temperature and the viscosity, which changes with temperature. The standard $g_1(\tau)$ vs. τ plot results in a $g_1(\tau)$ vs. $\tau \cdot q^2 \cdot \eta^{-1} \cdot T$ plot (Chapter 5.4.5).

The mass M of any particle relates with its radius R depending on its topology corresponding to relationship 2.13

$$M_w \sim R^{\upsilon} \qquad (2.13)$$

The exponent υ is the so-called fractal dimension of the particle. It provides information on the topology of the particles summarized in Table 2.2. It can be determined by plotting the measured R_H versus the molecular mass M_w of the scattering particles in a double logarithmic plot (see Chapter 4.4). The slope of the linear regression yields the fractal dimension υ.

Table 2.2: Topology of a particle related to a certain fractal dimension

topology	υ
ideal coil	1/2
coil in good solvent	3/5
sphere	1/3
disc	1/2
rod	1

The characterization of ELPs and ODN-ELP diblock copolymers by light scattering are discussed in Chapter 4.4 and 5.4.5.

3 DNA four-arm junctions

One of the basic elements for the network formation by DNA self assembly are stable four-arm DNA junctions. The junctions connect the building blocks of the network. The stability of the formed network depends on the stability of these connection points. Therefore a detailed study of the thermal stability is necessary to verify the concept of nano networks by DNA hybridization. Besides the thermodynamic stability, the hybridization of different junction generations has to be tested in parallel to ensure a defined structure formation.

This chapter provides the results of the formation of stable DNA junctions, their hybridization behavior and studies on competing DNA junctions. The experiments concerning the thermal stability were performed in cooperation with Dr. Nils Heimann [120].

3.1 Thermal Stability of the Seeman junction J1

The first reported stable DNA four arm junction was designed by N. Seeman et al. [121]. This junction consists of four individual oligonucleotides with 16 bases each. The strands are partially complementary to form a cross junction with four arms, which consist of eight base pairs each. The geometry of this junction is discussed in Chapter 2.1.5.

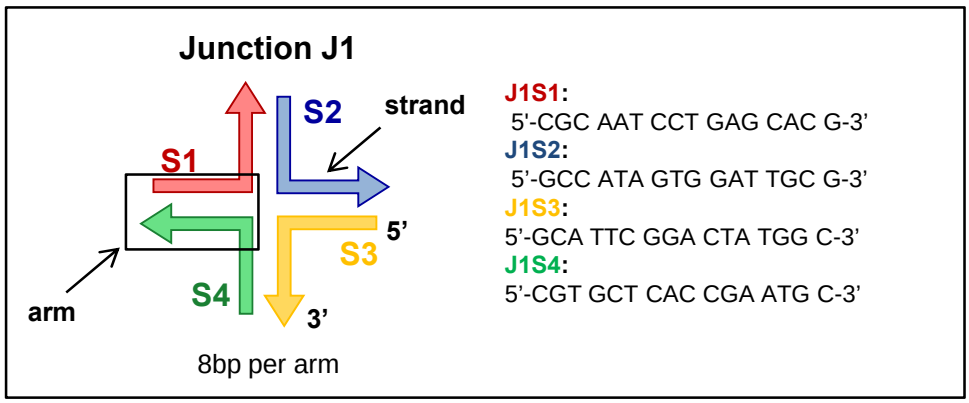

Figure 3.1 Schematic of the four-arm DNA junction J1 with strand sequences J1S1-J1S4 designed by N. Seeman [33]

Important for the use of such four-arm DNA junctions in DNA self assembly is their thermal stability to ensure a formation of stable and defined assemblies. Thus the thermal stability of the Seeman junction J1 was tested at different temperatures. Figure 3.2 shows the native gel electrophoresis of the junction J1 and its equimolar strand combinations performed at 5-6°C.

All gels presented here are vertical gels. The samples were applied at the top of the gel and migrated through the matrix to the anode at the bottom of the gel. Due to the constant charge to mass ratio of DNA the separation is mass dependent. Larger molecules migrate slower than smaller ones. Hence, in a gel picture bands at the bottom correspond to small species and bands closely to the top refere to larger species. Usually a marker was applied on each gel to indicate the DNA size. Lane 1-4 contain the individual strands S1-S4 with 16 bases each. The differences in migration of the single strands result from the different base composition. The following lanes 5-10 display the six possible dimer combinations. For example, lane 5 shows the resulting dimer of S1 and S2. Its electrophoretic mobility is slower than the single strand mobilities. In lane 6 no dimers are formed because here the strands S1 and S3 are mixed which should not assemble. The same result occurs for the combination of S2 and S4 in lane 9. The lanes 13-16 contain the four equimolar trimer combinations. The trimers migrate slower than the dimers but seem to be unstable. The bands in lane 14 and 15 for example are undefined. One possible explanation of this behavior is an unfavourable geometry of the triplet combinations which leads to the degeneration of the trimers. In lane 12 all four strands are combined. A single band slower than the trimers is present. This band corresponds to the tetrameric complex of the strands. The single band indicates the complete hybridization of the four strands. All these observations verify the correct sequence design of the junction and all strand combinations behave as expected. The electrophoretic pattern correponds to the published data by M. Kallenbach et al.[121]

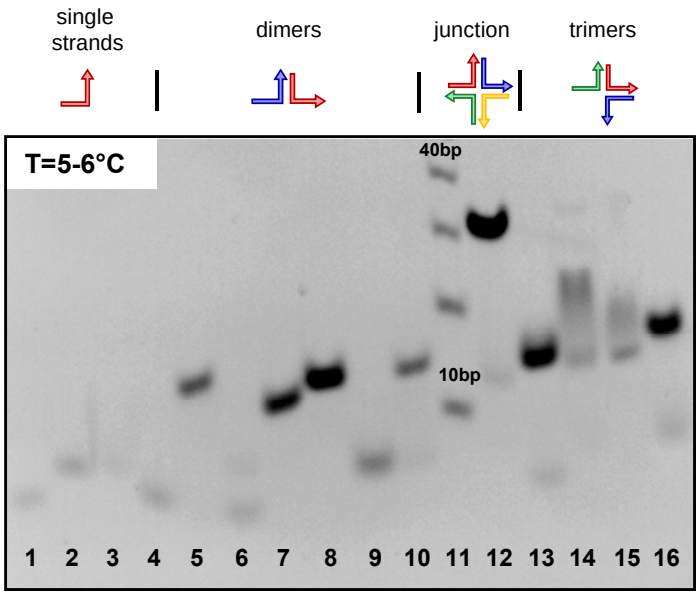

Figure 3.2 Native polyacrylamide gel electrophoresis of oligonucleotide strands of J1 and mixtures. Lane 1-4: strands S1-S4; Lane 5:S1+S2, Lane 6: S1+S3; Lane 7: S1+S4; Lane 8: S2+S3; Lane 9: S2+S4; Lane 10: S3+S4; Lane 11: Marker 10bp; Lane 12: S1+S2+S3+S4 (J1); Lane 13: S1+S2+S3: Lane 14: S1+S2+S4; Lane 15: S1+S3+S4, Lane 16: S2+S3+S4

Figure 3.3 shows the same analysis of the junction performed at elevated temperatures. For these experiments the gel chamber is constantly heated at the indicated temperature. The analyses at 35°C and at 45°C show only the individual strands S1-S4 and the tetrameric mixture. At 25°C the results are comparable to the analysis at 5-6°C. One difference can be seen in the mobility of the trimers. They completely migrate in the range of the dimer combinations. This corresponds to the former observation that the trimers seem to be thermodynamically unstable. They are fully degenerated into dimer combinations and single strands.

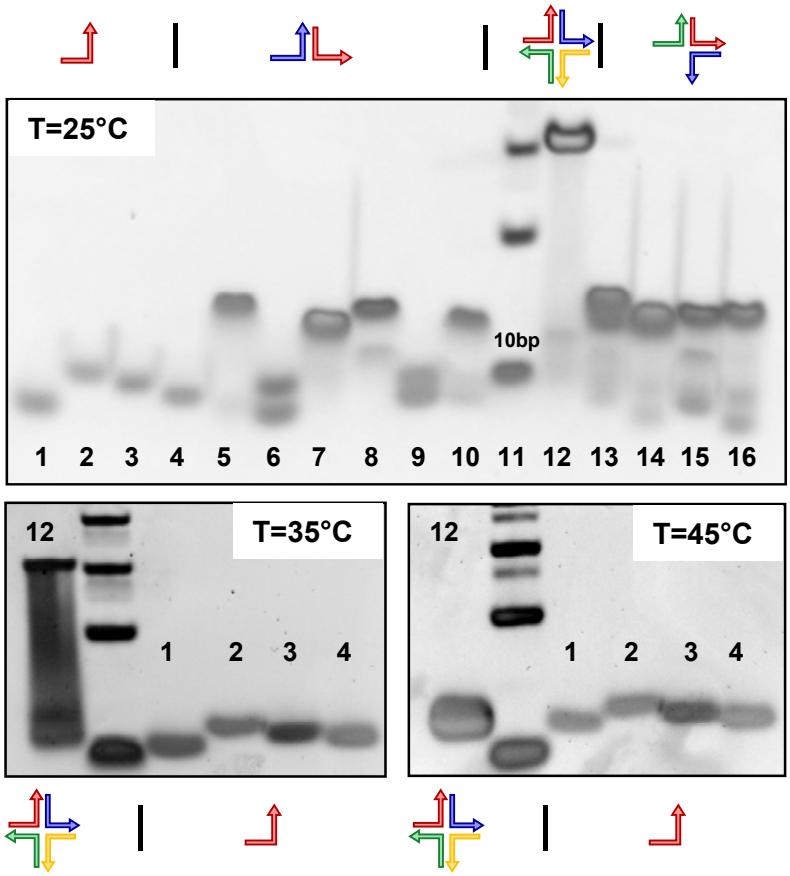

Figure 3.3 Native polyacrylamide gel electrophoresis of oligonucleotide strands of J1 and mixtures performed at different temperatures. Lane 1-4: strands S1-S4; Lane 5:S1+S2, Lane 6: S1+S3; Lane 7: S1+S4; Lane 8: S2+S3; Lane 9: S2+S4; Lane 10: S3+S4; Lane 11: Marker 10bp; Lane 12: S1+S2+S3+S4 (J1); Lane 13: S1+S2+S3: Lane 14: S1+S2+S4; Lane 15:S1+S3+S4, Lane 16: S2+S3+S4

Another difference can be seen in lane 12. Besides the single band for the tetrameric complex a slight background is detected, starting at the mobility of the single strands up to the band of the junction complex. This effect is enhanced at 35°C. It can be explained by the dissociation of the junction into its smaller components during gel electrophoresis: single strands, dimers and trimers. If the degeneration takes place at the beginning of the gel electrophoresis the resulting components, the individual strands, migrate like the single

strands. If the junction dissociates during gel electrophoresis, assemblies with various electrophoretic mobilities are created. The pure single strands are the fastest species. The complete junction has the lowest electrophoretic mobility. The thermal energy at 35°C is insufficient for the complete degeneration of the tetrameric complex. Therefore also dimers, trimers and remaining tetramers are detected. The mixture of these components results in a continuous distribution of the electrophoretic mobility. The junction is completely degenerated into its single strands at 45°C. That corresponds to the reported melting point of the junction J1 in the range of 40°C.[121]

The studies on the thermal stability of the Seeman junction showed that the formation of stable associations at room temperature is not ensured. The degeneration of the junction starts at ambient temperatures. An increased junction stability can be achieved by the increase of base pairs per arm. The following section provides the observation on a newly-designed junction with 23 base pairs per arm.

3.2 Four-arm DNA junction K4 with 23bp per arm

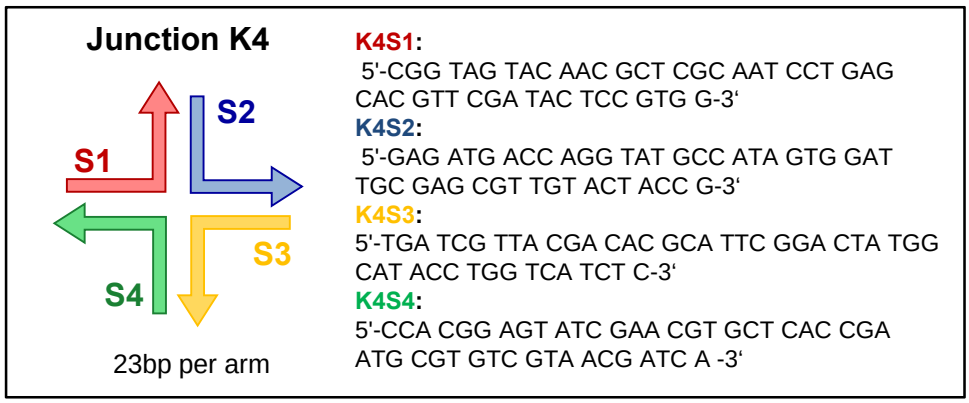

Figure 3.4 Schematic of the four-arm DNA junction K4 with the designed strand sequences

For stable DNA self assembly a junction with increased thermal stability is necessary. Therefore based on Prof. Seeman's work a new junction with increased arm length was designed. The junction core corresponds to the junction J1. The arm length is increased to 23bp per arm by the described designing rules in Chapter 2.1.4. Longer arms provide an enhanced stability by additional hydrogen bonding and base stacking. For example an oligonucleotide of 12 bases shows a melting temperature in the range of 34°C depending on base, sequence buffer and salt concentration. When the length of the oligonucleotide is doubled to 24 bases the melting temperature increases to approx. 55°C.

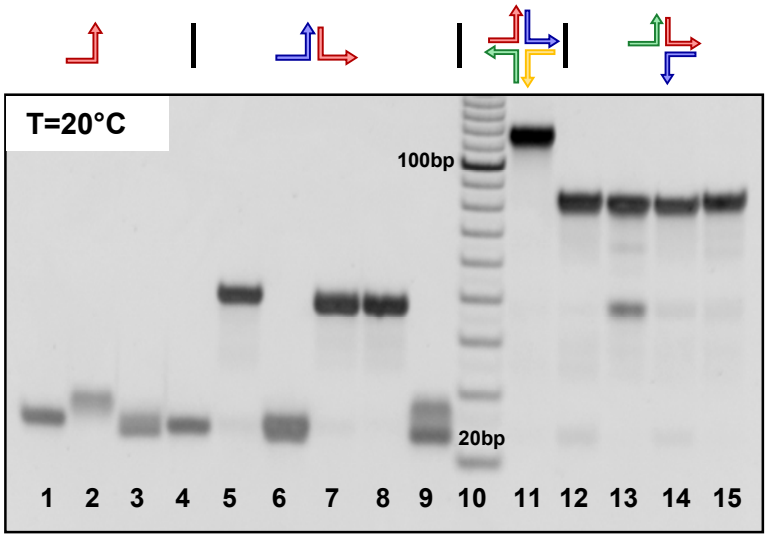

Figure 3.5 Native polyacrylamide gel electrophoresis of oligonucleotide strands of K4 and mixtures performed at T=20°C. Lane 1-4: strands S1-S4; Lane 5: S1+S2, Lane 6: S1+S3; Lane 7: S1+S4; Lane 8: S2+S3; Lane 9: S2+S4; Lane 10: Marker 10bp; Lane 11: S1+S2+S3+S4 (K4); Lane 12: S1+S2+S3: Lane 13: S1+S2+S4; Lane 14: S1+S3+S4, Lane 15: S2+S3+S4; (dimer combination S2+S3 has been omitted).

Figure 3.5 shows the native gel electrophoresis of the newly designed junction K4 performed at 20°C. The electrophoretic mobility of junction K4 shows the same pattern as detected for the junction J1. Most important is that no degeneration of the junction occurs. It has to be highlighted that for this junction with 23bp per arm the trimer combinations are also stable at ambient conditions. They migrate slower than the dimer combinations. The junctions K4 in lane 11 travel as a single band in the range of 120bp. The electrophoretic mobility is a function of size, shape and base pairing. If only the number of base pairs is taken into account, a migration of the junction in the range of 92bp is expected. Therefore the geometry decreases the mobility of the junction in the gel. This effect is also valid for the trimers. They migrate with the speed of 80bp instead of the expected 69bp. The dimers are traveling in the estimated range of 46bp. It has to be noted that the single strands K4S1-K4S4 with 46 bases migrate as fast as 23 base pairs (two bases = one base pair).

The junction K4 has a melting temperature of T_m=67°C determined by temperature depending UV absorption measurements (Figure 3.6) (see Chapter 2.4.4). They confirm the increased thermal stability compared to the junction J1 with a melting temperature of T_m=40°C.

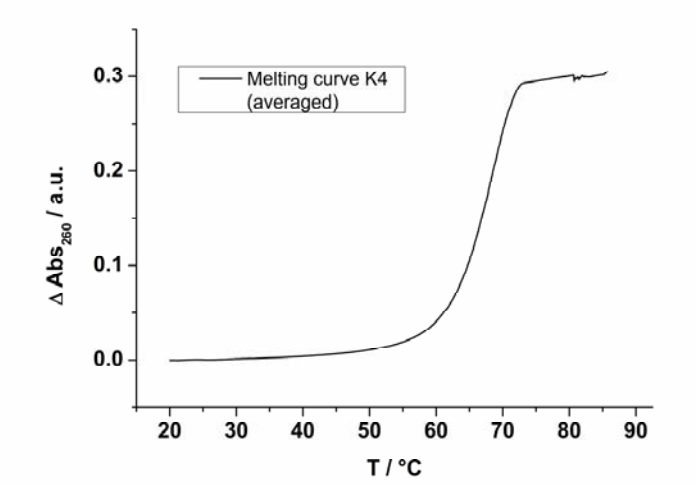

Figure 3.6 Averaged thermal transition profile of an equimolar mixture of the strands of K4 measured at 260nm. The measurement was performed twice in 1mM $MgCl_2$ solution. The results were baseline corrected and averaged.

The thermal stability of the four-arm DNA junction is one key element for the self-assembly, but it is also important to see how dangling ends influence the hybridization of the junction. Dangling ends are a model for the later modification of the oligonucleotide with the polypeptide. Is this additional element decreasing or increasing the stability of the junction? Does it have an influence on the hybridization efficiency? Those questions are answered in the following section.

3.2.1 Effect of dangling ends on the hybridization efficiency

A simple approach to the question how dangling ends might influence the hybridization, is the modification of the junction K4 with a single stranded DNA sequence, which is non-complementary to the junction itself, at all four arms. This junction is named K3. The strands of this junction consist of the 46 bases that form the DNA junction, and additionally 23 bases with the same sequence at the 5'end of each strand. The sequence of the 23 bases was designed to be non-complementary to the junction sequences. Junction K3 shows a similar behavior in the native gel electrophoresis as the junction K4 as well as a comparable thermal stability. Its melting temperature is slightly decreased to T_m= 65°C (see Appendix 9.1.1). The additional dangling ends seem to have no further effect on the hybridization efficiency. This conclusion was verified by additional native gel electrophoresis of all possible tetrameric and one trimeric mixture of K3 and K4 sequences varying the numbers of dangling ends. The results are presented in Figure 3.8.

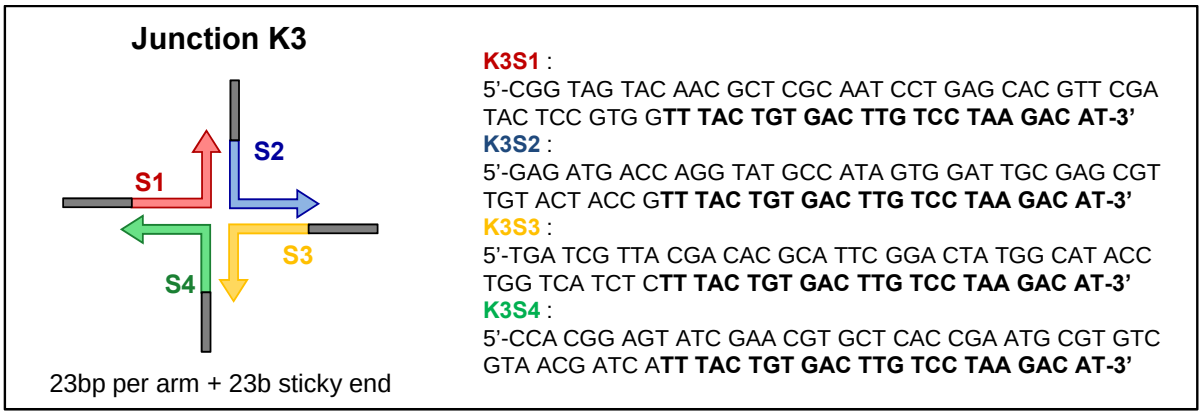

Figure 3.7 Schematic of the four-arm DNA junction K3 with dangling ends and its strand sequences.

Lane 1 of Figure 3.8A contains the K3 junction with four dangling ends. Lane 2-5 contain junction K3 with one sequence substituted by the corresponding sequence of K4. For example lane 2 contains the mixture of the sequences K3S1, K3S2, K3S3 and K4S4. In lane 6-10 two sequences of K3 were replaced. These complexes represent a four-arm DNA junction with two dangling ends. The lanes 10-13 show the migration behavior of junctions with one dangling end. Lane 14 contains the junction K4 with no dangling ends. The addition of dangling ends decreases the electrophoretic migration as expected. Nevertheless it makes no difference if the dangling ends are attached at the neighboring strands or at opposite ones.

In Figure 3.8B the stability of trimers with varying number of dangling ends was tested. Lane 2 shows the mixture of K4S1, K4S2 and K4S3. In lane 3-5 each one of the K4 strands was substituted by the corresponding strand of K3. This resulted in trimers with one

dangling end. For lane 6-8 a second strand of K4 was replaced to yield trimers with two dangling ends. Finally, the trimer with three dangling ends is shown in lane 9. All analyzed trimers are stable at the given temperature of T=20°C. The migration time decreases with the addition of dangling ends comparable to the results for the tetramers shown in Fig 3.8A.

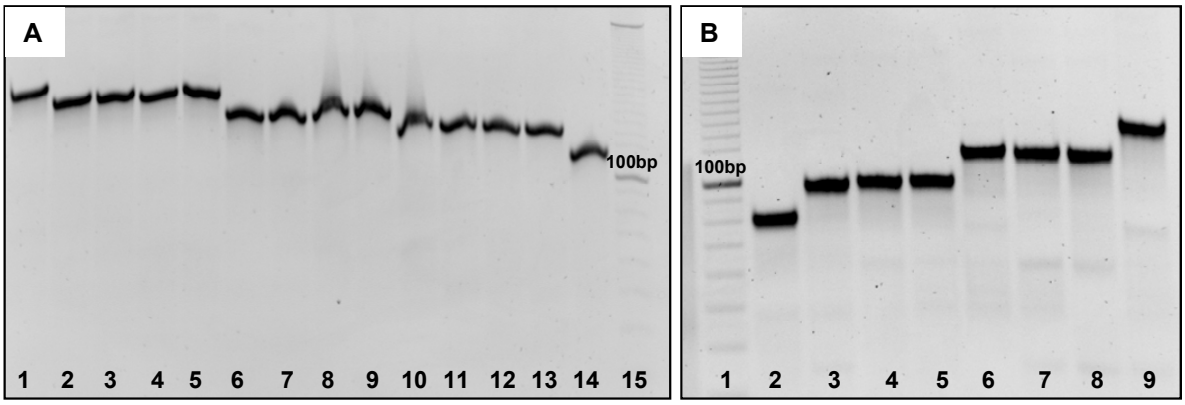

Figure 3.8 Native polyacrylamide gel electrophoresis of oligonucleotide strands of K4,K3 and their mixtures performed at T=20°C. A) tetrameric complexes; Lane 1: K3, four dangling ends; Lane 2-5: three dangling ends, Lane 6-9: two dangling ends; Lane 10-13: one dangling end; Lane 14: K4, no dangling ends; Lane 15: 10bp marker; B) trimeric complexes; Lane 1: K4 trimer, no dangling end; Lane3-5: one dangling end; Lane6-8: two dangling ends; Lane 9: K3 trimer, three dangling ends.

3.2.2 Rehybridization efficiency

An important aspect for the formation of nanostructures by self-assembly is the rehybridization efficiency. As reported by N. Heimann [120] a decrease of the hybridization efficiency was detected after isolation and rehybridization of a PCR dimer. The PCR dimer was constructed by synthesizing two polymerase chain reaction (PCR) products each of 600bp carrying complementary sticky ends of 23 bases. These two PCR products were hybridized, extracted and rehybridized. The junction K3 and K4 were treated in the same manner. First, the junctions were hybridized (Figure 3.9A) and isolated by gel extraction. This procedure includes the complete denaturation of the samples. Afterwards, the isolated products were rehybridized (Figure 3.9B). Lane 3 and 4 in Fig 3.9B show the hybridization performed by a temperature controlled program Hyb90 (see Chapter 8.1.3). Lane 1 and 2 contain the same samples left at room temperature without further treating. The gel analysis shows that the hybridization is quantitative in all cases. No smaller fragments of the junction were detected after rehybridization. It can be concluded that the tetrameric complexes fully rehybridized in contrast to the hybridization of linear PCR products with sticky ends, which only reassemble with a yield of 70%.[120]

The comparison of the different hybridization techniques, room temperature versus temperature controlled program, Figure 3.9B shows that the controlled heating and cooling

procedure is more specific. In the case of the room temperature hybridization, lane 1 and 2, additional bands with a lower electrophoretic mobility are detected. The lower mobility corresponds to a higher molecular weight species, which could be aggregates of the junctions. The room temperature samples were mixed and not denaturated prior to hybridization. Therefore, aggregates formed by unspecific self-assembly can exist. These unspecific interactions are destroyed by applying the temperature program which heats the samples first to T=90°C for 5min. The sample is steadily cooled down to room temperature over a time interval of 2h after the denaturation. This ensures a specific formation of the thermodynamically most favorable structure.

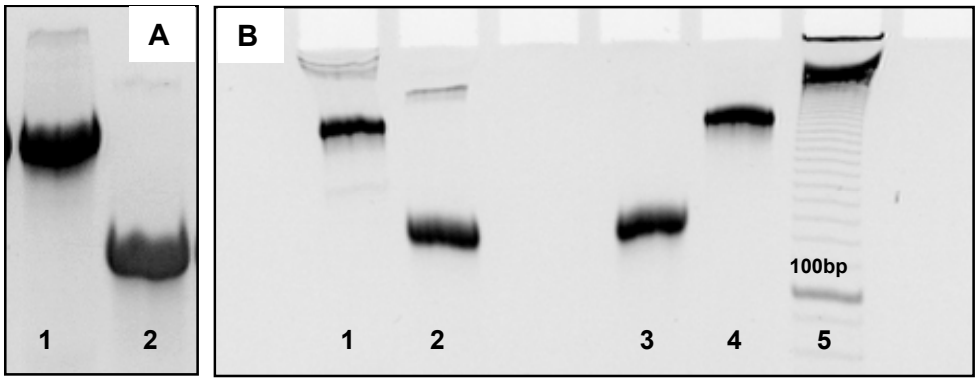

Figure 3.9 Native polyacrylamide gel electrophoresis of tetrameric complexes of K4 and K3 mixtures performed at T=20°C. A) before extraction; Lane 1: K3; Lane 2: K4 B) after extraction; Lane 1: K3 rehybridized at RT, Lane 2: K4 rehybridized at RT; Lane 3: K4 rehybridized with Hyb90, Lane 4: K3 rehybridized with Hyb90.

3.2.3 Effect of hybridization procedure

The observed influences of the hybridization procedure led to a more detailed study. In Figure 3.10 the results for the hybridization of junction K3 and K4 under various conditions are presented. All samples were mixed and incubated at RT for different time periods. Lane 1 and 8 show the junctions K4 and K3 respectively, hybridized over night for 18h. For the samples in lane 2 and 7 the hybridization time was increased to 26h and for lane 3 and 6 to 4 ½ days. Lane 5 and 4 contain samples of K4 and K3 treated with the standard temperature controlled program Hyb90. In all cases, no major differences were detected. Junction K4 showed quantitative hybridization for all four procedures. Therefore, the hybridization procedure seems to have no influence on the hybridization efficiency of the junction K4. For junction K3 small amounts of remaining single strands, dimers and trimers are found. The amount of trimer is less for the temperature controlled program than for the hybridizations at room temperature. One can argue here that the temperature program yields the highest specificity in junction formation due to the complete denaturation at the beginning of the hybridization procedure. This denaturation ensures the complete destruction of any

unspecific secondary structure formations. The observed single stands, dimers and trimers might also result from a non-equimolar mixture of the strands. The four samples were pipetted independently. The amounts that are used of each strand are less than 10µl. The error in pipetting in this volume range is not negligible. Hence, a defined dependence of the hybridization failur on the hybridization procedure can not be given due to the possible error in pipetting and/or error in UV concentration determination.

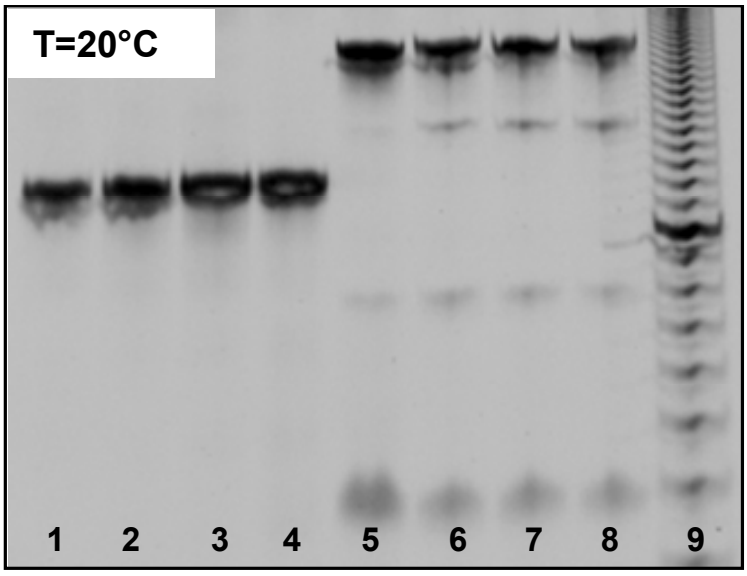

Figure 3.10 Native polyacrylamide gel electrophoresis of junctions K3 and K4 hybridized under different conditions. Lane 1:K4 hyb over night; Lane 2: K4 hyb for 26h; Lane 3: K4 hyb for 4 ½ days; Lane4: K4 hyb for 2h10min (Hyb90 program) Lane 5: K3 hyb for 2h10min (Hyb90 program); Lane 6: K3 hyb for 4 ½ days; Lane 7: K3 hyb for26h; Lane 8: K3 hyb over night; Lane 9: 10bp marker.

The previous chapters investigated the formation of four-arm DNA junctions differing in arm length, their thermal stability and their hybridization procedures. The next section deals with the formation of a four-arm junction build up by oligonucleotides of 46 bases as well, but designed to form independently in the presence of the former discussed junction K4.

3.3 2nd Generation junction K5

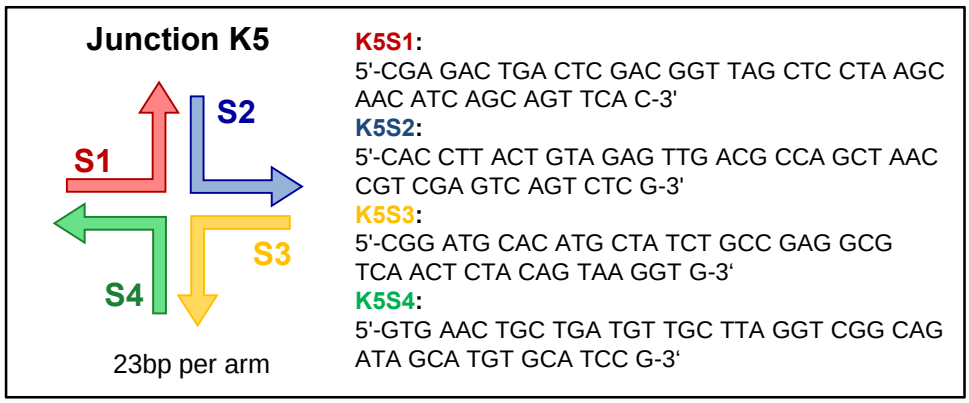

Figure 3.11 Schematic of the second generation four-arm DNA junction K5 and its strand sequences.

For the formation of DNA network structures at least two junction generations have to be designed (see Chapter 1). The junction sequences have to be unique. The strands of the first junctions are not allowed to interfere with the second junction strands to ensure defined structure formation. Therefore, a second and a third oligonucleotide four-arm junction, named K5 and K6, with 23bp per arm were designed. Junction K5 shows comparable thermal stability and the same hybridization pattern as junction K4.

The specific hybridization was tested by mixing the eight strands of junction K4 and K5 pair wise, resulting in 16 possible combinations. If no interference occurs between the strands of the different junctions, the native gel analysis shows simply single strands. Fig 3.12 shows the resulting native gel electrophoresis performed at 20°C. The single strands in lane 18 to 25 all show similar electrophoretic mobilities. One exception is strand K4S2 (lane 24) with a retarded mobility compared to the other single strands. This retardation was already observed in the junction hybridization K4 in Figure 3.5. It is sequence specific. The dimer combinations of one strand of K4 and one strand of K5 in Lane 2-17 show the same electrophoretic mobility as the single strands except the combination of K4S3 and K5S3 in lane 7. Here a blurry band, which starts at the electrophoretic mobility of a dimer and stretches up to the mobility of a single strand, is detected. These two strands interfere with each other in an undefined manner. If a stable dimer was formed, a single band at around 46bp would appear. The smearing of the band refers to a minor interaction of the two strands. However, this interaction can have an influence on the junction formation.

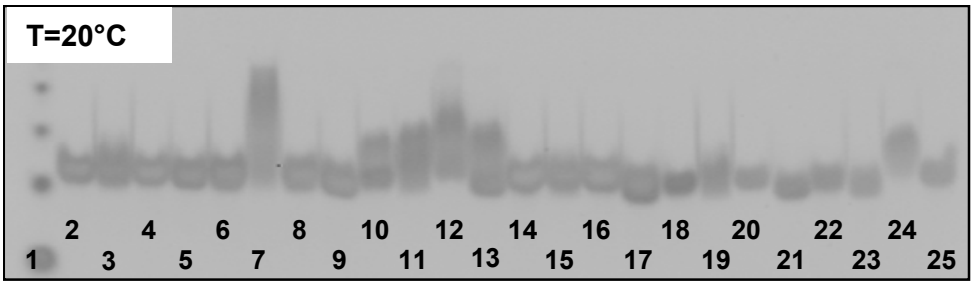

Figure 3.12 Native polyacrylamide gel electrophoresis of oligonucleotide strands of K4 and K5 and their dimer mixtures performed at T=20°C. Lane 1: 10bp marker; Lane 2-17: dimer mixtures; Lane 18-25: single strands.

Therefore, the junction hybridization of K4 and K5 was tested in the presence of the single strands of the competing junction. Lane 5 and 6 in Fig 3.13 show the junctions K4 respectively K5 on their own. In Lane 1-4 one of the four strands of K5 was mixed with the four strands of K4. The junction K4 hybridized completely in all four cases as shown by a single band. The intensity of the junction bands is comparable with the junction K4 hybridized on its own. The bands with higher electrophoretic mobility represent the added junction strands of K5. Also strand K5S3, which showed interactions with the Strand K4S3, has no effect on the efficient hybridization of K4. A destabilization or interference would be shown by an undefined junction band. The same result is obtained for the hybridization of K5 in presence of single strands of K4 (Lane 7-10 in Fig 3.13). The stability of the junction K5 is unaffected by the competing strands of K4.

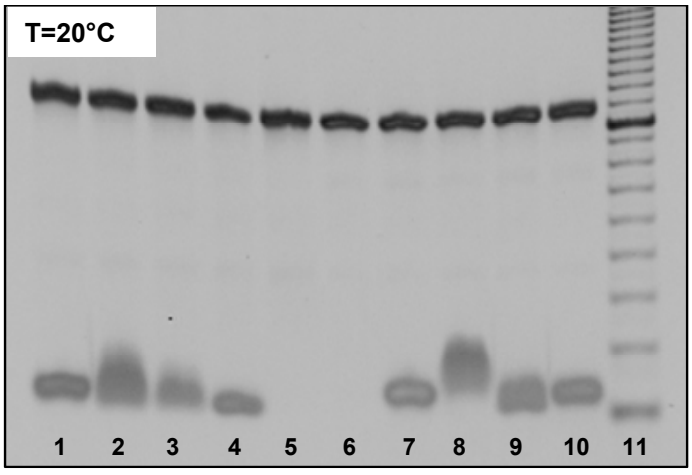

Figure 3.13 Native polyacrylamide gel electrophoresis of oligonucleotide strands of K4 and K5 performed at T=20°C. Lane 1: K4+K5S4; Lane 2: K4+K5S3; Lane 3: K4+K5S2; Lane 4: K4+K5S1; Lane 5: K4; Lane 6:K5; Lane 7: K5+K4S1; Lane 8: K5+K4S2; Lane 9: K5+K4S3; Lane 10: K5+K4S4; Lane 11: 10bp marker.

The discussed hybridization experiment showed that the minor interaction between the strand K4S3 and K5S3 is negligible and the two junctions can hybridize independently in presence of each other.

3.4 3rd Generation junction K6

In addition to the second generation junction K5, a third junction, named K6, was designed. According to the strand design described in Chapter 2.1.5, all three junction sequences were compared. Some of the designing rules had to be altered, because with the increasing amount of base pairs the criton length N_c (series of overlapping sequences) had to be increased from $N_c<5$ to $N_c<6$ (see Chapter 2.1.4). The criton length is the maximum length of a base sequence that can be repeated with the same sequence in all strands.

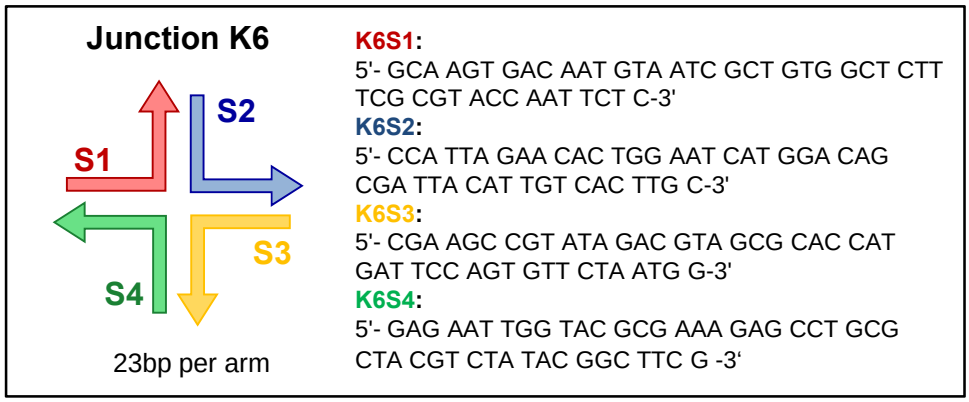

Figure 3.14 Schematic of the third generation four-arm DNA junction K6 and its strand sequences

Figure 3.15 shows the hybridization pattern of the new junction K6. It is similar to the patterns of junction K4 and K5 except for the single strand K6S2 in lane 2. Instead of one band in the range of 23bp a second band appears at the size of a dimer. This strand forms a homodimer. This observation has no effect on the complete hybridization of the junction in combination with all strands, but the homodimer formation inhibits a correct concentration determination. The absorption coefficient for single stranded DNA is higher than the one for double stranded DNA (Chapter 2.4.2). The concentration of a mixture of single stranded and dsDNA, as it exists with the homodimer, cannot be measured accurately. However, it is necessary to mix the strands equimolar to create tetramers with no impurities of trimers, dimers or single strands. This is not ensured for the formation of K6 with the designed sequence K6S2. Therefore, the junction K6 has to be redesigned. This work is in progress. After the verification of the complete hybridization of K6, the competing hybridizations of K4 and K5 are going to be tested.

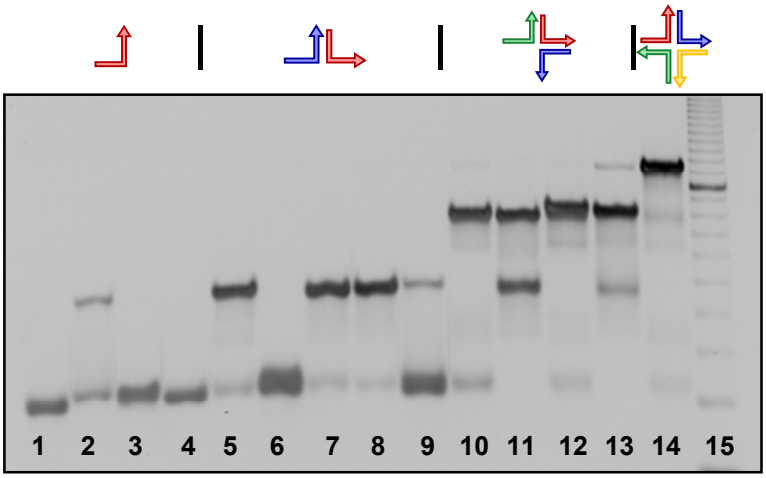

Figure 3.15 Native polyacrylamide gel electrophoresis of oligonucleotide strands of K6 and mixtures performed at T=20°C. Lane 1-4: strands S1-S4; Lane 5: S1+S2, Lane 6: S1+S3; Lane 7: S1+S4; Lane 8: S2+S3; Lane 9: S2+S4; Lane 10: S1+S2+S3; Lane 11: S1+S3+S4; Lane 12: S1+S2+S4; Lane 13: S2+S3+S4; Lane 14: S1+S2+S3+S4 (K6), Lane 15: Marker 10bp; The dimer combination S3+S4 has been omitted.

3.5 Summary

The study of the thermal stability of the junction J1 with eight base pairs per arm shows an insufficient thermal stability. Hence, the junction arms were increased to a length of 23base pairs per arm to yield a stable DNA four-arm junction at room temperature. This junction exhibits quantitative rehybridization. The addition of dangling ends with 23 bases to all four strands has no major influence on the thermodynamic stability or the hybridization efficiency of this junction. Furthermore, the hybridization in parallel of two junctions, K4 and K5, shows a specific hybridization of each junction itself. No interfering interactions between the junction sequences are detectable.

4 Hydrophobic cysteine functionalized ELPs

In the following chapter the synthesis and characterization of new Elastin-like polypeptide (ELP) libraries is described. The properties of the new libraries were chosen to be suitable for further conjugation of the polypeptides with oligonucleotides. The polypeptides were designed to carry chemically reactive groups at each chain end. At the N-terminus the free amino group is able to react under various reaction conditions, for example with activated esters. At the C-terminus of the polypeptide one cysteine residue was incorporated in the terminating sequence to perform thiol conjugation reactions. The repeating amino acid sequence carries only non-reactive hydrophobic amino acids to prevent any side conjugation. The known ELP library E4 with valine as guest residue was modified with the single cysteine residue in the terminating sequence. Additionally, a new library E26 with alanine as guest residue is going to be discussed. The polypeptide sequences are shown in Fig. 4.1.

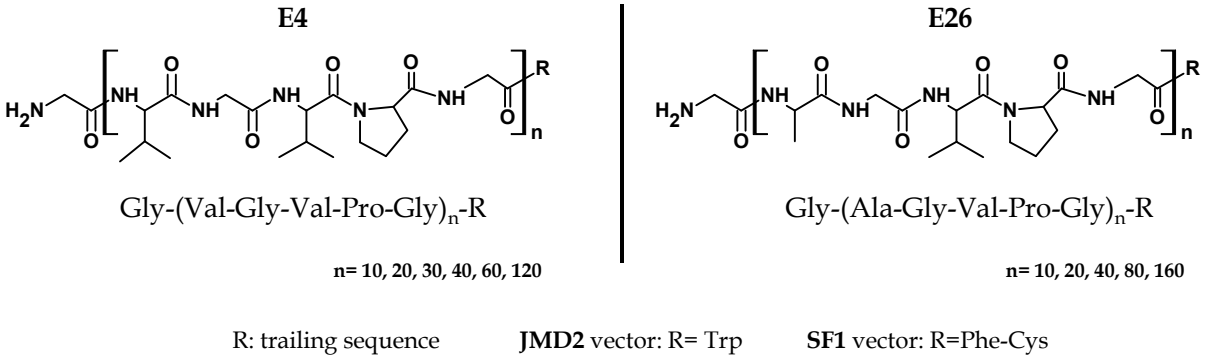

Figure 4.1 Amino acid sequences of the ELP libraries E4 and E26 with vector dependent trailing sequences.

The genetic engineering and the polypeptide expression were performed in the laboratory of Prof. A. Chilkoti at Duke University, North Carolina under the supervision of J.A. MacKay (currently Assistant Professor at the USC School of Pharmacy) and J. McDaniel (PhD student, Prof. Chilkoti).

4.1 Genetic engineering

Monodisperse ELPs are produced by genetic recombination. The detailed procedure of molecular cloning for ELPs is described in Chapter 2.3. For this work two different vectors were used for the gene oligomerization of the desired ELPs. Both vectors are based on the

pET24a(+) T7 *lac* expression vector (Appendix 1.3.3). The vector JMD2 simply encodes a tryptophan as termination codon for the polypeptide. The SF1 vector carries no leading amino acids. The trailing sequence is designed to produce a cysteine-phenylalanine termination of each polypeptide at its C-Terminus. The new SF1 vector was constructed by annealing complementary, chemically synthesized oligonucleotides SF1r and SF1f and then ligating those into a pET24(+) plasmid. The oligonucleotides encode the leading and terminating sequences of the desired polypeptides. Both vectors described can as well be used as expression vectors.

The SF1 vector could not be employed in the new RDL method (Chapter 2.2.2), because the position of the recognition site of RE2 only allows one amino acid codon for the terminating sequence. In SF1 the trailing sequence encodes a phenylalanine and a cysteine. Therefore the clones of E26 were synthesized by using the vector JMD2. The oligomers of 40, 80 and 160 peptide repeat units were produced. The clones for 10, 20 and 40 repeat units had already been synthesized by Jonathan McDaniel. The 10-mer and the 40-mer of E26 were transferred into the SF1 vector.

Table 4.1 Restriction enzymes and their cutting sites for the SF1 and JMD2 vector

enzym	**cutting site**
BseRI	5'…..GAGGAG(N)$_{10}$…..3' 3'…..CTCCTC(N)$_8$….. 5'
AcuI	5'…..CTGAAG(N)$_{16}$…..3' 3'…..GACTTC(N)$_{14}$…..5'
BglI	5'…..GCCNNNNNGGC…..3' 3'…..CGGNNNNNCCG…..5'
XbaI	5'…..TCTAGA…..3' 3'…..AGATCT…..5'
BamHI	5'…..GGATCC…..3' 3'…..CCTAGG…..5'

Table 4.1 gives an overview of the important restriction sites of the vectors. For the RDL method the cutting sites BseRI (RE1) and AcuI (RE2) were used. The vector was designed to give GG/CC sticky ends after digestion for both enzymes. The JMD2 vector was prepared to be used in the new RDL method with the third restriction enzyme BglI (RE3). After cutting the plasmid an insert, which encoded the desired peptide sequence, was ligated into the

plasmid. The ligation is catalyzed by ligases, which seal breaks in the phosphate sugar backbone of the DNA.

After each ligation step a digestion with the enzymes Xba1 and BamH1 was performed to isolate the new plasmid insert, which encodes the peptide sequence. The isolated inserts were first subject to agarose gel electrophoresis to confirm the correct length. Second, an automated DNA sequencing analysis was performed to determine the DNA sequence.

The different ELPs synthesized are distinguished using the notation EX-Y. The number X specifies the encoded guest residue Xaa. The E26 library encodes an ELP library with alanine as guest residue. The guest residue of the E4 library is valine. The Y represents the number of Val-Pro-Gly-Xaa-Gly repeat units. For example, E4-40 is an ELP of 40 pentapeptide repeat units (corresponding to 200 amino acids) carrying the guest residue valine. The E26 library was already synthesized up to inserts of 40 repeat units. The clones encoding 80 and 160 repeat units were synthesized by the new RDL method described in Chapter 2.2.2 in the JMD2 vector. The inserts produced in this vector were transferred into the SF1 vector, which encodes the terminating sequence of phenylalanine and cysteine.

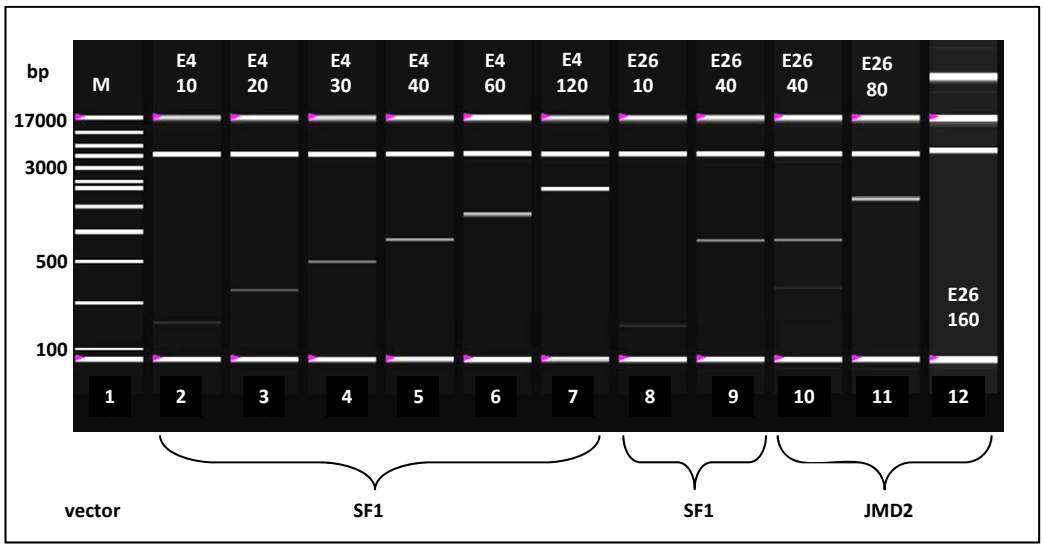

Figure 4.2 Automated gel electrophoresis (Experion, Bio-Rad) of the diagnostic digests of the produced E4 and E26 libraries.

Figure 4.2 displays the produced gene libraries of E4 and E26. The analysis was performed by isolating the plasmid insert by a diagnostic digest. The inserts were subject to an automated gel electrophoresis analysis. The genes differ only in the number of repeat units. The corresponding number of repeat units is labelled above each lane. All ELP-4 shown are based on the SF1 vector. The lane on the left shows the DNA ladder with indicated base pair

sizes. Each sample contains a small DNA fragment, lowest band, which marks the lower exclusion limit for the automated system. The upper bright band corresponds to the upper exclusion limit. The lanes 2-7 correspond to the E4 gene library in the SF1 vector. The gene library for the E26 is shown on the right hand side. Lane 10-12 contain the inserts of the JMD2 vector with 40, 80 and 160 repeats. In lane 8 and 9 the inserts of E26-10 and E26-40, which were transferred into the SF1 vector, are analyzed. All inserts exhibit the expected size compared to the marker except the insert for E26-160. The insert size can be calculated by multiplying the repeat units of the amino acid sequence by five, because every repeat unit contains five amino acids. This gives the number of amino acids encoded by the insert. Additionally, the calculated number has to be multiplied by three, because each amino acid is encoded by three nucleotides. The insert for E4-40 for example has a size in the range of 600bp. In lane 12 the insert for the E26-160 shows a lower electrophoretic mobility than expected. The same sample showed in the regular agarose gel electrophoresis the expected size. This discrepancy was not investigated further because studies on the expression of the E26 (JMD2) showed low yield peptide expression (see Chapter 3.2.2). The insert for E26-40 in the JMD2 vector (lane 10 in Fig. 4.2) shows a shallow band in the range of an insert of 30 repeat units. The mixture of two inserts occurs, if two cell colonies containing plasmids with different inserts grow close-by. This mixture of plasmids cannot be used further for the polypeptide expression. It would yield a mixture of polypeptides differing in length.

The genes with 10, 20 and 40 encoded repeat units of E26 were already synthesized with the JMD2 vector by Jonathan McDaniel. Only the inserts encoding 10 and 40 repeat units were successfully transferred into the SF1 vector. Additionally to the automated gel analysis an automated sequencing analysis was performed to ensure the correct base sequence. All samples shown in Figure 3.1 encoded the desired amino acid sequence.

4.2 Polypeptide Expression

For the expression of the polypeptide, the produced plasmids were transferred into BLR(DE3) expression cells. DE3 strains carry the RNA polymerase gene of the T7 phage, which is controlled by the *lac* promoter. This promoter is activated by isopropyl-1-thio-β-D-galactopyranoside (IPTG), but the overexpression of most ELPs doesn't require the addition of IPTG. In some cases the addition can increase the overall yield. No IPTG was used in the protein expressions reported here.

The overexpression of polypeptides can be monitored by SDS polyacrylamide gel electrophoresis (SDS-PAGE). The following sections show the characterization of the synthesized ELPs by SDS-PAGE. In all cases gradient gels were used to provide a wider range of molecular weight resolution.

The E26 gene library was first synthesized in the JMD2 vector. The produced clones were transformed into BLR expression cells and test cultures were made. Figure 4.3 shows the analysis of the supernatant after cell lysis and a first centrifugation step. Lane 1 contains a peptide standard marker which is labelled in kilodaltons. On the right hand side samples of the E26 cultures of 40-, 60- and 120mers in the JMD2 vector are presented. In comparison to that lane 2-4 show the later produced E4 polypeptides in different lengths (E4-60, E4-120). These lanes show a large band in the region of the overexpressed peptide. The E26 samples do not show any overexpressed peptide bands. A reason for the poor expression is so far unknown. Other experiments showed that the expression yield depends on the amino acid sequence of the ELP. For example, ELPs containing phenylalanine in their repeat unit are poorly or not expressed. One possibility to enhance the overexpression is the addition of IPTG, which stimulates the lac promoter to produce more mRNA, but this work was focused on the successful synthesis of the E4 library.

The expressed polypeptides were purified by inverse transition cycling (ITC) (see Chapter 2.2.2). This process involves the repeated aggregation of the polypeptide by heating and/or NaCl salt addition. After each precipitation the mixture is centrifuged at T=40°C (hot spin) to remove any soluble contaminants of the cell lysate. The resulting peptide pellet is resolubilized in cold buffer and centrifuged at T=4°C (cold spin) to remove any remaining insoluble matter. To obtain highly pure polypeptide the inverse transition cycling is repeated until no impurities are detected by SDS-PAGE (at least five times and up to seven times).

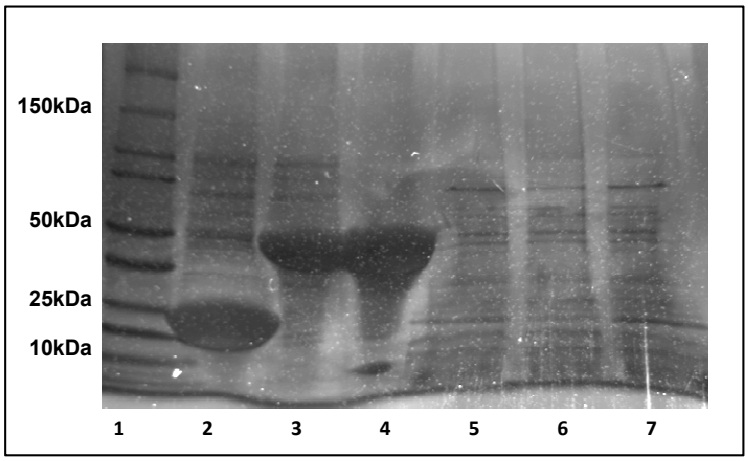

Figure 4.3 Gradient 4-20% SDS-PAGE Gel of the first supernatant of E26-40, E26-80 and E26-120 (JMD2 vector, lane 5-7) after cell lysis and centrifugation. Lane 1: commercially available peptide marker; Lane 2: E4-60 after the second cold spin; Lane 3 and 4: unpurified samples of E4-120 (two batches)

Figure 4.3 illustrates the ITC process. In Lane 2 of Fig 4.3 a sample of E4-60 (M_w=26.9kDa) after the second cold spin is shown. This sample still contains cell contaminants of higher molecular weights (fine bands above the thick ELP band). Lane 3 contains a sample of E4-120 (M_w=49.1kDa) which has been purified by five transition cycles. This sample already shows fewer contaminants. After two additional cycles the polypeptide has no higher molecular weight impurities as shown in Lane 4.

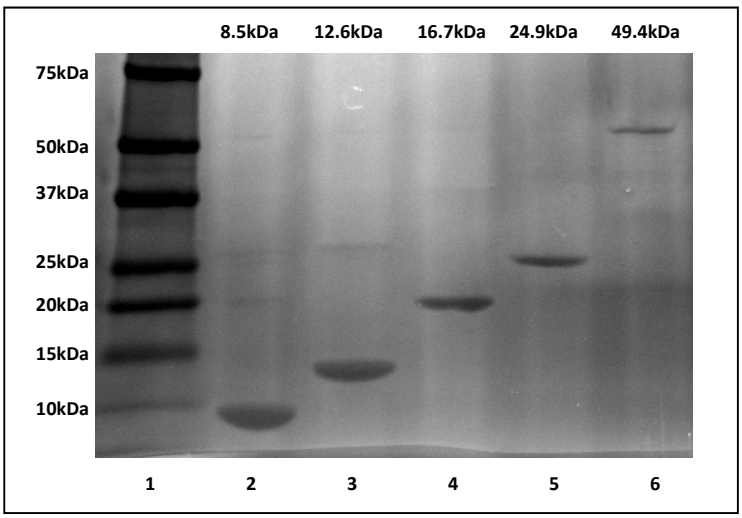

Figure 4.4 Gradient 4-20% SDS-PAGE Gel of the purified E4-library under reducing conditions. Lane 1: peptide marker; Lane 2: E4-20, Lane 3: E3-40; Lane 4: E4-40; Lane 5: E4-60, Lane 6: E4-120

Figure 4.4 shows the SDS-PAGE gradient gel of the purified E4 library. The left lane contains a peptide standard ladder which is labelled in kilodaltons. The expected molecular weight of each ELP is indicated on the top of the corresponding lane. Especially the larger ELPs migrate slower than expected. This trend has already been observed in former studies [63].

To verify the existence of the cysteine residue in each peptide the SDS-PAGE was performed without adding reducing agent to the loading buffer. The result is shown in Figure 4.5. Each polypeptide sample shows a second band with a decreased electrophoretic mobility in the gel analysis. In comparison to the marker lane the slower migration corresponds to a species of the double molecular weight of the corresponding polypeptide. This indicates the formation of polypeptide dimers by thiol oxidation.

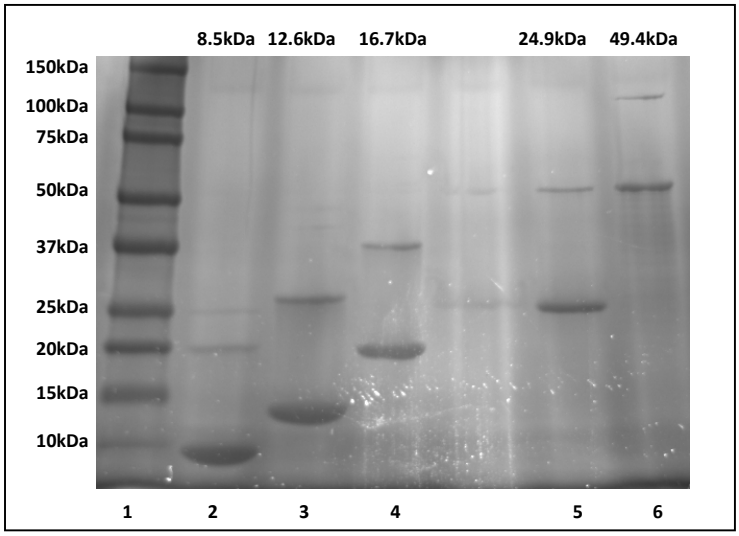

Figure 4.5 Gradient 4-20% SDS-PAGE Gel of the purified E4-library under non-reducing conditions. Lane 1: peptide marker; Lane 2: E4-20, Lane 3: E3-40; Lane 4: E4-40; Lane 5: E4-60, Lane 6: E4-120

Besides the characterization by SDS-PAGE the properties of the new polypeptide library were tested by UV cloud point measurements as well as by dynamic light scattering. The following chapters summarize the results of these characterization methods.

4.3 UV cloud point measurements

One key feature of Elastin-like polypeptides is their inverse transition temperature. This property can be analysed by temperature depending UV measurements. Figure 4.6 shows the temperature dependent UV scans of E4-20 in PBS buffer (10mM phospate; 140mM NaCl and 3mM KCl, pH=7.4). The optical density at 350nm is monitored as a function of the temperature. The peptide concentration varies from 5µM up to 100µM.

The cloud point temperature T_t is defined as the temperature of the inflection point of the measured cloud point curve. The measurement shows that the cloud point temperature depends on the peptide concentration: the cloud point temperature decreases with increasing peptide concentration. Table 4.2 gives the transition temperatures for the E4 library of the SF1 vector. The decrease in absorption for the sample E4-120 at 100µM at T>55°C is due to sedimentation of the aggregated ELP.

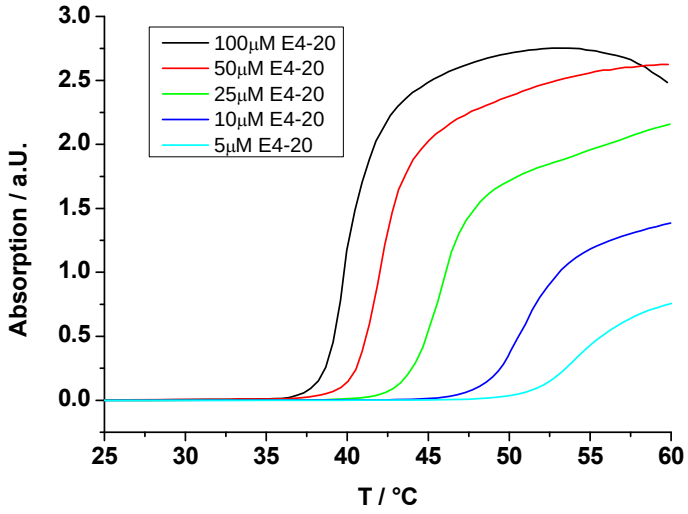

Figure 4.6 Temperature depending UV-Scans at 350nm of E4-20 solutions with different concentrations (heat rate: 1°C/min, scan frequency: 1s).

Table 4.2 also shows the values for a former E4 library based on the JMD2 vector. The solutions of the different libraries were prepared differently. The JMD2 ELPs carry a tryptophan at the C-Terminus of the peptide. Therefore their concentration can be estimated by UV-spectroscopy. This is not possible for the SF1 based ELPs. They contain a phenylalanine instead of a tryptophan. The molar extinction coefficient of phenylalanine (ε_m= 195 $M^{-1}cm^{-1}$ at 257.5nm) is 30x smaller than the extinction coefficient of tyrosine (ε_m= 1285 $M^{-1}cm^{-1}$ at 280nm). Additionally the cysteine residue also shows absorption in the same range (ε_m= 155 $M^{-1}cm^{-1}$ at 275.5nm), which makes the concentration determination by UV difficult. Therefore all samples were lyophilized after purification and the solutions were

prepared by weight. A calibration curve for the UV absorption at 230nm (Appendix 9.1.2). was measured with ELP samples of known concentration. Hence, the peptide concentration of unknown samples could be estimated.

Both libraries show comparable values regardless of the preparation method. The transition temperature decreases with increasing peptide concentration and with increasing peptide length except for the sample E4-30 (SF1). It shows lower transition temperatures than the sample E4-40. The sample E4-30 was measured after being dissolved in buffer for a few months, which could have led to the formation of disulfides by oxidation. The formed disulfides correspond to a polypeptide with 60 repeat units, which should have a comparable transition temperature like the E4-60 sample. The transition temperatures for the E4-30 are close to the values of the E4-60. The slightly higher values could result from a mixture of non-oxidized and oxidized E4-30.

Table 4.2 Cloud point temperatures of E4 library (SF1 vector) and of E4-30, E4-60 and E4-120 (JMD2 vector). All transition temperatures are given in °C for different peptide concentrations. The concentrations of JMD2 ELPs were determined by UV-measurements at 280nm. The solutions of SF1 ELPs were prepared by weight after lyophilization.

SF1	**E4-20**	**E4-30**	**E4-40**	**E4-60**	**E4-120**
	T_t/°C	T_t/°C	T_t/°C	T_t/°C	T_t/°C
100 µM	39.6	33.9	35.4	30.9	25.6
50 µM	41.9	34.4	37.8	32.5	27.0
25 µM	46.0	37.0	40.8	34.5	28.0
10 µM	51.0	39.6	43.8	36.4	29.4
5 µM	53.8	40.6	46.6	38.4	30.3

JMD2		**E4-30**		**E4-60**	**E4-120**
		T_t/°C		T_t/°C	T_t/°C
100 µM		44.5		32.3	28.1
50 µM		47.5		33.3	28.6
25 µM		51.1		35	29.6
10 µM		55.9		37.7	30.9
5 µM		60.6		39.0	31.8

The concentration dependence of the transition temperature, plotted in Figure 4.7, can be fitted as a logarithmic function of concentration:

$$T_t = m \log c + b \tag{4.1}$$

The negative slope increases with decreasing peptide length. This relation has already been reported for other ELP libraries [68]. One exception is again the sample E4-30. Its slope suits to the slope of E4-60. This observation fits to the assumption of disulfide formation.

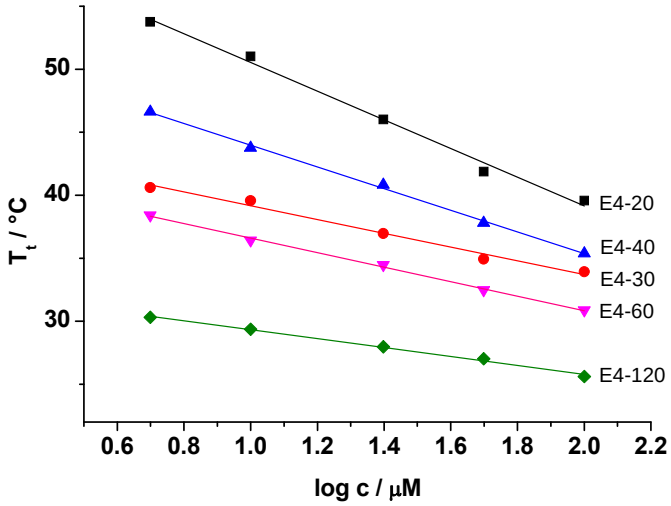

Figure 4.7 T_t as a function of the log of peptide concentration in µM. The linear fits are in good agreement for all data points with an average r^2 for these fits between 0.983 and 0.997.

4.4 Dynamic light scattering (DLS)

The dynamic light scattering measurements were performed to determine the hydrodynamic radii and the purity of the ELPs. The ELPs were dissolved in 20mM NaCl for the LS measurements at a concentration of 5mg/ml. All presented measurements were performed at an angle of 30°. The scattering intensity showed no angular dependence. The correlation functions for E4-20, E4-30 and E4-60 decayed single exponentially. The measurements of E4-40 and E4-120 had to be done in presence of reducing agent (TCEP) to remove an arising slower relaxation caused by bigger particles. As mentioned before, the SF1 ELPs can form dimers by thiol oxidation, which disturb the DLS measurements. The formation of disulfides may have been occurred because the samples E4-40 and E4-120 were kept at RT for several days before the measurement. The slow mode disappeared completely after the addition of reducing agent.

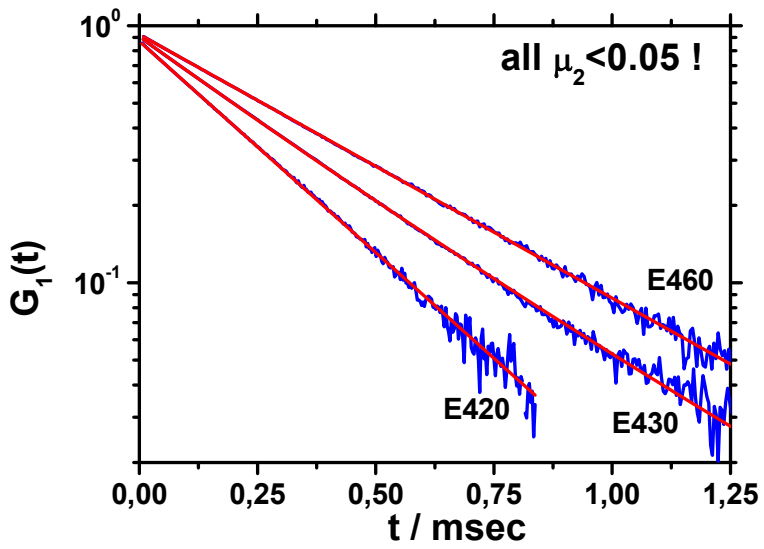

Figure 4.8 Correlation function G_1 (t) of E4-20, E4-30 and E4-60 (all SF1) plotted vs. the correlation time t in a semi logarithmic scale.

Figure 4.8 shows the dynamic light scattering measurements for the E4-20, E4-30 and E4-60. The amplitude correlation function is plotted versus the correlation time in a semi logarithmic scale. The linear dependence indicates that the samples are monodisperse. The normalized 2nd cumulant μ_2, a measure for the polydisperstiy of the sample, was determined $\mu_2<0.05$, which is taken as an indication of monodisperse samples.

Table 4.3A shows the hydrodynamic radii for the E4-SF1 library determined by dynamic light scattering and in comparison to that the results of former measurements on different ELP and ELP diblock samples synthesized and measured by M. Dreher (Table 4.3B)[70]. The

values, plotted in Figure 4.9, are in good agreement. The measurements of the ELP4 library all showed a single exponential decay of the correlation functions which demonstrates that they are mono modal and free of any larger impurities. The hydrodynamic radii for the samples of M. Dreher were determined by analysing the fast mode in presence of a slow mode. Therefore, these values were not used in further analysis.

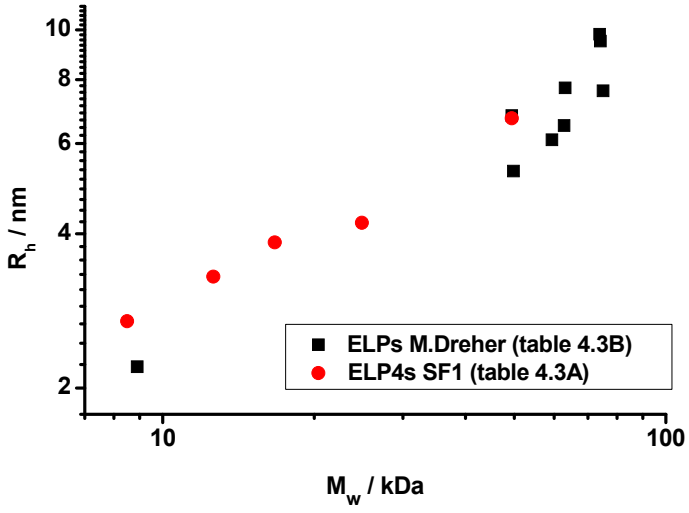

Figure 4.9 Plot of the measured hydrodynamic radii vs. the molecular weight for the E4 SF1 library and the ELPs synthesized by M. Dreher.

A

	M_w/kDa	R_h/nm
E4-120	49,4	6,7
E4-60	24,9	4,2
E4-40	16,7	3,9
E4-30	12,6	3,3
E4-20	8,5	2,7

B

	M_w/kDa	R_h/nm
E4-20	8,9	2,2
ELP2-64,4-60	49,4	6,8
ELP2-32, 4-90	49,8	5,3
ELP1-150	59,4	6,1
ELP2-64,4-90	62,8	6,5
ELP2-96,4-60	63,1	7,7
ELP2-96,4-90	73,9	9,8
ELP2-64,4-120	74,1	9,5
ELP2-128,4-60	75,1	7,6

Table 4.3 Theoretical molecular weight and the hydrodynamic radii of different ELPs measured by dynamic light scattering at 30° at 20°C. The SF1-ELPs (A) were measured in 20mM NaCl solution. All others (B) were measured in 1x or 1/10x PBS buffer.

The relationship between the measured hydrodynamic radius R_H and the calculated molecular weight M_w of the SF1-ELPs was analyzed by a double logarithmic plot shown in Figure 4.10. The data points can be fitted with a linear fit function with a slope of 0.5. The

slope corresponds to the fractal dimension υ which relates the mass to the topology of a particle.

$$M_w \sim R^{\upsilon}$$

The fractal dimension υ is associated with the geometry of a polymer in solution. A fractal dimension of 0.5 complies with an ideal coil in theta solution.

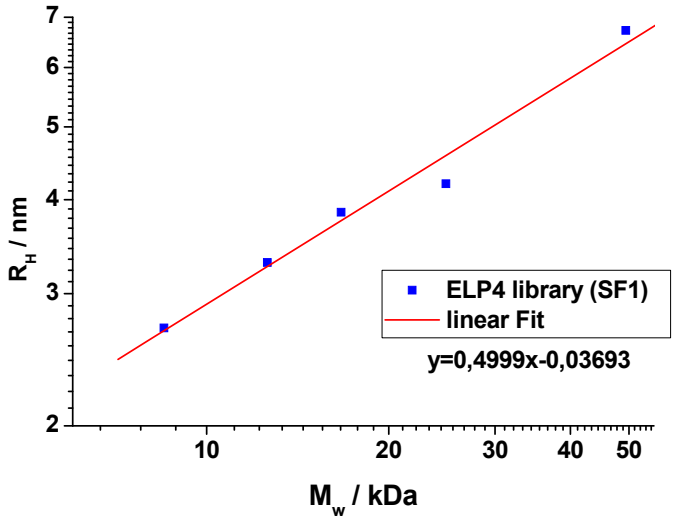

Figure 4.10 Double logarithmic plot of the calculated molecular weights and the measured hydrodynamic radii for the E4 library (SF1). The data points fit a linear function (r^2=0.989) display above.

The Yamakawa-Fujii theory[122, 123] based on the wormlike chain model[124] relates the hydrodynamics of a chain to its stiffness. The Kuhn statistical length l_k, a measure for the chain stiffness, can be obtained nummerically by fitting a theoretical R_H value to match the measured R_H[125]. The parameters needed are the length per repeat unit b and the effective chain cross-section d_{eff}. In Figure 4.11 the double logarithmic plot of the hydrodynamic radius of the ELPs versus the number of repeat units is shown. The calculated fits were obtained by taking b=0.365nm and assuming different values for the effective chain cross-section d of 0.5, 1.0 and 1.5, which is impossible to exactly calculated for non rigid particles. Given the different side chain size of the amino acids in ELPs the chosen d values include the extremes of a very small hydrodynamic effect of the side chain (d=0.5) and a maximum effect reflecting the maximum extension of the largest amino acid side chain (Valine). Hence, the best fit with d_{eff}=1.0 reveals a Kuhn length of l_k=2.4. The length per repeat unit was calculated by the well-known peptide bond lengths and angles[126].

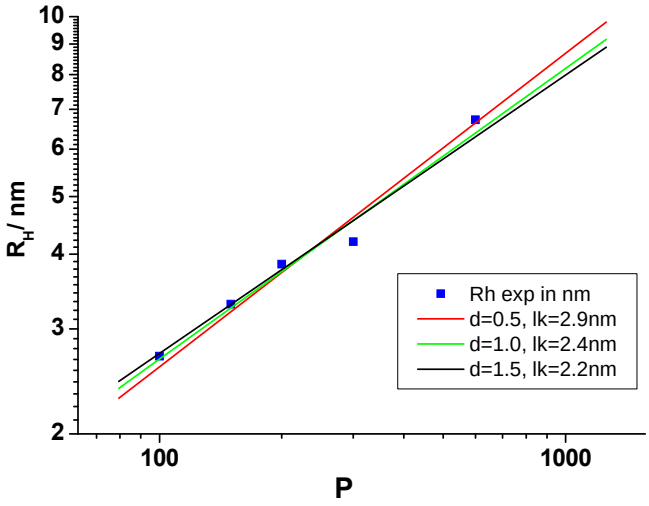

Figure 4.11 Double logarithmic plot of the hydrodynamic radius R_H vs. the number of repeat units P. The lines represent the best fits for the indicated effective chain cross section d assuming a repeat unit length b of 0.365 and the resulting Kuhn length l_k. The fits are compared with the measured hydrodynamic radii (data points) of the ELP4 library.

Given the experimental scatter of R_H data, all three d-values fit the data equally well. The most resonable value d=1.0nm leads to a Kuhn length l_k=2.4nm, which is seen to only slightly depend on d. It should be noted that l_k=2.4nm is much larger than $l_k \leq$ 0.4nm based on force distance curve analysis[127], which is frequently reported to yield unphysically small Kuhn lengths[128]. It should be noted that the contour length utilized in the analysis ignores possible secondary structures of ELP such as helices, hair pins etc. Since such effects would shorten the contour length, the Kuhn length would become even larger, i.e. the presently reported value constitutes a minimum value.

4.5 Summary

The previous sections showed the successful genetic engineering and expression of elastin-like polypeptides functionalized with one cysteine residue at the C-Terminus. The synthesized ELPs carry only hydrophobic, unreactive amino acids in their repeat units and are therefore only reactive at their terminal amino acids: the thiol moiety of the cysteine and the free amino group of the N-Terminus. The new ELP library consists of five polypeptides differing in length from 20 repeat units up to 120. The characterization by SDS-PAGE and DLS demonstrated the well defined, monodisperse properties of the ELPs. Furthermore, cloud point measurements were carried out to define one of the important properties, the transition temperature, of the new polypeptides which relates to former measurements of similar polypeptides.

5 ODN-ELP Diblocks

The main object of this thesis is the synthesis of oligonucleotide (ODN) polypeptide conjugates. The options for the coupling of biomacromolecules are manifold. In Chapter 2.3 a selection of possible coupling techniques for the conjugation of ODNs and ELPs was introduced. The following chapter presents the experimental results of the conjugation reactions. First, a one step approach to ODN-ELP conjugates by using methacrylate modified ODNs is discussed. The second approach introduces the concept of linker functionalization of amino modified ODNs for further conjugation by thiol addition. The addition reactions were all tested by introducing various thiol containing components before the conjugation of ELPs themselves was analyzed. In a third approach the formation of the desired ODN-ELP conjugates by activated ester chemistry is presented. The latter differs from the first approaches by utilizing oligonucleotides bound to solid support. The detailed conditions for all reactions reported are summarized in Appendix 9.2.1.

5.1 Thiol Addition to methacrylate modified ODN

The Michael-type addition[78] of thiols to double bonds is widely used in bioconjugation as discussed in Chapter 2.3.2. The first synthetic approach (Figure 5.1) to oligonucleotide conjugates presented here is a one step procedure. It involves the addition of a thiol active molecule to a methacrylate modified oligonucleotide. This modification is commercially available under the trademark Acrydite™ (IDT, Integrated DNA technologies) (see Chapter 2.1.2).

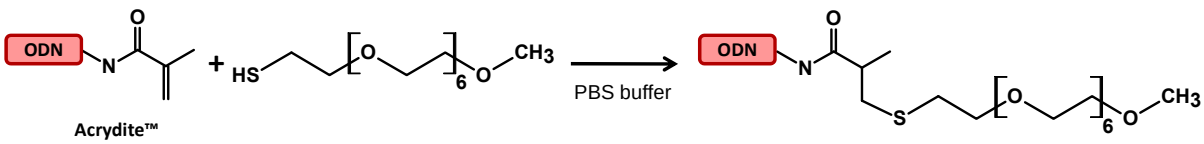

Figure 5.1 Synthesis scheme of Acrydite™ addition reaction

This synthetic approach was first tested with monodisperse mono-methoxy poly(ethylenoxid) (mPEO) with six repeat units carrying a thiol end group. The reaction was performed with a high excess of the thiol component. Figure 5.2 shows the gel analysis of the reaction between a methacrylate modified oligonucleotide of 23 bases and the thiol

mPEO. All experiments on the left hand side (Figure 5.2A) were performed in phosphate buffer at pH=7.5 with a 1000x excess of the thiol component. Lane 2 contains the pure oligonucleotide. In lane 3 the reaction was performed at room temperature and in lane 1 the temperature was raised to 40°C. In both cases a second band appeared with a lower electrophoretic mobility. This band can be assigned to the PEO-oligonucleotide conjugate, which migrates slower because of the higher molar mass and a higher mass to charge ratio. The reaction yield increases with temperature from approximately 8% at room temperature (RT) to 40% at T=40°C determined by band intensities.

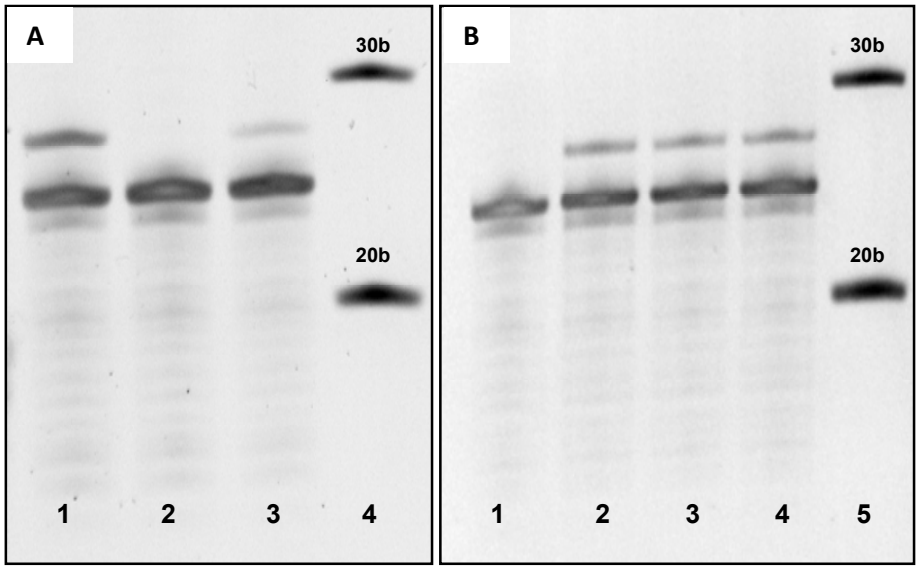

Figure 5.2 Addition reaction of mPEO thiol to Acrydite™ ODN with 23 bases. A) All reactions performed at pH=7.5. Lane 1: at T=40°C; Lane 2: pure Acrydite™ ODN; Lane 3: at T= RT; Lane 4: 10b marker. B) All reactions performed at T=40°C Lane 1: pure Acrydite™ ODN; Lane 2: pH=6.7, Lane 3: pH=7.5; Lane 4: pH=8.3; Lane 5: 10b marker.

Further, the influence of the pH was investigated (Figure 5.2B). All reactions analyzed in lane 2-4 were performed in 1000x excess of the thiol component and at a reaction temperature of 40°C. The pH value of the phosphate buffer was varied from pH=6.7 (lane 2), pH=7.5 (lane 3) to pH=8.3 (lane 4). Lane 1 contains the pure Acrydite™ ODN. The reaction yield was around 22-25% in all cases. No influence of the pH value on the reaction yield was detectable. Comparing lane 1 of Figure 5.2A and lane 3 of Figure 5.2B the yield decreased around 20%. The reactions were carried out under the same conditions except for a decreased in reaction time from 25h in Figure 5.2A to 19h in Figure 5.2B, which could explain the change in yield.

The described test reaction showed that a thiol coupling to an Acrydite™ modified oligonucleotide is possible. Therefore, the reaction approach was tested with other thiol containing components (Figure 5.3) as well. The results are summarized in Table 5.1. One

major constraint for all following thiol components is their availability. Although the synthesis of oligonucleotides and short peptides has been commercialized, the amounts are limited and still costly. Hence, the conditions of the PEO test reaction had to be modified to a lower excess of the thiol component. A synthetic approach to yield oligonucleotide-polypeptide conjugates is only implementable, if all components are used at a minimum loss.

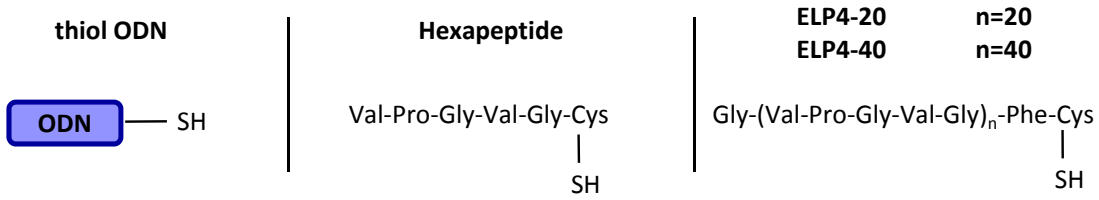

Figure 5.3 Thiol components tested in the addition reactions of Acrydite™-ODNs.

The addition of a thiol oligonucleotide to the methacrylate oligonucleotide was performed under various conditions. The reaction was performed at different pH values as well as at different temperatures. Additionally a water-soluble Lewis acid catalyst $Sc(OTf)_3$ [88, 129]was applied. All conditions gave the same result: the addition of a thiol oligonucleotide to Acrydite™ is not possible in an equimolar manner under the chosen conditions.

Table 5.1 Reaction components, applied reactant ratios and yield of the thiol addition reaction to Acrydite™ functionalized ODNs.

thiol component	oligonucleotide	ratio	yield
thiol ODN	Acrydite™	equimolar	0%
hexapeptide	Acrydite™	160x excess peptide	0%
E4-20	Acrydite™	equimolar	0%
E4-40	Acrydite™	equimolar	0%

The reaction between the methacrylate oligonucleotide and a hexapeptide containing one cysteine residue at the C-terminus showed the same results. The hexapeptide was used in 160x excess. However, no addition product was observed. Similar results were obtained for the addition of the elastin-like peptides E4-20 and E4-40. The thiol addition to a methacrylate modified oligonucleotide was therefore only successful in the case of the thiol PEO used in large excess.

The Acrydite™ modification of ODNs has been used in the copolymerization with acrylamide producing ODN functionalized hydrogels.[130, 131] The company IDT (Integrated DNA Technologies) also postulates that Acrydite™ ODNs can be immobilized on surfaces by thiol coupling.[132] No literature reports on this subject have been published so far. The conjugation of thiol containing components to Acryidte™ ODNs in aqueous solution are unknown as well. Hence, a quantitative comparison is not possible. The coupling efficiency of the here reported Acrydite™ conjugations can be qualitatively compared to the labeling of thiol containing compounds with acrylodan, an acryloyl functionalized fluorescent probe.[133-135] The conjugation efficiency of acrylodan labeling to enzymes ranges from 76-95% (5x excess of acrylodan), which demonstrates the ability of conjugating thiol compounds to acryloyl containing molecules.[136] In the case of acrylodon, a low-molecular weight species (M_w=225g/mol) was coupled to proteins with high molecular weights. In the case of the Acrydite™ coupling the acryloyl functionality is bound to the ODN, a high molecular weight species. This fact alters the reaction conditions tremendously. Therefore, no quantitative comparison is possible.

These findings led to a change in the synthesis approach. The Acrydite™ modified oligonucleotide was replaced by an amino oligonucleotide which can be functionalized with a variety of different well known bifunctional linkers (Chapter 2.3). The disadvantage of the new approach is the additional functionalization step which leads to a two-step procedure for the synthesis of oligonucleotide-polypeptide conjugates. The different functionalization and conjugation reactions are discussed in the following chapter.

5.2 Modification of amino oligonucleotides by heterobifunctional linkers

The conjugation of biomolecules by different homo- or heterobifunctional linkers is widely used. In this section the modification reactions of 5'- amino functionalized ODNs consisting of 23 bases with several linkers (Figure 5.4) are presented. All chosen linkers are heterobifunctional. Their common features are the reactive end groups: an activated N-hydroxysuccinimide (NHS) ester and a maleimide. The latter one is sulfhydryl reactive and forms a covalent linkage during the conjugation reaction with thiol containing compounds.

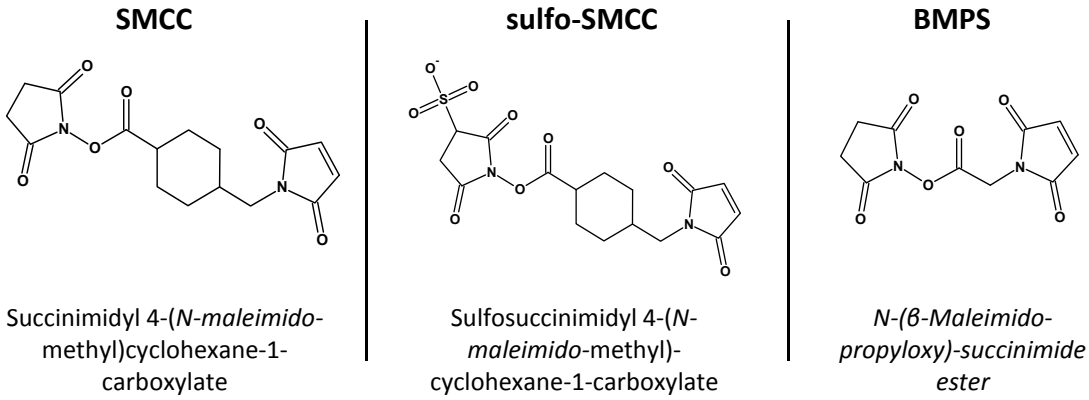

Figure 5.4 Chemical structures of the heterobifunctional linkers SMCC, sulfo-SMCC and BMPS.

5.2.1 Hydrolysis kinetics of crosslinkers with NHS ester functionality

One major problem of the linker modification by activated ester chemistry is the hydrolysis of the NHS ester. The modification reactions are usually performed in aqueous solution due to the insolubility of biomolecules in organic solvents. The hydrolysis is a competing reaction to the modification reaction and its rate increases with pH. This problem is taken into account by using the linker in high excess and by performing the reaction at a nearly neutral pH value between 7.2 and 7.5. At this pH values the hydrolysis is slow compared to the aminolysis.

Figure 5.5 shows the kinetics of the hydrolysis for the linkers sulfo-SMCC, BMPS and SMCC. The latter two are insoluble in water and were dissolved in DMF prior to the measurements, which were performed in PBS buffer (0.1M phosphate, 0.15M NaCl, pH=7.2) at T=20°C. The kinetics were studied by detecting the absorption at 280nm. At this wavelength the N-Hydroxysuccinimid (NHS), that is the product of the hydrolysis of the active ester, is detected. The decrease of the active ester was calculated by (1-Abs_{280nm}).

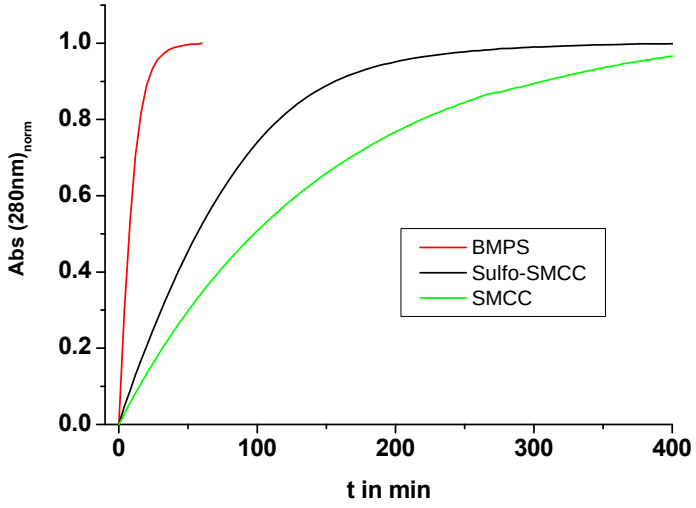

Figure 5.5 Kinetic study of the NHS hydrolysis of the linkers sulfo-SMCC, SMCC and BMPS. The kinetic was measured by UV absorption at 280nm detecting the produced N-Hydroxysuccimide.

The rate constants k_H of the hydrolysis were determined by linear regression of a semi log plot of (1-Abs_{280nm}). The linear regression shows that the hydrolysis of the different linker follows a first-order reaction at this pH. The calculated slopes correspond to the hydrolysis rate of the linker. The determined rates are given in Table 5.2. BMPS shows the fastest hydrolysis with a half life of only 14 min. For sulfo-SMCC a hydrolysis rate of 7.4 min^{-1}, which results in a half life of 94 min, was evaluated. The slowest hydrolysis occurs for SMCC with a half life of 207min. The hydrolysis rate can be related to the spacer arm of the linker. BMPS with a simple ethylene bridge shows the fastest hydrolysis. In the case of sulfo-SMCC and SMCC the cyclohexane bridge increases the stability of the linker against hydrolysis.

Table 5.2 Hydrolysis rate constants k_H of BMPS, sulfo-SMCC and SMCC determined by UV measurements at 280nm.

linker	BMPS	sulfo-SMCC	SMCC
rate constant k_H (10^{-3} min^{-1})	49	7.4	3.4

The hydrolysis constant determined for sulfo-SMCC corresponds to previously reported values of $5.85 \cdot 10^{-3}$ min^{-1} at pH=7.0 and $9.85 \cdot 10^{-3}$ min^{-1} at pH=7.6 by Tournier et al.[137] The hydrolysis of the active ester competes with the nucleophilic substitution of the amino

compound that is modified by the linker. Therefore, a small hydrolysis constant is desirable to increase the modification yield. The SMCC linker meets this demand best.

5.2.2 Modification of amino ODNs by BMPS and sulfo-SMCC

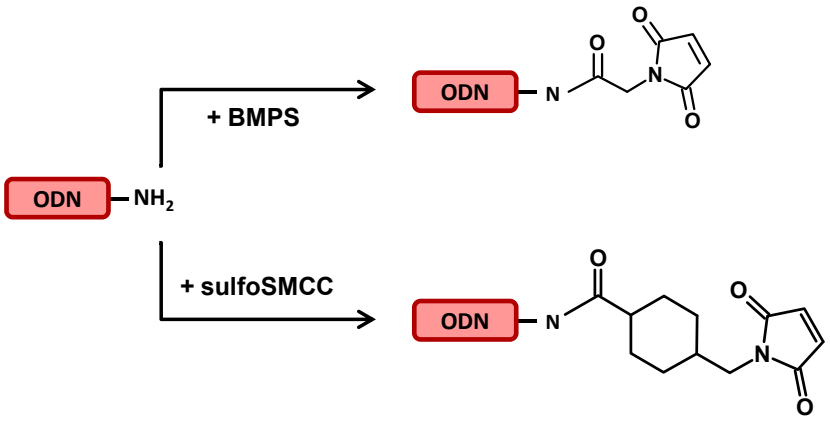

Figure 5.6 Reaction scheme of an amino ODN modified by BMPS and sulfo-SMCC.

The different linkers were all tested in modifying an amino functionalized oligonucleotide. The reaction scheme for the BMPS and sulfo-SMC modification is shown in Figure 5.6. The gel analysis of the two reactions is presented in Figure 5.7. The modification by sulfo-SMCC in lane 1 results in a mixture of products. Three bands are detected for this reaction. One can be assigned to the pure oligonucleotide (lane 3). The other two bands may be the desired product and a side-product. It was not possible to characterize the different products of this reaction further. In lane 2 the reaction products of the BMPS modification are shown. Here the main band corresponds to the remaining pure oligonucleotide, which indicates that the conversion of this reaction was low. A weak band with a slightly decreased electrophoretic mobility is detected which corresponds to the modified oligonucleotide. A third band arose at around 50 bases. This band is in the regime of the double molecular weight of the oligonucleotide. The reactive maleimide group may be attacked by the free amino group of the oligonucleotide to yield an oligonucleotide-linker-oligonucleotide conjugate. The addition of amines to maleimides is usually very slow at neutral pH. Its reaction rate is 1000x smaller than the one for the reaction with thiols.[78] At higher pH values the reactivity of the amines increases. Hence, both modification reactions yield undesired products in an uncontrollable way. The modification by sulfo-SMCC and BMPS are not useful for a defined functionalization of oligonucleotides. The high hydrolysis rate at first place and the observation of side products in the second place exclude them from further application.

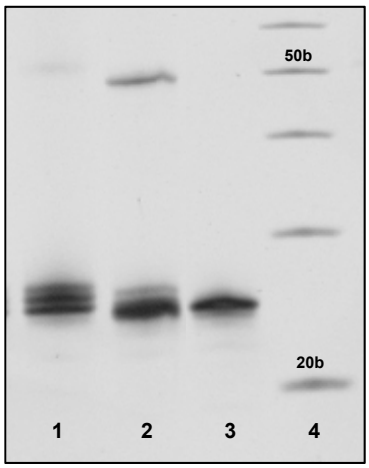

Figure 5.7 Modification of ODN with two different bifunctional linkers. Lane 1: Sulfo-SMCC; Lane 2: BMPS; Lane 3: pure ODN with 23bases (sequence S2); Lane 4: 10b marker.

5.2.3 Modification of amino ODNs by SMCC

In Chapter 5.2.1 the hydrolysis of three linkers was tested. The latter section showed that two of them, sulfo-SMCC and BMPS, are not applicable. The functionalization by SMCC, the linker with the slowest hydrolysis, is discussed in the following part.

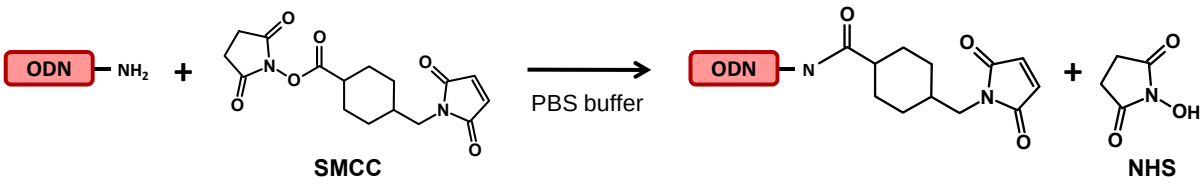

Figure 5.8 Reaction scheme of SMCC modification.

Results of the functionalization of an amino oligonucleotide by the SMCC linker are presented in Figure 5.9A. The reaction was carried out in phosphate buffer (0.1M phosphate, 0.15M NaCl, pH=7.2) for 4h at room temperature with a 100-fold excess of SMCC. Lane 1 contains the pure amino oligonucleotide. In lane 2 the reaction products are shown. Here only one additional band with a slightly decreased electrophoretic mobility was detected, which can be assigned to the modified oligonucleotide. The yield is around 49% by band intensities. This result is promising for a defined introduction of a maleimide group to amino modified ODNs.

Hereupon, several reaction conditions were tested to increase the conversion. Figure 5.9B shows the results for the same reaction carried out in degassed buffer and under argon. [138] The pH of the buffer (0.1M phosphate, 0.15M NaCl) was increased to pH=7.3 and the excess of linker was decreased to 50-fold. The reaction yield increased under these conditions to 70%. The best results were obtained by performing the reaction in degassed PBS buffer

(0.01M phosphate, 0.015 NaCl, pH=7.3) at RT for 4h under argon and using an 120x molar excess of SMCC applied in two portions (addition of the second portion after 2h). In Figure 5.13 the HPLC measurements of the SMCC modification under these optimized conditions are presented and show a yield >90% after 4h reaction time.

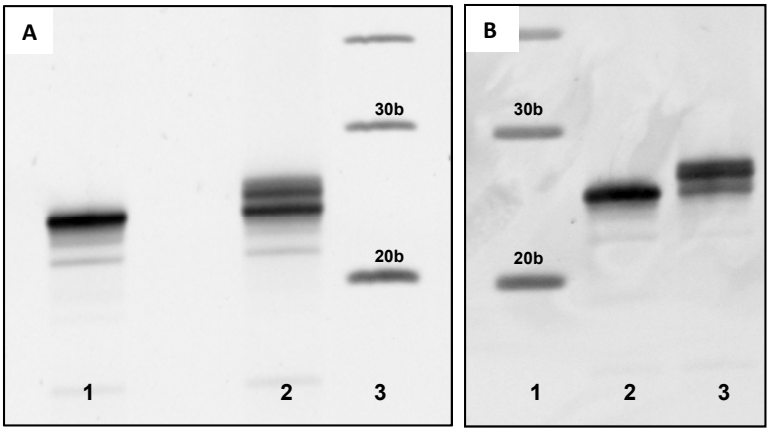

Figure 5.9 Denat. 20% PAGE analysis of the ODN modification by SMCC. A) Lane 1: pure ODN with 23 bases; Lane 2: after SMCC modification; Lane 3: 10b marker. B) Lane 1: 10b marker; Lane 2: pure ODN23; Lane 3: after SMCC modification

The modification of oligonucleotides by SMCC was also tested by using an amino functionalized oligonucleotide bound to a solid support. This solid phase synthesis has the advantage of an easy purification after the reaction. The excess reactant can be washed off before the oligonucleotide is cleaved of the solid support. Hence, no impurities of the excess linker are present. This reaction was tested by applying SMCC in pure DMF or in a mixture of DMF/PBS buffer.

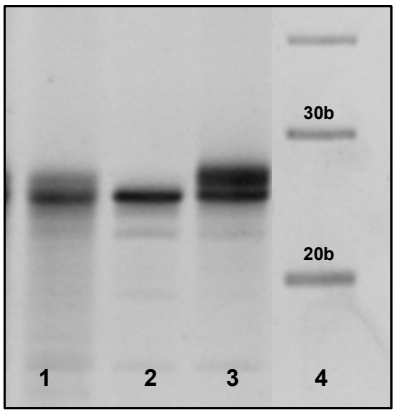

Figure 5.10 Denat. 20% PAGE analysis. Comparison of the SMCC modification of solid support bound amino ODN vs. the modification in solution. Lane 1: solid support base reaction; Lane 2: pure amino ODN with 23 bases; Lane 3: modification in aqueous solution; Lane 4: 10b marker

In Figure 5.10 the solid support mediated reaction (lane 1) is compared to the modification reaction in aqueous solution (lane 3). Lane 2 contains the unmodified ODN. Both reactions

still contain unfunctionalized ODNs. The reaction in solution shows an intense second band with a lower electrophoretic mobility, which corresponds to the modified ODN. In comparison the solid support reaction exhibits only a faint staining above the pure ODN band. Hence, the conversion of the reaction between SMCC and a solid support bound amino ODN is very low. The yield could not be increase by changing the reaction conditions. Therefore, the SMCC modification of amino ODNs in aqueous solution is the synthesis of choice. The following section presents the detailed analysis of the SMCC modification reaction by HPLC.

5.2.4 HPLC analysis of the SMCC modification reaction

Furthermore, the SMCC modification was followed by IP-RP-HPLC (ion pair reversed phase HPLC, see Chapter 2.4.3) to monitor the reaction process. The HPLC conditions were optimized by the measurement of oligonucleotides functionalized with different end groups during solid phase synthesis.

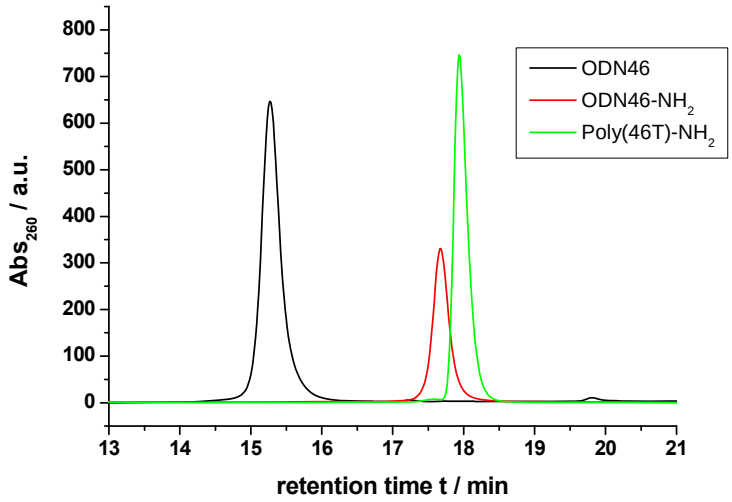

Figure 5.11 IP-RP-HPLC measurements of an unmodified ODN with 46 bases (mixed sequence, K4S1), an amino functionalized ODN with the same sequence and an amino functionalized poly(dT) ODN of 46 bases. The measured absorption at 260nm is plotted vs. the retention time. The measurements were performed under the following conditions: C18 column; flow rate 0.5ml/min; T=25°C; Mobile phase A: TEAA (0.1M, pH=7); Mobile phase B: acetonitril; Gradient starts at 0% B and ends after 30min at 60% B.

Figure 5.11 shows the separation of a non-functionalized 46mer, the corresponding amino functionalized oligonucleotide and a poly(46dT)-amino oligonucleotide that carries 46 thymine bases. The non functionalized oligonucleotide exhibits the shortest elution time. Hence, the amino functionalization enhances the interaction of the analyte and the stationary phase. Despite this aspect, the difference in retention time between the two amino functionalized oligonucleotides, the ODN46NH2 and the poly(46dT)-NH2, is not significant

enough to yield a relation between the base sequence and its influence on the elution behavior.

The influence of the oligonucleotide length and the base sequence on the retention time were tested in an additional set of measurements. Five oligonucleotides differing in length and sequence are compared in Figure 5.12. The indicated GC content takes into account the different base sequences of the oligonucleotides. It is usually a measure of thermostability. A double stranded DNA with a high GC content is more stable than an oligonucleotide with a low GC percentage, because GC pairs exhibit a higher stabilization of the double helix by base stacking and hydrogen bonding. Here, it accounts for the hydrophobicity of the different bases which increases from C < G < A < T.[115] Therefore an oligonucleotide with a low GC content is more hydrophilic than one with a higher GC content. The hydrophobicity of the analyte is one factor that influences the retention in HPLC measurements. The elugrams show a statistical variation of the retention time that relates neither to the oligonucleotide length nor to the base sequence. Thus, it is not possible to separate oligonucleotides according to their length or their sequence under the chosen conditions, but they are applicable to separate oligonucleotides by their end group as shown previously.

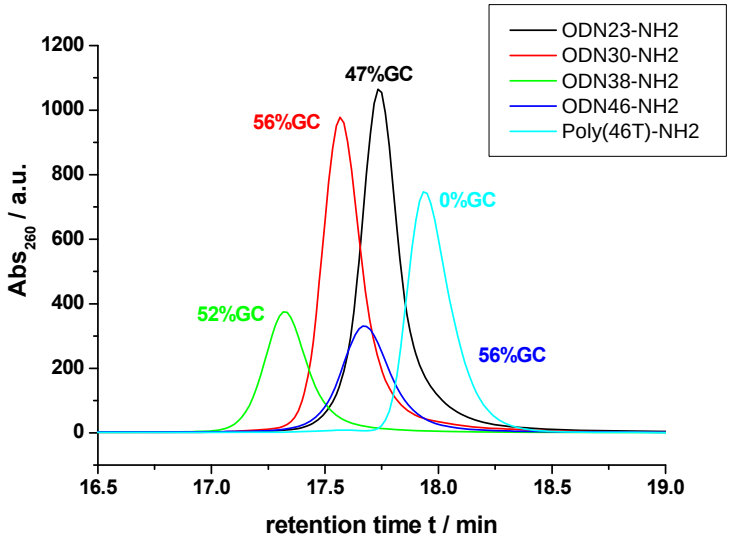

Fig 5.12 IP-RP-HPLC measurements of amino modified ODNs differing in length and/or sequence. The measured absorption at 260nm is plotted vs. the retention time. The measurements were performed under the following conditions: C18 column; flow rate 0.5ml/min; T=25°C; Mobile phase A: TEAA (0.1M, pH=7); Mobile phase B: acetonitril; Gradient starts at 0% B and ends after 30min at 60% B.

The modification of the amino oligonucleotide by SMCC changes the free amino end group of the oligonucleotide into a maleimide group. In Figure 5.13 the reaction between an amino modified oligonucleotide with 30bases (ODN30) and the SMCC linker was monitored by IP-

RP-HPLC. The peaks of the pure oligonucleotide and the maleimide functionalized oligonucleotide are baseline separated under the chosen conditions. The maleimide functionalized oligonucleotide shows an increased retention time (t=19.0min) in comparison to the amino oligonucleotide (t=17.3min). The measurements show the decrease of the reactant peak and the simultaneous increase of the product peak. After 250min the conversion is >90%.

The achieved modification efficiency is comparable to reported values in literature. For example, the modification of an amino ODN (8 bases) with SMCC (15x excess) in 0.1M phosphate buffer at pH=7.8 yielded 80% modified ODN confirmed by HPLC.[139] The SMCC or sulfoSMCC modification of biomolecules has been described under various conditions.[140-143] The modification efficiency was not determined in most cases, because the modified compounds were immediately used in thiol conjugation reactions.

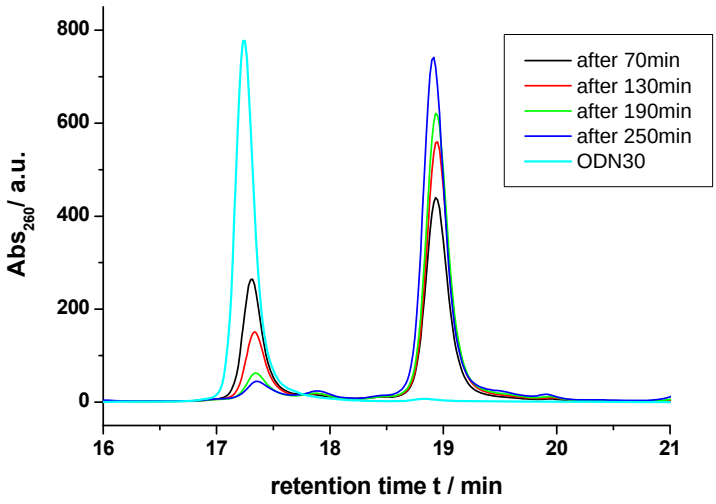

Fig 5.13 IP-RP-HPLC measurements following the reaction progress of the modification of an ODN with 30 bases by SMCC. The retention time is plotted vs. the measured absorption at 260nm. The measurements were performed under the following conditions: C18 column; flow rate 0.5ml/min; T=25°C; Mobile phase A: TEAA (0.1M, pH=7); Mobile phase B: acetonitril; Gradient starts at 0% B and ends after 30min at 60% B.

In contrast to the other linker systems the SMCC modification shows a defined and reproducable reaction behavior. The amino oligonucleotide can be modified by SMCC to introduce a thiol reactive maleimide group.

5.3 Synthesis of ODN conjugates by thiol addition

The previous chapter discussed the modification of amino functionalized oligonucleotides by SMCC in detail. The reaction transforms the free amino group into a maleimide functionality. In order to test the reactivity of the new introduced maleimide group several thiol containing reactants were tested comparable to the addition reactions of the Acrydite™ modified oligonucleotide in Chapter 5.1. The results of these conjugation reactions are presented in the following sections.

5.3.1 Addition of thiol-PEG to maleimide modified ODNs

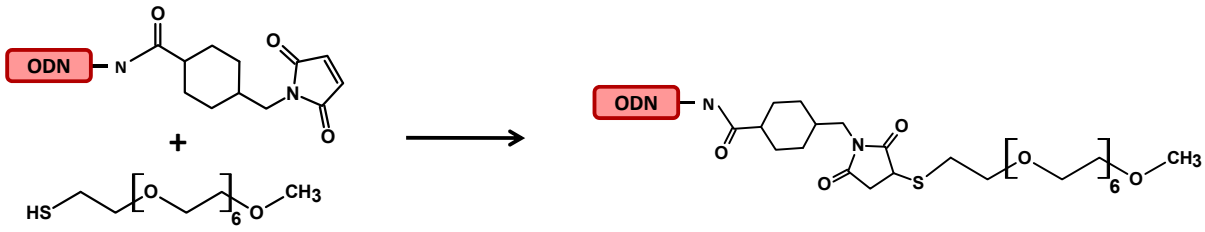

Fig 5.14 Reaction scheme for the addition reaction of thiol-PEG to maleimide functionalized ODNs.

Monodisperse thiol PEG has already been used in Chapter 5.1 to test the addition reaction of Acrydite™ functionalized ODNs. The following experiment uses the thiol PEG to investigate the reactivity of the maleimide group introduced by SMCC modification of ODNs.

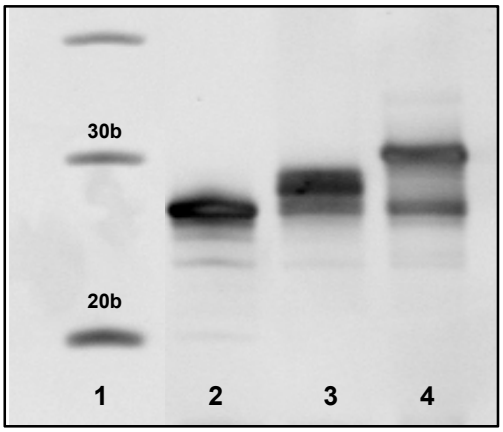

Figure 5.15 Denat. 20% PAGE analysis of the maleimide functionalization and the following thiol addition reaction of an ODN with 23 bases and thiol PEG. Lane 1: 10b marker; Lane 2: pure ODN23; Lane 3: after SMCC modification; Lane 4: after thiol addition of PEG.

The thiol addition reaction of PEG is presented in Figure 5.15. Here, the amino oligonucleotide in lane 2 was first modified with SMCC (lane 3). The modified oligonucleotide was immediately incubated with an excess of a short monodisperse thiol PEG. The reaction was performed in degassed PBS buffer at pH=7.3 for two days. The gel

analysis of this reaction (lane 4) shows two bands. The band with the higher electrophoretic mobility corresponds to the amino oligonucleotide. The band corresponding to the maleimide modified oligonucleotide disappeared completely. Instead a band with a lower electrophoretic mobility is detected that can be assigned to the PEG-oligonucleotide conjugate. Its higher mass leads to the decrease in electrophoretic mobility. In this reaction the maleimide oligonucleotide is completely converted into a PEG-oligonucleotide conjugate by gel intensities. These results show that the maleimide group introduced by SMCC modification is reactive towards thiol components.

5.3.2 Addition of thiol functionalized ODNs to maleimide modified ODNs

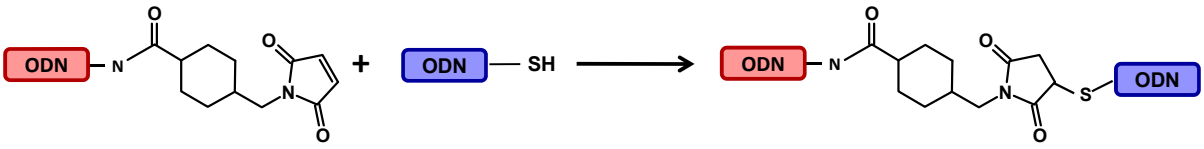

Figure 5.16 Reaction scheme of the addition of thiol functionalized ODNs to maleimide modified ODNs.

The thiol addition was additionally tested with thiol modified oligonucleotides (Figure 5.16). Lane 2 of Figure 5.17 contains the pure amino oligonucleotide with 23bases. This oligonucleotide was reacted with SMCC (lane 3). After the modification the excess of SMCC was removed by column chromatography and the maleimide oligonucleotide was immediately reacted with a thiol oligonucleotide with 23 bases in 1.2x molar excess.

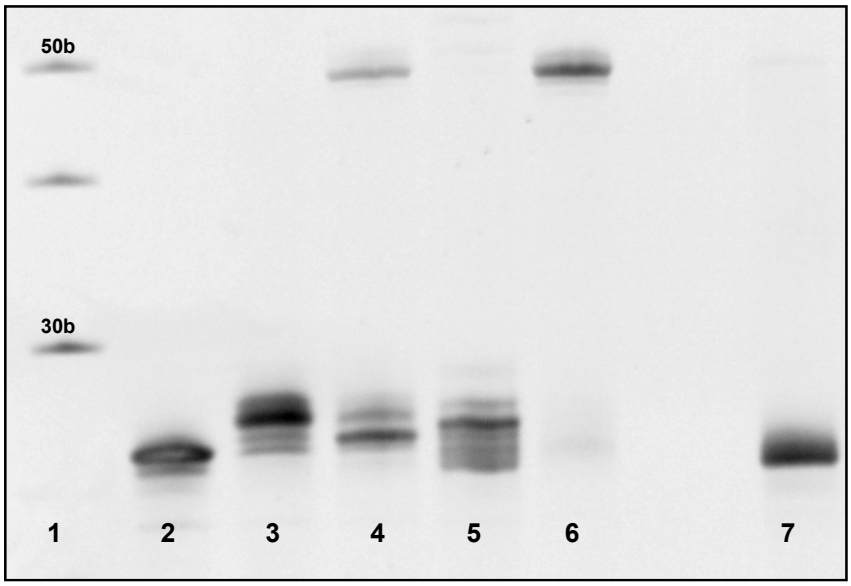

Fig 5.17 Denat. 20% PAGE analysis of the maleimide functionalization and the following thiol addition reaction of an ODN with 23 bases (ODN23) and thiol modified ODN with 23 bases (ODN23SH). Lane 1: 10b marker; Lane 2: pure ODN23; Lane 3: after SMCC modification; Lane 4: reaction mixture after thiol addition of ODN23SH; Lane 5: reaction mixture after thiol addition of ODN23SH with reducing agent; Lane 6: pure ODN23SH, fully oxidized; Lane 7: pure ODN23SH with reducing agent.

The reaction mixture of the addition reaction is shown in lane 4. If a conjugate formed during the reaction, a band in the range of 46 bases appears. In lane 4, a band in this size range is detected, but if a reducing agent is added to the same mixture the band disappears (lane 5). The band can be assigned to the dimer of the thiol oligonucleotide, which is formed by disulfide bridging. Lane 6 contains the pure thiol oligonucleotide without reducing agent and lane 7 shows the reduced thiol oligonucleotide. The addition reaction of the thiol oligonucleotide to the maleimide modified one was not achieved under the described conditions. The reaction kinetics of the addition may be slower than the thiol oxidation or the maleimide hydrolyzed prior to the addition reaction. One determining factor could also be the electrostatic repulsion of the oligonucleotides, which decreases the reaction rate.

5.3.3 Addition of cysteine containing hexapeptide to maleimide ODNs

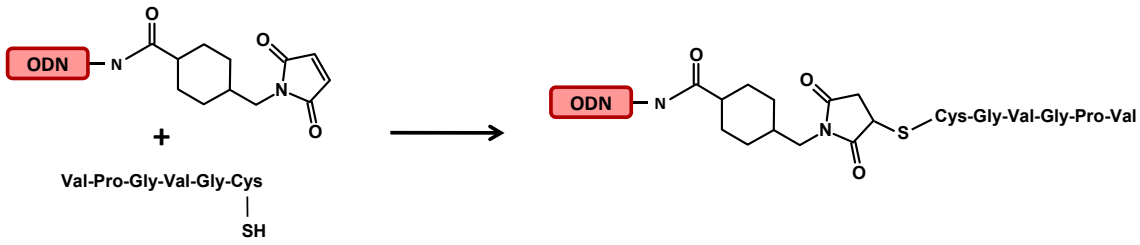

Figure 5.18 Scheme of the reaction between a cysteine containing hexapeptide and a maleimide functionalized ODN.

The analysis of the addition of a hexapeptide (Figure 5.18) containing one cysteine residue to a maleimide functionalized oligonucleotide with 23 bases is presented in Fig 5.19. The reaction was performed in degassed PBS buffer (pH 7.3) with a 300x molar excess of the hexapeptide. Lane 2 of Figure 5.19 shows the pure oligonucleotide. In lane 4 the results of the SMCC modification and in lane 3 the reaction mixture after the addition of an excess of hexapeptide are presented. The latter lane shows two bands. One corresponds to the unmodified amino oligonucleotide. The second band exhibits a decreased electrophoretic mobility compared to the maleimide functionalized oligonucleotide. It can be assigned to the oligonucleotide-hexapeptide conjugate.

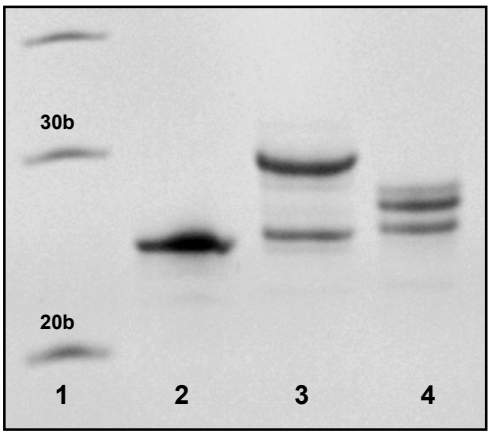

Fig 5.19 Denat. 20% PAGE analysis of the maleimide functionalization and the following thiol addition reaction of an ODN with 23 bases and a cysteine containing hexapeptide. Lane 1: 10b marker; Lane 2: pure ODN23; Lane 3: after thiol addition of the hexapeptide; Lane 4: after SMCC modification.

The conversion of the addition reaction in Figure 5.19 is quantitative comparable to the addition reaction of the thiol PEG in Chapter 5.3.1. The restrictions that applied to the addition of the thiolated oligonucleotide to a maleimide ODN seem to have no impact on this addition reaction. This is important for the desired synthesis of the oligonucleotide-polypeptide block copolymers. The synthesis of ODN-peptide conjugates by coupling a maleimide functionalized ODN to a cysteine residue of a peptide has already been reported under various conditions. Harrison et al.[139] reported the conjugation of heptapeptides to maleimide functionalized 8mers (ODN with 8 bases) under comparable conditions (5-7x excess of peptide compound, 0.1M phosphate buffer, pH=7.0, 3h). The conjugation yield variied from 40-96% mainly depending on the peptide sequence. In comparison the conjugation of SMCC modified oligonucleotide (34 bases) to a cysteine containing peptide (12 amino acids) performed in PBS buffer (10x excess peptide, no details on ionic strength and pH of PBS buffer given) reported by Zanta et al.[141] yielded 30% of the desired ODN-peptide conjugate. In contrast to this low conjugation yield, Tung et al.[140] demonstrated the coupling of a 15mer ODN to a cysteine containing tetrapeptide in 0.1M phosphate buffer at pH=6.6 (240x excess of peptide) with an efficiency of 86%. These three examples show that the conjugation reactions reported differ extremely in the applied reaction conditions and the resulting yields. The quantitative conjugation of a hexapeptide to a SMCC functionalized ODN, reported in this work here, provides conditions for a full conversion, if the cysteine compound can be used in high excess.

5.3.4 Addition of ELPs to maleimide modified ODNs

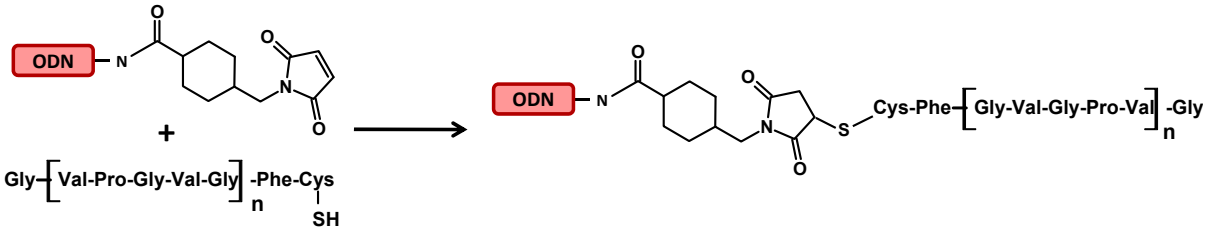

Figure 5.20 Reaction scheme: Addition of cysteine functionalized ELPs to amino ODNs modified by SMCC.

The main aim of this work is the synthesis of ODN-ELP conjugates. The previous chapters showed the synthesis of ODN conjugates with lower molecular weight compounds. This chapter discusses the synthesis of ODN-ELP diblock copolymers by thiol conjugation to maleimide functionalized ODNs. The reaction scheme is presented in Figure 5.20. Both reactants can be varied. The ELP can be chosen from the synthesized library E4 (see Chapter 4) to yield block copolymers with different peptide block lengths. The oligonucleotide sequence and/or number of bases can be changed to alter the hydrophilic block of the copolymers.

In Figure 5.21 the denaturating gel analysis of various conjugation reactions is presented. The reactions differ in their reactants, but in all cases the peptide compound was used in excess. Lane 1 shows the 10 base marker. Lane 4, 6, 9 and 12 contain the pure ODNs with 46 poly(T) bases (46poly(T)), 46 bases (sequence K4S1, 46mer), 38 bases (38mer) and 30 bases (30mer). The sequences for the 38mer and the 30mer were designed by shortening the K4S1 sequence (see Chapter 8.1.2.). Lane 2, 5, 7 and 10 show the conjugation reaction of E4-40 to the different oligonucleotides. The samples show a band of the pure oligonucleotide and a band with a much lower electrophoretic mobility, which corresponds to the ODN-ELP conjugates. All conjugate (though differing in oligonucleotide length) exhibit the same migration behavior. The difference of 16 bases at maximum can not be resolved with this gel analysis. In Figure 5.22 the SDS PAGE analysis is shown where the size differences are detected. In lane 3, 8 and 11 the conjugates of the different ODNs with E4-20 are shown.

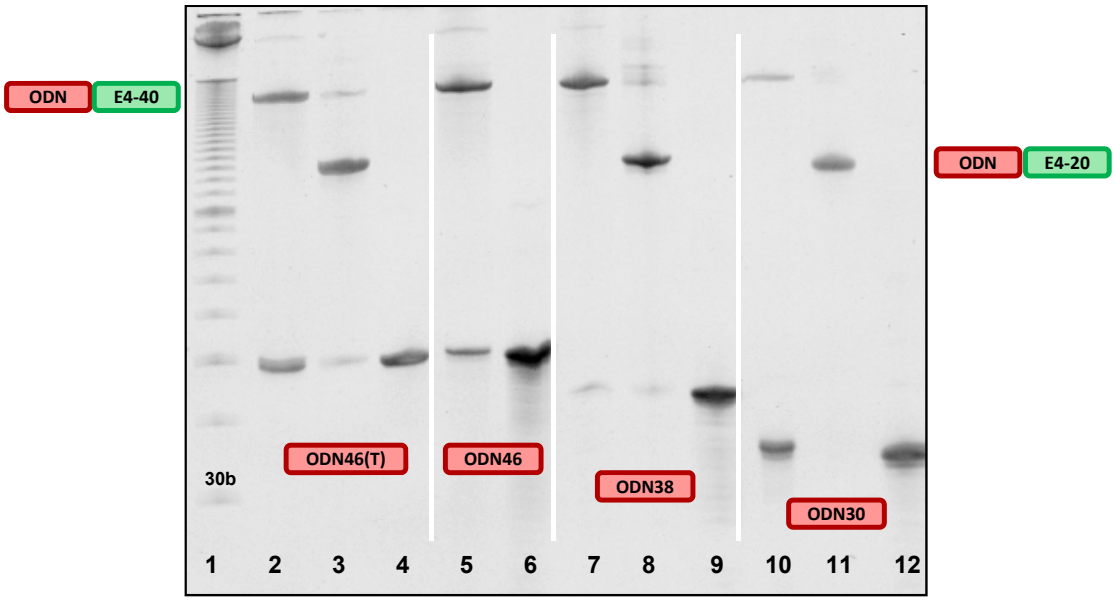

Figure 5.21 15% denat. PAGE of ELP conjugation to SMCC functionalized ODNs of different length. Lane1: 10b marker; Lane 2: reaction of E4-40 and ODN 46poly(dT); Lane 3: reaction of E240 and ODN 46poly(dT); Lane 4: pure ODN 46poly(dT); Lane 5: reaction of E4-40 and ODN 46mer; Lane 6: pure ODN 46mer; Lane 7: reaction of E4-40 and ODN 38mer; Lane 8: reaction of E4-20 and ODN 38mer; Lane 9: pure ODN 38mer; Lane 10: reaction of E4-40 and ODN 30mer; Lane 11: purified reaction of E4-20 and ODN 30mer, resolubilized pellet of salt precipitation; Lane 12: pure ODN 30mer.

Although the size difference of the conjugates synthesized with the same ELP block is not detectable, a major difference in migration of the conjugates with the same ODN block and varying ELP blocks is seen. Comparing lane 2 to lane 3, which show the conjugate of the 46poly(dT) with E4-40 and E4-20, it is pointed out how the ELP block length changes the migration behavior. The larger the uncharged ELP block the slower the conjugate migrates in the electric field. The reactions presented in lane 2, 3, 5, 7 and 8 all show an additional weak band with a smaller electrophoretic mobility than the conjugate. Those species migrate in the range of the double size, nicely seen by comparing lane 2 and 3. The weak band in lane 3 migrates as slow as the conjugate in lane 2. This observation leads to the conclusion that a conjugate with two peptide units, linked via a disulfid bridge, is formed during the reaction. The free thiol of the peptide forms a covalent bond with the maleimide residue of the ODN and is therefore unable to form disulfide bridges. One possible explanation is that amines are able to perform a Michael addition to maleimides as well as thiols[144]. The free amino group at the N-terminus of the polypeptide might react with the maleimide group to form conjugates of the same size, but carrying a free thiol group at the end. These thiol groups are able to form disulfide bridges by oxidation. Usually the reaction of amines is much slower than the addition of the thiols to the maleimide double bond at the chosen pH value (see Chapter 2.3.2), but the polypeptide was used in a large excess and high concentration, which could alter the conditions for the competing addition reactions. It also

has to be noted that the formation of the dimeric peptide conjugate only occurs to a minor degree (< 5% by gel intensities).

The purification of the synthesized diblocks is challenging, because two components have to be separated from the conjugates. The polypeptide was used in excess and has to be removed as well as unreacted oligonucleotides. Therefore, the purification approach involves two steps. The first step is a salt coprecipitation of the conjugate and the remaining polypeptide to remove the unconjugated ODN. The precipitation is done by the addition of saturated NaCl solution to the reaction mixture. By additional heating the polypeptide and the conjugate aggregate. The oligonucleotide stays in solution. The precipitate can be isolated by centrifugation and is resolubilized in buffer. Lane 11 in Figure 5.21 shows the purified diblock copolymer of E4-20 and the 30mer after salt precipitation and resolubilization. In comparison to lane 10 no pure oligonucleotide is detected after the precipitation step. If the separation is not complete, the salt precipitation can be repeated.

The samples purified by salt precipitation still contain a mixture of the block copolymer and the pure polypeptide. Now, the properties of the oligonucleotide are exploited to perform the separation. In the field of molecular biology the use of DNA binding columns is common, for example, to isolate plasmids from cell residues. The oligonucleotide binding is based on adsorption of DNA to silica.[145] For this work oligonucleotide binding spin columns (nucleotide removal kit, Qiagen) were used. The ODN is applied to the spin columns in high-salt buffer at low pH containing a chaotropic salt. The bound oligonucleotide, here the ODN-ELP block copolymer, is washed several times to remove any impurities and can be eluted by applying a low-salt buffer with a higher pH. Figure 5.22 shows the results of the column purification. A gradient SDS-PAGE analysis was performed using ethidium bromide (EtBr) as staining.

In lane 1 of Figure 5.22B pure E4-40 with the addition of reducing agent is shown. Lane 2 contains E4-20 under reducing conditions. The staining of the peptide with EtBr is weak. Usually EtBr is used to stain DNA by intercalation, but the hydrophobic nature of the polypeptide also shows weak interactions with the dye. After the EtBr staining, the gel was subject to peptide silver staining, but here the diblock conjugates are difficult to detect. The ODN-polypeptides do not seem to be affected by the fixative step of the silver staining protocol and are washed out of the gel during the staining and washing steps of the staining procedure.

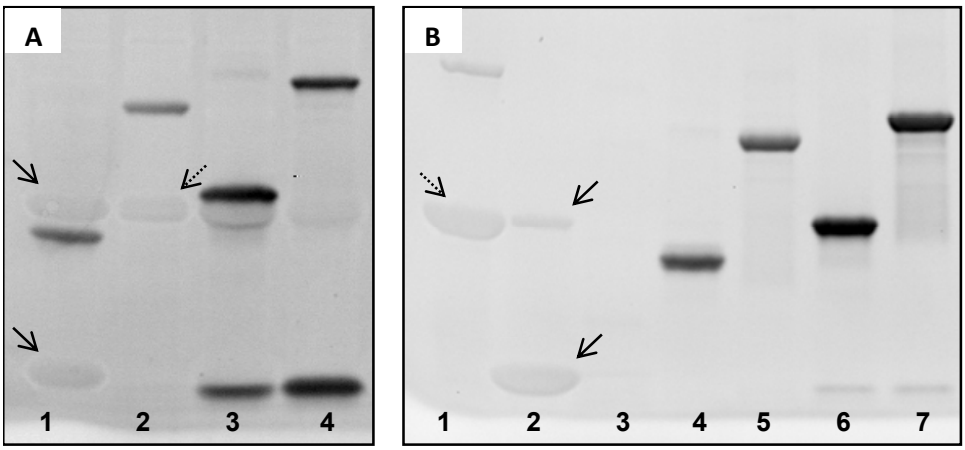

Figure 5.22 Gradient SDS-PAGE (10-20%) analysis. A) reaction mixtures of ELP-ODN conjugation by thiol addition prior to spin column purification. Lane 1: ODN30-E4-20; Lane 2: ODN30-E4-40; Lane 3: ODN38-E4-20; Lane 4: ODN38-E4-40. B) ELP-ODN conjugates after spin column purification. Lane 1: pure E4-40, Lane 2: pure E4-20; Lane 3: peptide marker, not stained by EtBr; Lane 4: ODN30-E4-20; Lane 5: ODN30-E4-40; Lane 6: ODN38-E4-20; Lane 7: ODN38-E4-40.

Figure 5.22A shows the diblock conjugate before the two purification step. Figure 5.22B shows the same samples after the purification step. Lane 1 of Figure 5.22A for example contains a sample of the E4-20-30mer synthesis. Besides the dark stained band of the conjugate two weak bands appear. The band with the higher electrophoretic mobility corresponds to the pure E4-20. During the synthesis the used E4-20 is partially oxidized to form a disulfide bridged dimer. This dimer is detected by the weak band above the diblock band. The migration behavior of the E40-20 dimer, which equals an E4-40 with 40 repeat units, is similar to the pure E4-40 detected in lane 2 as weak band. In all reactions displayed in lane 1-4 the remaining polypeptide is detectable. In lane 3 and 4 of Figure 5.22A the unreacted oligonucleotides are detected at the lower exclusion limit of the gel.

In Figure 5.22B the same samples are shown after the purification by salt precipitation and by spin column chromatography. Lane 1 and 2 contain the pure polypeptides under reduced conditions as discussed earlier. The polypeptides are not completely reduced. A low amount of disulfide dimer is still detected. Lane 3 contains the peptide marker, which is not stained by EtBr. The remaining lanes contain the pure ODN-ELP conjugates. In lane 4, a sample of the E4-20-ODN30 is analyzed. Compared to lane 1 of Figure 5.22A, no residual polypeptide is found. This is valid for all conjugates shown in Figure 5.22B. Therefore the described purification procedure is applicable to obtain pure ODN-ELP conjugates formed by thiol addition. One major draw back of this purification protocol is the small yield. At the end of the purification process an overall yield of <15% is achieved. Compared to the gel intensities in the denat. PAGE of the crude reaction mixture a conjugation yield of >50% was expected.

Reasons for this high loss are first of all the low recovery of the diblock from the spin-columns. For the short oligonucleotides a recovery of 60-80% for oligomers of 17-40mers is guaranteed.[146] Second, the salt precipitation of ELPs always goes along with a loss of ELP due to adsorption of the ELP to the vial.

In comparison to literature, the coupling efficiency is comparable to other reported conjugation reactions. The coupling of sulfo-SMCC modified ODNs (24 bases) to the enhanced yellow fluorescent protein (EYFP, M_w=31kDa) was perfomed by Kukolka et al.[147] with a yield of 50% conjugation (1.3x excess EYEP, 0.1M phosphate, 0.15M NaCl, pH=7.3). The only publication on ODN-ELP conjugates synthesized by a maleimide-cysteine conjugation protocol gives no conjugation yield.[74] It can be estimated by the gel picture shown to be in the range of 50%. Hence, the conjugation efficiency is similar to the here reported values.

At the moment a new approach for the purification is tested by using preparative gel permeation chromatography (GPC) to reduce the loss of the desired diblock copolymer. The challenge of this method is the determination of a suitable column material and the optimal separation conditions. Measurements of polymer oligonucleotides conjugates by GPC[148, 149] have already been performed as well as of standard peptide samples[150]. The characterization of ELP-ODN conjugates by GPC or further the separation of ELPs and ODNs by GPC has not been accomplished yet. Another alternative is the purification by anion exchange chromatography as reported by Schweller et al[74]. This techniques is going to be tested as well.

5.3.5 Translocation of ODN-ELP diblock copolymers

The synthesized monodisperse ODN-ELP diblock copolymers were subject to translocation measurements performed by S. Fakhouri (Group of Prof. Muthukumar, Unversity of Massachusettes). Translocation of single stranded DNA through a protein pore has been studied intensively.[151] The diblock copolymers are interesting subjects due to the uncharged polypeptide block, which corresponds to a weight that the DNA has to carry through the pore. The measurements are performed by preparing a lipid bilayer membrane incorporating a single transmembrane protein. Here α-hemolysin (α-HL) was employed. It forms a beta-barrel pore (Figure 5.23A) with a length of 100 Å and a diameter ranging from 14 Å to 46 Å.[152] The migration of an analyte through the pore is measured by the blockage of the constant current level, which is caused by the transmembrane potential. The α-HL pore has a transmembrane potential of 120mV with a positive sign at the beta-barrel side

(trans). A typical translocation time for single stranded DNA is in the range of 0.1ms. Figure 5.23B shows a translocation trace for the ODN23-E440 block copolymer. A drop of the current , also called event, to zero is attributed to a translocation event. The analyte entered the beta barrel and blocked the pore completely in this case. If the analyte only moves into the vestibule and does not translocate through the pore, a smaller drop of the current is observed to approx. 50pA.

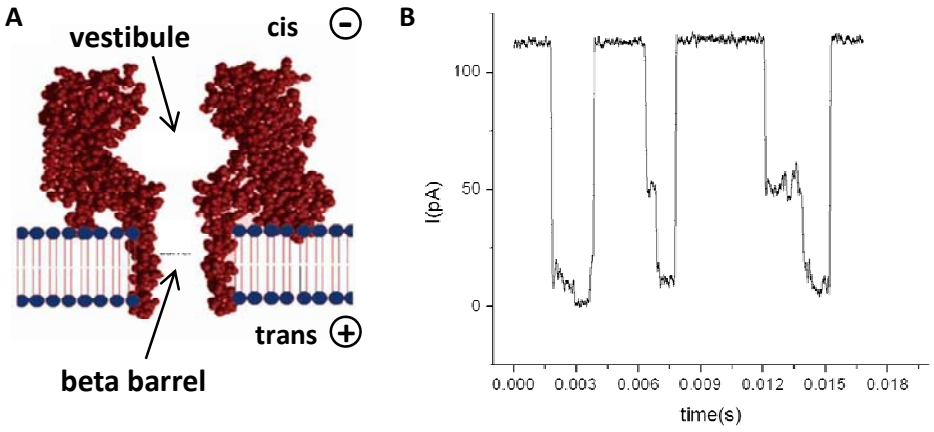

Figure 5.23 A) Schematic of the beta-barrel structure of α-Hemolysin. B) Current trace of the translocation measurements of ODN23-E4-40. Complete current blockages are attributed to a translocation of the analyte. Small current drops correspond to the migration of the analyte into the vestibule without translocation through the beta barrel.

The translocation data is analyzed by plotting the event count versus the measured translocation time giving the most probable translocation time. Figure 5.24 shows the histograms resulting form the translocation of an ODN23-E4-20 (Figure 5.24A) and ODN23-E4-40 (Figure 5.24B). The measurements demonstrate that the translocation time increases with increasing peptide length, which was expected. The translocation measured is approx. one magnitude larger in comparison to the translocation of single stranded DNA indicating the hindered motion of the DNA. Further studies with varying oligonucleotide length and base sequences are performed. An overall picture on the translocation behavior of the diblock copolymers can not be given yet.

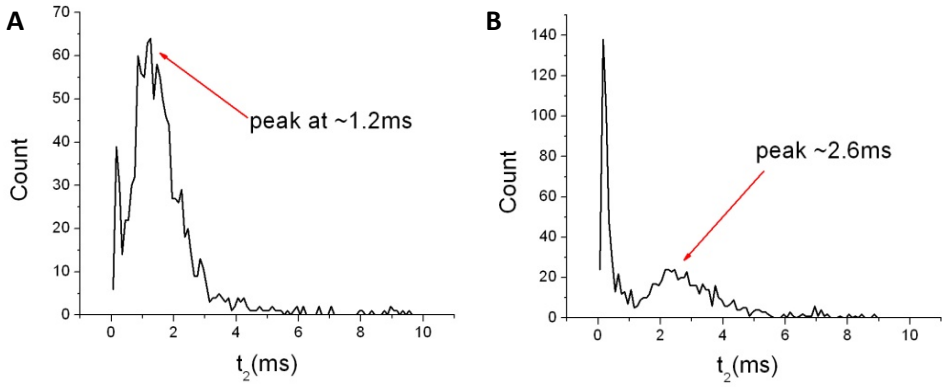

Figure 5.24 A) Event histogram of the translocation measurements of ODN23-E4-20. The peak indicated corresponds to the most probable translocation time of 1.2ms. B) Event histogram of the translocation measurements of ODN23-E4-40 with the most probable translocation time of 2.6ms.

In summary, Chapter 5.3 showed in detail the synthesis of ODN conjugates formed by the thiol addition to maleimide functionalized oligonucleotides. In Chapter 5.3.4 the synthesis of monodisperse ELP-ODN conjugates was discussed. These conjugates carry a free amino group at the end of the peptide block, which can be used for further modification. The following chapter is going to highlight the synthesis of ODN-ELP conjugates by the reaction of the free amino group of the peptide with an oligonucleotide carrying an activated ester. Therefore, these conjugates still carry the free thiol group of the C-terminus of the peptide. Each synthesis approach leads to monodisperse ODN-ELP diblock copolymers equal in composition, but differing in their end group.

5.4 Synthesis of ODN conjugates by Activated Ester Chemistry

The synthesis of oligonucleotide conjugates by using oligonucleotides functionalized with a succinimidyl activated carboxyl group (Figure 5.25) goes back to the PhD work of Dr. Nils Heimann.[120] He modified the reported conjugation of alkyl amines to oligonucleotides with an activated carboxyl group [153] by using monoprotected α,ω-diamino-polyethylenoxid to create ODN-PEO diblock and triblock copolymers. The synthesis of ODN-PEO multiblock copolymers has been continued by Tina Kiefer .

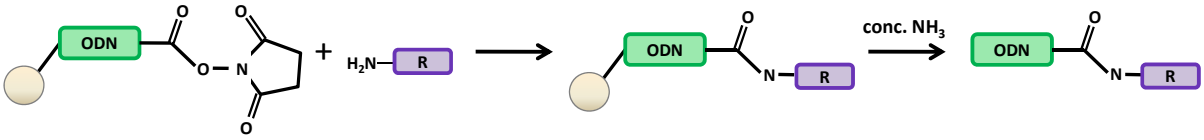

Figure 5.25 Reaction scheme for the conjugation of amino compounds to solid support bound oligonucleotides functionalized with a succinimidyl activated carboxyl group and the following cleavage of the solid support.

The linker carrying the activated carboxyl group can be introduced at the 5′-end of the oligonucleotide during standard solid phase synthesis. After the synthesis the oligonucleotide is usually cleaved of the solid support by concentrated ammonia. In the case of the activated ester functionalization it is necessary to perform the coupling of the amino component prior to the cleavage, because the succinimidyl ester reacts with the ammonia to yield an unreactive amid end group. The coupling prior to cleavage has two main advantages. The bases of the oligonucleotide bound to the solid support are fully protected. Therefore the coupling reactions can be performed in organic solvents which diminishes the hydrolysis of the active ester compared to the widely performed coupling in aqueous solution and prevents side reactions caused by the unprotected amino groups of the nucleotides. A second advantage is the easy handling and purification of the solid support. The amino component can be used in high excess to increase the coupling efficiency and is easily removed by washing the solid support after the reaction.

The reported coupling of monoprotected α,ω-diamino-polyethylenoxid to succinimidyl ester functionalized oligonucleotides was performed in dichloromethane containing 10% triethylamine with yields >90% [120] comparable to the coupling efficiency of the alkylamines [153]. This conjugation protocol is not applicable in the case of polypeptides as amino compounds due to their insolubility in the used solvents. The synthesis of ODN-ELP diblock copolymers has to be performed in aqueous solution because of the insolubility of the ELP in organic solvents. The following section demonstrates the successful synthesis of ODN-ELP diblock copolymers by coupling polypeptides to NHS activated oligonucleotides.

5.4.1 Protection of the cysteine moiety

In Chapter 4 the library of elastin-like polypeptides carrying one cysteine residue at the C-terminus of the peptide was introduced. These polypeptides are used to create ODN-ELP conjugates. The free thiol group of the cysteine is protected to minimize the formation of any side products and to have a selective coupling of the free amino group of the N-terminus with the succinimidyl ester functionalized oligonucleotide. The conjugation reaction follows a nucleophilic substitution mechanism. Hence, all presented nucleophiles are reactive, but the reaction of the sulfhydryl group with the NHS ester yields an unstable thioester[78], which hydrolyzes in aqueous solution. The thiol group can later be used as reactive functionality to create ODN-ELP-ODN triblock copolymers (Chapter 6).

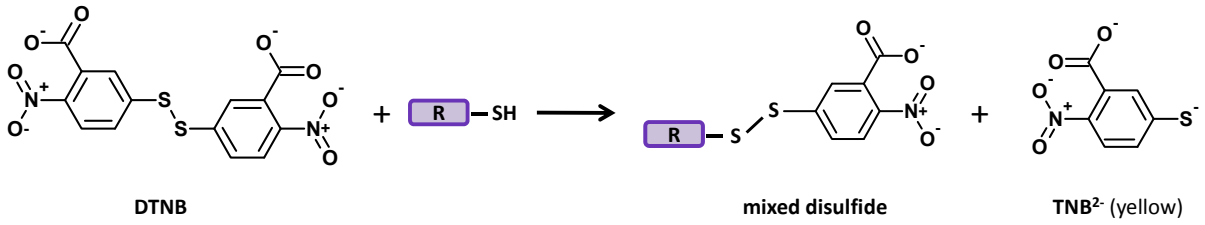

Figure 5.26 Reaction scheme of the thiol protection by Ellman's reagent DTNB.

The concentration of free thiol groups in peptide or protein solutions is usually determined by using the Ellman's assay[78]. This protocol involves the reaction of the thiol residues with 5,5'Dithio-bis-(2-nitrobenzoic acid) (DTNB). The DTNB reacts with the free thiol to yield a mixed disulfide and 2-nitro-5-thiobenzoic acid (TNB) (Figure 5.26). In solution the TNB anion is bright yellow and can be analyzed by UV-VIS spectroscopy. The concentration of TNB corresponds to the concentration of free thiols in the sample. The TNB extinctions are calibrated by using cysteine as standard compound.

The DTNB reaction can also be used to inactivate free thiols by creating a mixed disulfide. The advantage of this protection of the thiol group is its reversibility. The TNB protecting group can be cleaved off by the addition of reducing agent. The success of the deprotection can be followed by UV-Vis measurements because the resulting product is the TNB anion (yellow).

This DTNB reaction was used to protect the free thiol group of the E4 polypeptides for the synthesis of ODN-ELP diblock copolymers. Figure 5.27 shows a gel analysis comparing pure ELPs stored in solution to TNB protected ELPs. Lane 6 and lane 7 contain a sample of E4-120 and E4-60 stored in aqueous solution. In both cases the polypeptide dimer formed by thiol oxidation is detected. The amount of the dimers reaches almost 50% by gel intensities for the

unprotected ELPs. In contrast to this, the TNB protected ELPs show a dimer formation of less than 10%. Lane 1-5 contain the ELP library E4-20, E4-30, E4-40, E4-60 and E4-120. The peptides were incubated with reducing agent (TCEP) prior to the reaction with DTNB. The excess of DTNB was removed by column chromatography (Sephadex) in small scale experiments or by dialysis and salt precipitation of the polypeptide in large scale synthesis. The lower dimer content demonstrates the inhibition of the active thiol groups by the TNB protection. The remaining disulfide dimers are not interfering with the following conjugation reaction because they carry only reactive amino end groups. The thiol protected ELPs were used in the synthesis of ELP-ODN conjugates by activated ester chemistry described in the following section.

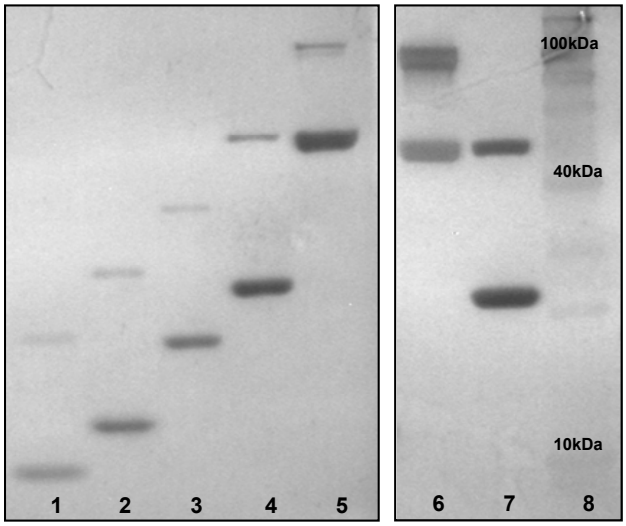

Figure 5.27 Gradient SDS-PAGE (10-20%) analysis of TNB protection reaction (silver staining). Lane 1: E4-20TNB; Lane 2: E4-30TNB; Lane 3: E4-40TNB; Lane 4: E4-60TNB; Lane 5: E4-120TNB; Lane 6: E4-120; Lane 7: E4-60, Lane 8: Peptide marker (Roti-Mark 10-150).

5.4.2 ODN-ELP diblock copolymers

The synthesis of ODN-ELP conjugates by activated ester chemistry is a two step procedure (Figure 5.28). The support-bound and linker modified oligonucleotide is incubated with a concentrated solution of the TNB protected polypeptide. The solid support is washed extensively after the reaction to remove any unreacted peptide. The oligonucleotide and its base protecting groups are cleaved off by the incubation with concentrated ammonia at elevated temperature (T= 47°C) over night.

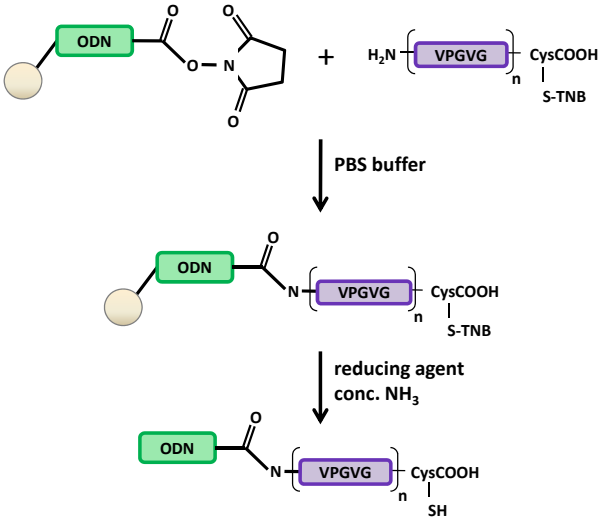

Figure 5.28 Scheme of the conjugation reaction of succinimidyl functionalized ODNs with ELPs by amide formation and the following cleavage of the solid support.

The synthesis results are going to be discussed on the example of the conjugation of an oligonucleotide with 23 bases (sequence S2) to E4-40 with TNB protected sulfhydryl groups. Figure 5.29A shows the analysis of a conjugation reaction performed with a peptide concentration of c=8mg/ml in 58mM PBS buffer at pH=7.3 by denaturating PAGE. In lane 2 the pure oligonucleotide shows the expected electrophoretic mobility of a 23mer. The reaction mixture after cleavage of the solid support in lane 3 yields three bands. The species with the highest electrophoretic mobility corresponds to unreacted oligonucleotide. The additional two bands show a very low electrophoretic mobility. The slowest species moves at the upper exclusion limit. The low electrophoretic mobility supports the conclusion that these are oligonucleotide-polypeptide conjugates, because the polypeptide carries almost no charges and therefore decreases the electrophoretic mobility dramatically. The movement in the electric field is exclusively due to the charges of the oligonucleotide. Two different ODN-polypeptide conjugates have formed, because two very slow species are detected. The distinction between the upper and the lower band was done by the addition of reducing agent to the sample prior to the electrophoretic analysis. Lane 4 shows the sample with reducing agent. In this case the slowest band disappears and the intensity of the other band increases. This experiment reveals the formation of a dimer conjugate by disulfide bridges. The remaining band therefore corresponds to the ODN-E4-40 conjugate.

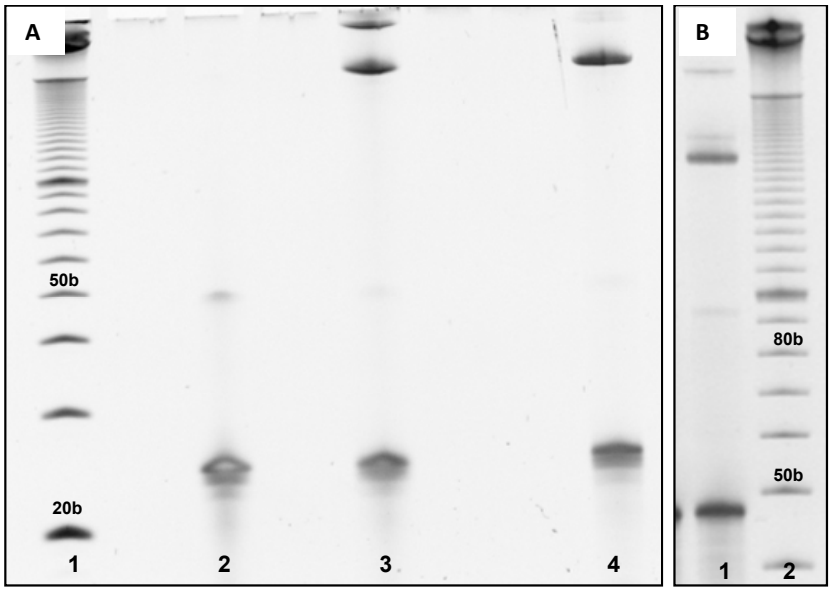

Figure 5.29 Denat. PAGE analysis of ODN-ELP conjugation by activated ester chemistry. A) 20% PAGE of the reaction of an ODN with 23bases (ODN23) and E4-40TNB. Lane 1: 10b marker; Lane 2: pure ODN23; Lane 3: reaction mixture of the conjugation after cleavage; Lane 4: reaction mixture of the conjugation after cleavage with the addition of reducing agent (TCEP); B) 10% PAGE of the conjugation of an ODN with 46 bases and E4-40TNB; Lane 1: reaction mixture of the conjugation after cleavage; Lane 2: 10b marker.

The dimer formation was expected to be suppressed by the introduction of the TNB protecting group, but it can be explained by taking the reaction conditions into account. The cleavage of the solid support is performed in concentrated ammonia, which acts as reducing agent under these harsh conditions[154]. For the following synthesis of ELP-ODN conjugates, an additional washing step of the solid support with reducing agent was usually applied. The washing step is also taken as indicator for the success of the reaction, because the reduced TNB results in a yellow coloring of the washing solution.

In Figure 5.29B the synthesis of E4-40 conjugated to an oligonucleotide with 46bases is presented. In this case the gel electrophoresis with an acrylamide percentage of 10% is used to give a higher resolution in the higher molecular weight regime. The difference between a gel with 20% and 10% acrylamide content can be seen in comparing Figure 5.29A and 5.29B. Resolution in the high molar mass range is enhanced for the gel with the lower acrylamide content (larger pore size) as expected. Compared to the marker lane also a difference in the electrophoretic mobility of the ODN-ELP diblocks is observed. This difference accounts for the change of the mass to charge ratio caused by the uncharged polypeptide block The mass to charge ratio is constant for DNA. Each base of the oligonucleotide carries the same charge in the given buffer. Hence, an oligonucleotide of unknown size can be characterized by its electrophoretic mobility compared to a commercially available marker. The presence of the ELP block increases the mass to charge ratio due to its coulombic neutral state. At the same

time the friction coefficient is increased by the larger hydrodynamic radius of the block copolymer in comparison to the pure unconjugated ODN. In sum, this determines the reduced electrophoretic mobility and the much slower migration velocity, which may be additionally reduced further by adsorption contributions of the ELP block to the gel matrix.

One important observation in Figure 5.29B is the detection of an additional band close to the ODN-ELP conjugate band. This shallow band was detected in a few independent diblock syntheses. The occurrence of this band was related to an oxidative impurity of the solid-phase synthesis. The purchased solid-bound, NHS functionalized oligonucleotide was normally received as white powder. The solid support showed in some cases a light yellow color. This color results from an insufficient washing of the solid support after the last step of the solid-phase synthesis, which involves the oxidation of the phosphate groups by iodine solution (Chapter 2.1.2). Residual iodine solution produces the yellowish color of the CPG and possibly accounts for the side product. The impurity is easily removed by additional washing steps after the solid-phase synthesis. This precaution prevents the formation of the side product.

5.4.3 Purification of ODN-ELP diblock copolymers

The last step of the solid support mediated synthesis of the ODN-ELP diblocks is the cleavage of the oligonucleotide off the solid support (CPG). The oligonucleotide is bound to the CPG by a covalent ester bond, which is cleaved by the addition of concentrated ammonium hydroxide solution. If the aminolysis is performed at elevated temperatures, it also removes the amino protecting groups of the bases, which are isobutyryl or benzoyl groups. In the resulting solution a mixture of the former protecting groups, the oligonucleotide and the oligonucleotide-polypeptide conjugates exists. The removal of the lower molecular weight impurities was done by extensive dialysis. In Figure 5.30 the dialysis of a diblock synthesis after cleavage was monitored by UV measurements. The crude solution (black) shows a high absorption at wavelengths smaller than 220nm. In comparison to the dialyzed sample, it also has an increased absorption in the range of 220-280nm. The determination of the ODN concentration by UV without dialysis is subjected to a huge error due to the absorption contribuition of cleavage side products. The dialysis was usually carried out for 5 days against Milli-Q water.

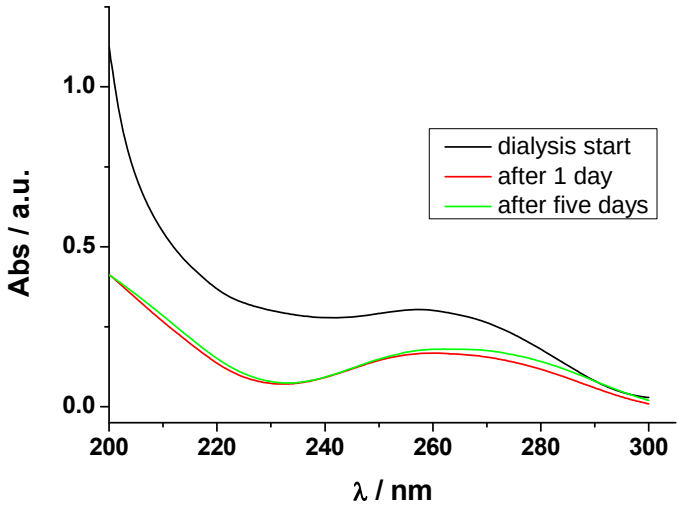

Figure 5.30 UV absorption measurements of the dialysis of a diblock synthesis after the solid support cleavage to monitor the removal of lower molecular weight impurities.

After the dialysis the solution still contains a mixture of the diblock and unreacted oligonucleotide. The unreacted polypeptide was removed earlier by washing the solid support after the reaction. The remaining oligonucleotide impurity contains shorter failure sequences caused by the solid phase synthesis (see Chapter 2.1.2), unfunctionalized oligonucleotides of the correct length and oligonucleotides whose active ester functionality was hydrolyzed during the reaction. To remove this oligonucleotide impurities, the salt precipitation, as already discussed in 5.3.4, was applied. The salt precipitation uses the nature of the ELP block to precipitate at high salt concentrations and/or elevated temperatures.

In Figure 5.31 the result of the purification by salt precipitation for a 46mer conjugated with E4-40 is presented. The gel analysis shows the supernatant (lane 1) containing the unreacted ODN. The resolubilized pellet (lane 2) shows only the desired diblock. If the salt precipitation in one step does not completely separate the two components, the procedure can be repeated several times. The yields of isolated diblock copolymers ranged from 15-30% in respect to the total DNA amount determined after dialysis. It has to be taken into account that this DNA amount contains the failure sequences of the solid-phase synthesis, the unfunctionalized DNA (no NHS linker) and the DNA hydrolyzed during synthesis. The reaction yield is therefore only an approximation. Depending on the coupling efficiency during solid-phase synthesis the yield of the targeted oligonucleotide is largely influenced (see Chapter 2.1.2). The efficiency of the NHS functionalization at the end of the solid-phase synthesis is also unknown. Hence, the amount of reactive oligonucleotide participating in the coupling reaction is lower than assumed.

In literature the reaction of the succinimidyl linker with alkyl amines has been reported to show a conjugation yield from 43% up to 77%.[153] The coupling of monodisperse PEO to NHS activated ODNs was reported to result in coupling efficiencies of >90%.[120] These reactions were performed in a triethylamine/DMF mixture in all cases, where no hydrolysis of the activated ester occurs. Therefore, the lower coupling efficiency in aqueous media is reasonable.

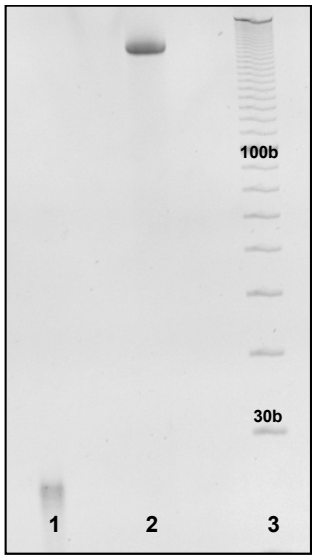

Figure 5.31 Denat. 15% PAGE analysis of the purification of ODN-ELP diblock copolymers by salt precipitation. Lane 1: supernatant containing the unreacted ODN; Lane 2: resolubilized pellet of the salt precipitation containing the diblock; Lane 3: 10b marker.

One major problem that occurred in large-scale synthesis of the diblocks was the poor solubility of the resulting pellet. Also, it was observed that the high concentrated diblock solutions showed precipitation after long time storage at 4°C. This precipitation always went along with a decrease in oligonucleotide concentration. Hence, a slow aggregation process of the diblock occurs. The insoluble matter was partially resolubilized in buffer containing SDS and/or reducing agent. The insolubility of the aggregates can not be fully explained. Several interactions between the diblocks are possible. The formation of dimers by disulfide bridging, as discussed earlier, is obvious. It is also reported that nucleotides can interact with aromatic amino acids.[155] The polypeptide block carries one phenylalanine residue besides the active thiol group. This could lead to an attractive interaction. Additionally, an unspecific hybridization of the non-complementary oligonucleotides is possible. All the interactions named can cause an aggregation of the synthesized diblock copolymers. The irreversibility of this aggregation is surprising, because by the addition of detergents, reducing agent and heat all interactions should be destroyed. The aggregation behavior and structure formations are under investigation.

An alternative method for the purification is the separation of the two components by preparative GPC. As mentioned in Chapter 5.3.4 tests of possible column materials and elution conditions are performed. This method would replace the salt precipitation and the irreversible diblock aggregation, hopefully.

Further characterization of the diblocks by dynamic light scattering is presented in Chapter 5.4.5. The next section shows the application of the activated ester chemistry to the ELP library to yield block copolymers with variable peptide blocks.

5.4.4 ODN-ELP diblock copolymer library

The following section provides an insight into the diversity of the discussed ODN-ELP diblock copolymer synthesis by activated ester chemistry. Both reactants can easily be varied in length and in sequence.

In Figure 5.32 the conjugation of an oligonucleotide with 23 bases and the five polypeptides of the E4 library are presented. Lane 1 contains the pure oligonucleotide. Lane 2 shows the conjugation reaction of the ODN with E4-120, the longest polypeptide with 120 repeat units. The following lanes contain the product of the conjugation between the ODN and E4-60 (lane 3), E4-40 (lane 4), E4-30 (lane 5) and E4-20 (lane 6).

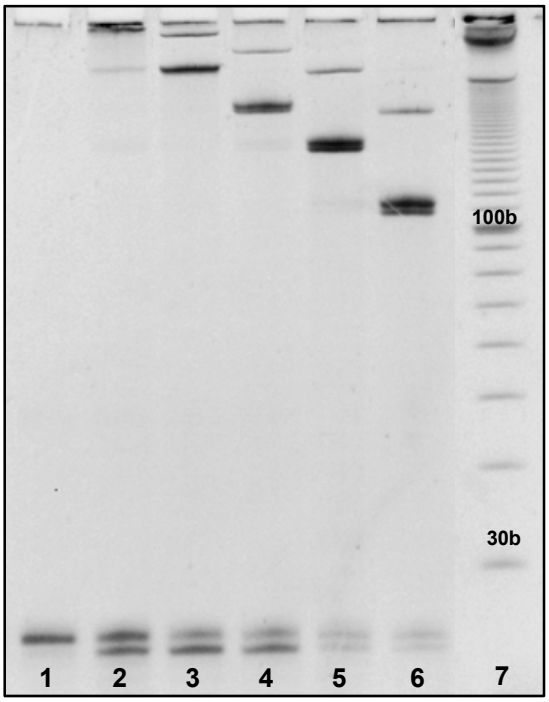

Figure 5.32 Denaturating PAGE (15%) analysis of the conjugation between an ODN of 23 bases and five ELPs (E4 library) differing in length. All samples were analyzed after the cleavage of the solid support without purification. Lane 1: pure ODN23; Lane 2: reaction of ODN23 and E4-120; Lane 3: reaction of ODN23 and E4-60; Lane 4: reaction of ODN23 and E4-40; Lane 5: reaction of ODN23 and E4-30; Lane 6: reaction of ODN23 and E4-20; Lane 7: 10b marker.

In general, the crude reaction mixtures exhibit three bands. The band with the highest electrophoretic mobility is caused by the pure ODN. The slowest migrating species corresponds to the diblock dimer formed by disulfide bridging and the most intensive band is assigned to the ODN-ELP diblock. The diblock dimer corresponds to an ODN-di-polypeptide-ODN triblock coplymer linked via a disulfide bridge. The oxidation of the thiol group in aqueous solution produces therefore a triblock copolymer carrying the same ODN sequence. In Chapter 6.2 the application of hexapeptide containing triblock copolymers in DNA self-assembly is discussed further. All diblock copolymers show a highly decreased electrophoretic mobility, which decreases with increasing polypeptide length. The largest conjugate, E4-120-23ODN, did not migrate at all. The sample remained in the well of the gel. Therefore the separation of the diblock and its dimer is not possible using this gel analysis. All samples are still contaminated with unconjugated oligonucleotide, which is identified by the comparison with the pure ODN in lane 1. Surprisingly , two bands are detected in this range for the reaction mixtures. As the electrophoretic mobility of the additional band is higher than the pure ODN, it has to be a shorter oligonucleotide or a higher charged species. The second band can not be explained by an error in solid-phase synthesis, because the reference ODN, which corresponds to the pure reactant, does not show the second band. A contamination by DNase, an enzyme which hydrolyzes DNA, is also unlikely, because degradation into the single bases should occur in this case. The band might correspond to a side-product of the active ester hydrolysis, but this has to be verified. The gel analysis though clearly shows that the synthesis with all five polypeptides is feasible and provides a tool for the preparation of ODN-ELP diblock copolymers with different block lengths. The oligonucleotide block can easily be altered as well, for example in length or base composition, by adapting the solid-phase synthesis.

The previous section showed the high potential of the NHS ester mediated synthesis of ODN-ELP diblock copolymers, which were so far characterized by gel electrophoresis. The next chapter will provide the characterization of the block copolymers by dynamic light scattering.

5.4.5 DLS characterization of ODN-ELP diblock copolymers

Dynamic light scattering (DLS) is a powerful tool to determine the diffusion coefficient and consequently the hydrodynamic radii of the scattering particles by applying Stokes-Einstein's law. It is also highly sensitive to impurities or heterogeneity of the sample. One demand of this work is the synthesis of monodisperse block copolymers. Hence, the following measurements by DLS will give a fundamental characterization of solution

properties of the synthesized conjugates, e.g. aggregation or phase separation. The measurements of an E4-40 polypeptide conjugated to a 46mer shown in Figure 5.33 were all performed at an angle of 17° at T=20°C in 32mM NaCl solution. None of the samples showed an angular dependence of the scattering intensity. Figure 5.33 presents the correlation function plotted versus the correlation time in a semi-log plot for a pure oligonucleotide with 46 bases (cODN46, black dots), the pure E4-40 (E4-40, blue dots), the conjugate of ODN46 and E4-40 (ssODN46-E4-40, red dots) and the conjugate hybridized with the complementary strand cODN46 (dsODN46-E4-40). All correlation functions show a single exponential decay indicating the monodispersity of the samples.

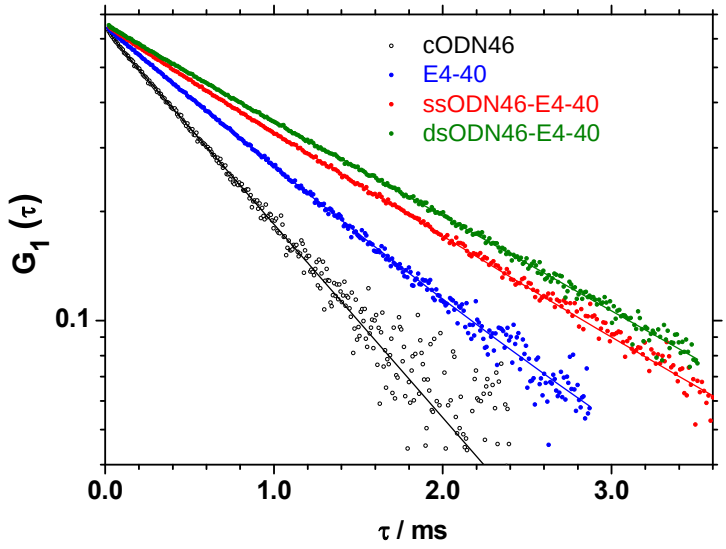

Figure 5.33 Correlation function $G_1(t)$ of cODN46, E4-40, ssODN46-E4-40 and dsODN46-E4-40 plotted vs. the correlation time t in a semi logarithmic scale.

The hydrodynamic radii were derived from the diffusion coefficient by using the Stokes-Einstein equation. The results are summarized in Table 5.3. The hydrodynamic radius of the oligonucleotide (R_H=2.6nm) is smaller than the radius of the pure polypeptide E4-40 (R_H=3.6nm). The radius increases to 4.6nm after the conjugation of the two components. The hybridization of the conjugate with the complementary strand cODN46 leads to the transformation of the coil structure into a coil-rod structure of the block copolymer, which shows a larger hydrodynamic radius of 5.4nm as expected.

Table 5.3 Hydrodynamic radii determined by dynamic light scattering and hydrodynamicall effective chain cross-section d_{eff} used for the determination of the Kuhn statistical length l_k.

	R_H / nm	d_{eff} / nm	l_k / nm
cODN46	2.6	2.0	2.4
E4-40	3.6	1.0	2.5
ssODN46-E4-40	4.6	1.5	2.4
dsODN46-E4-40	5.4	-	-

The measured hydrodynamic radii were used to obtain the Kuhn statistical length l_k as discussed in Chapter 4.4. For the nummerical analysis the length per repeat unit for single stranded DNA was assumed to be b=0.59nm.[14] The constants used for the effective chain cross-section d and the calculated values of l_k are summarized in Table 5.3. The values received for the Kuhn length demonstrate the consistency of the measured data. The analysis of the dsODN46-E4-40 is not possible, because no hydrodynamic theory has been developed so far for rod-coil structure.

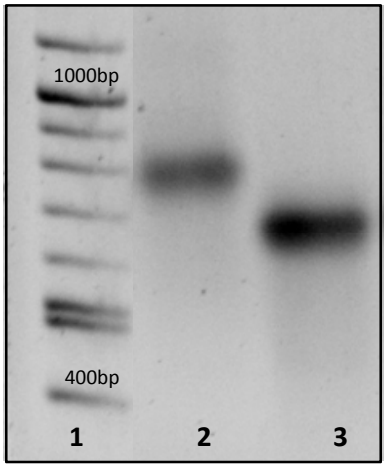

Figure 5.34 Native agarose gel electrophoresis (1.7%). Lane 1: 100bp marker; Lane 2: ssODN46-E4-40; Lane 3: dsODN46-E4-40.

The hybridization was also monitored by native agarose gel electrophoresis to ensure a uniform structure formation. Figure 5.34 shows the gel analysis of the pure ODN46-E4-40 in lane 2 and the product of the hybridization with the cODN46 (lane 3). The hybridized sample is migrating faster in comparison to the diblock carrying the single stranded ODN. The increase in electrophoretic mobility is due to the increase in charges by the addition of the second strand. The diblock hybridized completely with the complementary strand. Only

hybridized dsODN46-ELP is detected. This corresponds to the DLS result where no fast mode, which corresponds to lower molecular weight species, is found.

The ODN46-E4-40 conjugate and the corresponding hybridization product were also subject to dynamic light scattering measurements at elevated temperatures. As shown in Chapter 4.3, elastin-like polypeptides exhibit a phase transition at a characteristic temperature. The used E4-40 has a transition temperature in the range of 35-46°C depending on the peptide concentration and the ionic strength of the buffer. Therefore, the diblock copolymers were investigated at elevated temperatures to observe the collapse of the polypeptide block, which would result in a smaller hydrodynamic radius. The collaps of the ELP block might also be follow by an aggregation of the diblock copolymers into ordered structures like micelles or vesicles. For the single stranded sODN46-E4-40 intensity spikes were recorded by DLS immediately after heating the sample to T=55°C. This indicates the onset of phase separation of the block copolymer, i.e. micelle formation as observed for ELP-ELP diblock copolymer [70] does not occur.

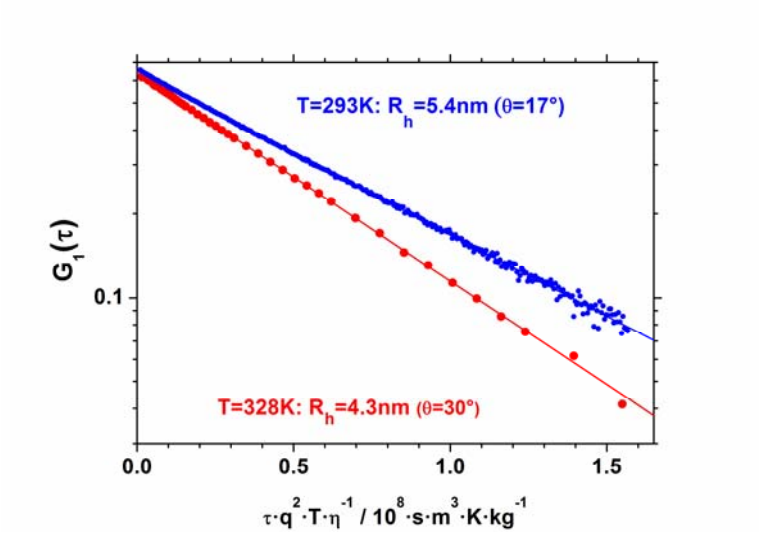

Figure 5.35 Comparison of the dynamic light scattering measurements of dsODN46-E4-40 at T=20°C and at T=55°C.

For the double stranded dsODN46-E4-40 a different behavior was monitored. Figure 5.35 shows the correlation function $G_1(\tau)$ plotted versus τ, which had to be normalized according to the measuring angle, the temperature and the viscosity, for the dsODN46-E4-40 at room temperature and at T=55°C. The measurement at elevated temperature shows a well detectable decrease in the hydrodynamic radii from 5.4nm at RT to 4.3nm at T=55°C. The smaller radius is close to the single strand ssODN46-E4-40 most propopably due to the collapse of the ELP block. Also the dehybridization can not be completely excluded, because

the UV melting profile shows a dissociation of 25% into ssODN at T=55°C. The ELP collapse has to be demonstrated by additional measurements with an increased salt concentration, which lowers the transition temperature of the ELP. After an incubation time of longer than 60min at higher temperature, intensive spikes occurred for the double stranded sample comparable with the observations for the single stranded block copolymer.

The discussed DLS measurements confirm the monodispersity and purity of the synthesized ODN-ELP conjugates, especially the absence of higher molecular mass impurities with high sensitivity. This has already been seen in the electrophoretic analysis, which additionally confirms the missing low molar mass impurities. The hybridization of a complementary strand to the diblock copolymer demonstrates that the single strand of the diblock are able to hybridize quantitatively and that they form well defined double stranded diblock copolymers. In the next section the possibility of a defined association by hybridization is going to be exploited to produce ODN-ELP diblock copolymer self-assemblies.

5.5 Self Assembly of ODN-ELP diblock copolymers

For the self assembly of ODN-ELP diblock copolymers into a four arm star, four different diblocks had to be synthesized. The diblocks varied in their oligonucleotide sequences. The sequences were chosen based on the K4 DNA four-arm junction, discussed in Chapter 3, and conjugated to the polypeptide E4-40. The conjugation was performed by the activated ester approach and followed by the described purification steps in Chapter 5.4.3. Figure 5.36 shows a schematic of the desired self-assembly.

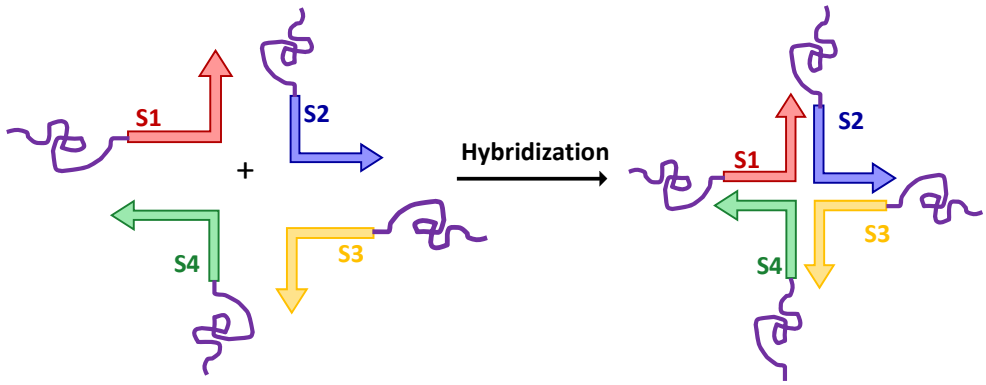

Figure 5.36 Schematic for the self-assembly of four ODN-ELP diblock copolymers into a four arm star.

The four ODN-ELPs were mixed in an equimolar ratio (c_{DNA}=1-4µg/µl) in TAE buffer containing magnesium acetate (12.5mM). The hybridization was performed by slowly cooling from 95°C to 8°C using a thermo cycler. The hybridization was investigated by

native agarose gel electrophoresis shown in Figure 5.37. The small schematics indicate the self-assembled structures corresponding to the samples applied on the gel.

In lane 7 of Figure 5.37 the migration behavior of a pure ODN-E4-40 diblock is observed. A mixture of a diblock copolymer carrying the K4S1 and the K4S2 sequences is analyzed in lane 6. Compared to the pure diblock a decrease in electrophoretic mobility is seen. This indicates the association of the two single strands of the diblocks. The band is well defined and discrete. Lane 6 also contains a mixture of two ODN-E4-40 diblocks, but here the diblocks with the K4S1 and K4S3 sequences were combined. The detected band migrates like the pure diblocks. Thus the chosen sequences do not hybridize, as expected.

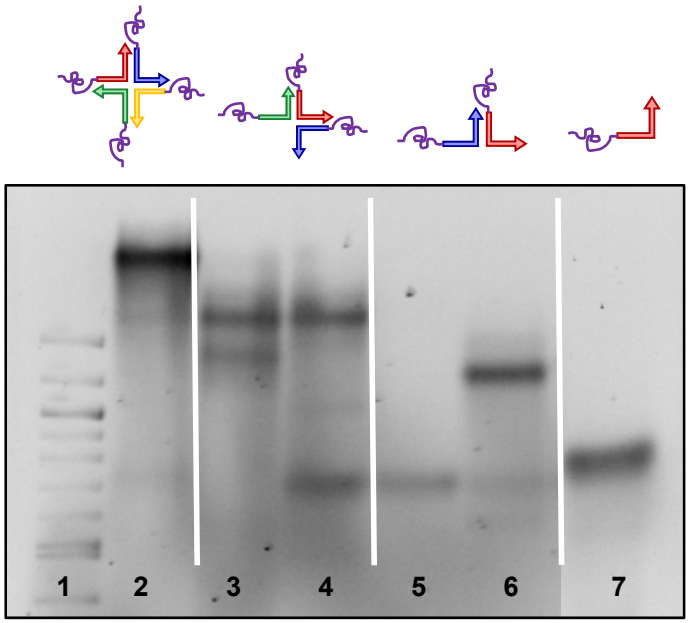

Figure 5.37 Native agarose gel electrophoresis (1.7%) of a diblock hybridization experiment. Lane 1: 100bp marker; Lane 2: mixture of four ODN-E4-40 diblocks with oligonucleotide sequences based on the four-arm DNA junction K4; Lane 3+4: mixture of three ODN-E4-40 diblocks; Lane 5: mixture of two ODN-E4-40 diblocks carrying the sequences K4S1 and K4S3; Lane 6: mixture of two ODN-E4-40 diblocks carrying the sequences K4S1 and K4S2; Lane 7: pure ODN-E4-40 diblock.

In lane 3 and lane 4 the combinations of three different diblock copolymers are analyzed. The resulting assemblies have a decreased electrophoretic mobility compared to the dimer formed in lane 6. Both trimer combinations show additional bands which migrate faster. In lane 4 the band corresponds to the pure ODN-E4-40. The additional band in lane 3 migrates in the range of the dimer in lane 6. These impurities are maybe caused by an error in mixing. If the concentration determination was not accurate, an equimolar mixing is not possible. Finally, in lane 2 the combination of all four ODN-E4-40 diblocks can be seen. The resulting band has the smallest electrophoretic mobility corresponding to a higher molecular weight

species. One major band is present, which indicates the formation of the desired four-arm diblock star.

This experiment showed that the hybridization of the ODN-ELP into defined structures is possible. The hybridization pattern matches the one observed for the simple ODN four-arm junction in Chapter 3.4. The ODN-ELP is therefore a potential building block for DNA self-assembly, which incorporates a flexible element, the peptide block, into the rigid structures formed exclusive by dsDNA.

5.6 Summary

The previous chapters discussed the synthesis of ODN-ELP diblock copolymers in detail. First, it was evaluated that a synthesis of these copolymers is not possible by the use of methacrylate functionalized oligonucleotides (Acrydite™). Using this approach, only the addition of low molecular weight species with a reactive thiol group was successful.

A second approach led to the modification of amino functionalized oligonucleotides by several heterobifunctional linkers with the aim to yield a thiol reactive functionalization. The kinetics of the linker hydrolysis and their reactivity towards oligonucleotides were tested. The functionalization by SMCC, a linker carrying a maleimide residue, revealed the best results. The kinetic of this reaction was analyzed by HPLC and several addition reactions with thiol compounds were investigated finally resulting in the conjugation of cysteine containing ELPs to maleimide functionalized oligonucleotides. This synthesis approach has been expanded to diblock copolymers with different block composition.

Additionally, the synthesis of ODN-ELP diblock copolymers has also been established by the use of succinimidyl functionalized oligonucleotides. The activated ester ODNs are bound to a solid support, which facilitates the handling and the purification of the ODN-ELP diblocks. This synthesis was also applied to generate diblock copolymers differing in block length. Thus, two synthetic approaches yielding ODN-ELP block copolymers differing in their reactive end group were established.The additional characterization by dynamic light scattering demonstrated the monodispersity of the synthesized block copolymers and investigated their hydrodynamic dimensions, which relate to the reactant compounds as expected.

The hybridization behavior of the ODN-ELP diblocks was tested by offering simply a complementary strand to yield a coil-rod compound. Furthermore, the formation of a diblock star with four arms was investigated by combining four different ODN-ELP

diblocks with partially complementary sequences. For both setups a complete structure formation was observed, which implies the possibility of using the ODN-ELP diblocks in DNA self-assembly. In the following chapter this approach is continued by discussing the synthesis of ODN-ELP triblock copolymers. The functionalization of the diblock copolymers with an additional single stranded oligonucleotide offers the possibility to create higher order structures, like the network structures introduced in Chapter 1.

6 ODN-Peptide-ODN Triblocks

The previous chapter demonstrated the synthesis of oligonucleotide-polypeptide diblock copolymers by thiol addition or by activated ester chemistry. These two approaches can be combined to synthesize oligonucleotide-Elastin-like polypeptide-oligonucleotide (ODN-ELP-ODN) triblock copolymers. These triblock copolymers can be used as building blocks for DNA self assembly. This chapter provides an insight into the synthesis and first characterization results of these triblock molecules.

6.1 ODN-Hexapeptide-ODN conjugates

The synthesis of ODN-Peptide-ODN triblock copolymers was first tested by using a hexapeptide (Val-Pro-Gly-Val-Gly-Cys) as middle block. The used hexapeptide (Figure 5.3) was already employed in the addition reactions to maleimide functionalized oligonucleotide (see Chapter 5.3.3). It carries a free amino group at the N-Terminus and a cysteine moiety at the C-Terminus. The synthetic approach for ODN triblock copolymer is presented in Figure 6.1.

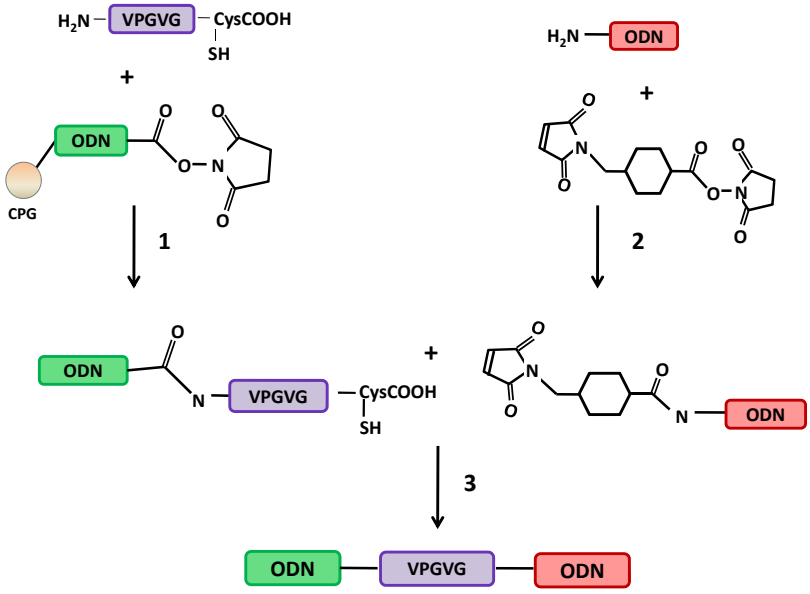

Figure 6.1 Scheme for the synthesis of ODN-Hexapeptide-ODN conjugates. In step 1 the conjugation of the hexapeptide to a succinimidyl functionalized oligonucleotide, which is bound to a solid support (CPG), is performed. The reaction follows the cleavage of the solid support. In step 2 an amino modified oligonucleotide is functionalized with SMCC to obtain a maleimide modified ODN. The third step involves the coupling of the ODN-Hexapeptide and the maleimide ODN by thiol addition.

The approach involves the combination of the ODN-hexapeptide diblock synthesis by activated ester chemistry with the thiol addition to a maleimide functionalized ODN. In Figure 6.2 a gel analysis of the ODN23-hexapeptide-ODN23 coupling is presented. The activated ester coupling (step 1 Figure 6.1) was performed by adding a concentrated hexapeptide (c=70mM) solution in 0.1M PBS (pH=7.3) to the solid support bound oligonucleotide. The mixture was incubated for 6h. Meanwhile the second step was performed by modifying an amino oligonucleotide with SMCC under the conditions described in Chapter 5.2.3. The excess SMCC was removed by gel column chromatography and the solution was immediately combined with the washed solid support of step 1. Lane 5 of Figure 6.2 contains the pure NHS-activated ODN23 (cleaved off the solid support) as reference. In Lane 2 a sample of the reaction after step 1, the hexapeptide coupling, was applied. Lane 3 and 4 contain the reaction mixtures after step 3 incubated for 22h and for 90h. Between the latter two samples no difference is observed. Both samples show multiple bands. In comparison to lane 5 the band with the highest electrophoretic mobility can be assigned to the pure ODN23. The band pattern of lane 2 and 3 are similar except that lane 3 shows an additional band in the middle part. Lane 2 exhibits only two distinct bands instead of three in this area.

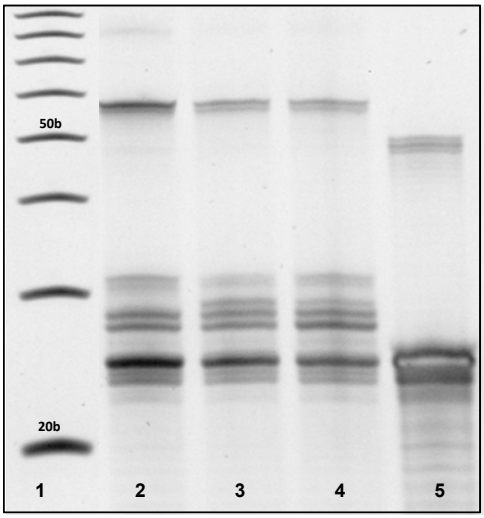

Figure 6.2 Denat. PAGE (20%) of the ODN23-hexapeptide conjugation reaction. Lane 1: 10b marker; Lane 2: sample of the ODN23-hexapeptide diblock synthesis by activated ester chemistry (step1); Lane 3: sample of the ODN23-hexapeptide after incubation with maleimide ODN23 for 22h (step3); Lane 4: sample of the ODN23-hexapeptide-ODN23 after incubation with maleimide ODN23 for 90h (step 3); Lane 5: pure ODN23.

The sample of lane 2 was investigated additionally after the addition of reducing agent. Figure 6.3 shows the denaturating gel analysis of a reduced (lane1) and a non-reduce sample (lane 2) of the reaction after step 1. Next to the gel picture an assignment of formed

conjugates to the observed bands is proposed. The addition of reducing agent reveals that the band with the lowest electrophoretic mobility consists of a disulfide bridged compound. In comparison to the marker lane in Figure 6.2 the compound migrates in the range of 55-60 bases, which indicates a conjugate with two oligonucleotides (2x 23bases) plus a linker molecule. Hence, taking disulfide bridging into account the proposed compound is the disulfide bridged dimer of the hexapeptide-ODN conjugate. The two additional bands in the range of 26-28 bases are assigned to the desired ODN-Hexapeptide conjugate and an ODN-hexapeptide conjugate with two peptide units joined by disulfide bridges. The reduced sample in lane 1 of Figure 6.3 does not reveal a clear distinction between those two compounds.

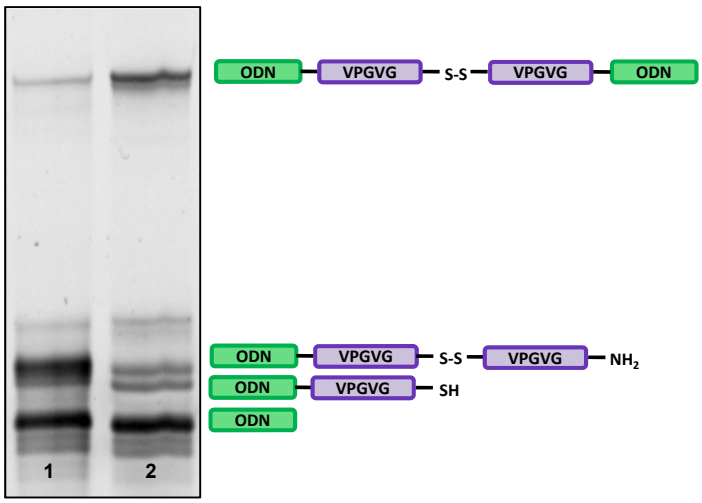

Figure 6.3 Denat. PAGE (20%) of the ODN-hexapeptide conjugation reaction. Lane 1: reduced sample of the reaction after step 1; Lane 1: non-reduced sample of the reaction after step 1 (compare to lane 2 in Figure 6.2).

The analysis of the sample after step 3 of the reaction with the addition of reducing agents also resulted in the disappearance of the band corresponding to the ODN-hexapeptide-ODN disulfide (Appendix 9.1.3). The desired ODN-hexapeptide-ODN conjugate should have migrated in the range of the ODN-di-hexapeptide-ODN disulfide. Therefore no triblock copolymer was formed.

As shown above the reaction did not yield the desired triblock copolymer, but the sulfide bridged ODN-hexapeptide dimer also corresponds to an ODN-di-hexapeptide-ODN triblock, which links two of the same ODNs with two hexapeptide units. This triblock molecule was isolated by gel extraction and small scale hybridization experiments were performed to investigate the association behavior.

6.2 Self assembly of ODN-di-hexapeptide-ODN triblocks

The oxidation of an ODN-hexapeptide diblock yields an ODN-di-hexapeptide-ODN triblock as discussed above. Both ODNs are connected to the hexapeptide at their 5′-end. This has to be considered for the design of complementary ODN to connect the triblock molecules. The triblocks can be linked by the addition of two partially complementary strands.

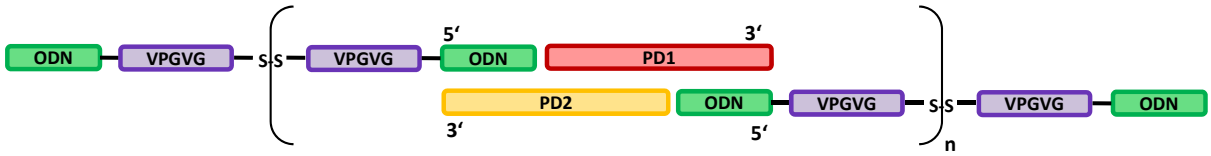

Figure 6.4 Scheme for the linear linkage of the ODN-di-hexapeptide-ODN triblock copolymers by hybridization with PD1 and PD2.

Figure 6.4 shows the scheme for a linear polymerization of the triblocks by the addition of strand PD1 and PD2, each composed of 60 bases. The strands were chosen to be complementary to the 23 bases of ODN sequence at their 3′ end. The remaining 37 bases of the 5′ end are complementary to the second strand (PD1, PD2). The resulting oligomer has a repeat unit of 83 base pairs plus two hexapeptide units, which decrease the electrophoretic mobility in the range of 5 base pairs (see denaturating gel analysis Figure 6.2, note two bases equal one base pair). The monomer unit has therefore an estimated electrophoretic mobility of 88bp.

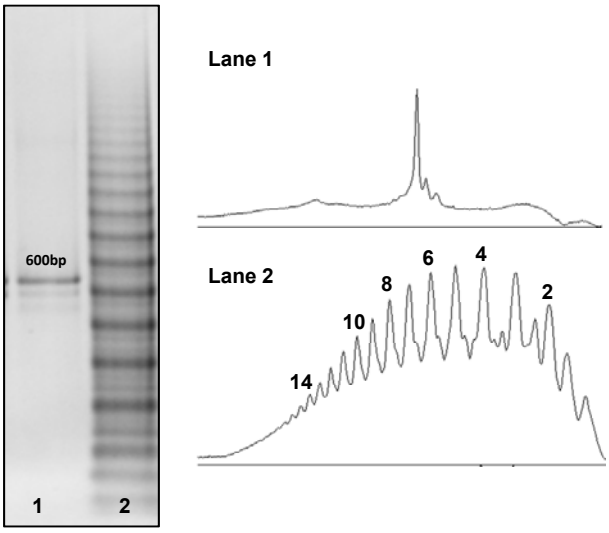

Figure 6.5 Agarose gel electrophoresis (3%) and gel intensity profiles of the hybridization of ODN-di-hexapeptide-ODN with PD1 and PD2. The degree of polymerization is indicated at the intensity profile for lane 2. Lane 1: 600bp DNA; Lane 2: oligomerized ODN-di-hexapeptide-ODN.

In Figure 6.5 the gel analysis of a hybridized sample of the synthesized triblock mixed with PD1 and PD2 is presented. The gel picture clearly shows an oligomerization of the triblock (lane 2) for the hybridization performed at RT overnight (no heating involved, only mixing). The hybridization resulted in the formation of large oligomers. The intensity profiles picture a weight averaged distribution function of the resulting polymers comparable to a Schulz-Flory distribution. Lane 1 in Figure 6.4 contains a dsDNA with 600 base pairs. Compared to this reference the degree of oligomerization can be assigned to the different bands using the calculated electrophoretic mobility of the monomer unit. The degree of oligomerization is indicated at the intensity profile of lane 2. The indication is based on the calculated values (P_i=i•88bp) in table 6.1.

Table 6.1 Degree of polymerization P_i and corresponding size in base pairs (bp).

P_i	1	2	3	4	5	6	7	8
Size in bp	88	176	264	352	440	528	616	704

In Figure 6.6 the scheme for a second hybridization experiment is presented. The 5′ ends of the linking strands (T2A, T2B, 60 bases each) were designed to be complementary to the ODNs at the triblock. The linking topology of the formed hybrids is therefore different to the former one shown in Figure 6.4.

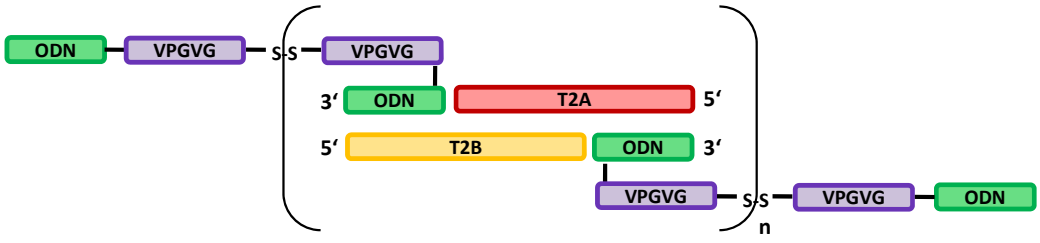

Figure 6.6 Scheme for the linkage of the ODN-di-hexapeptide-ODN triblock copolymers by hybridization with T2A and T2B.

The tail of the triblock at the 5′ end of one ODN is displaced by the double strand linkage of T2A and T2B. Figure 6.7 shows the native agarose gel analysis and the resulting intensity profiles of the different samples. In lane 1 the hybridization was performed with a temperature controlled program (Hyb90nig), which cools the sample from 90°C to RT over 18h. Lane 2 contains a sample hybridized by utilizing a temperature program (Hyb90) with a cooling interval of 2h. The third sample in lane 3 was also hybridized using the Hyb90 program and then stored for 5 days at 4°C. The samples in lane 1 and 3 show a higher degree of oligomerization than the sample in lane 2. The oligomerization seems to be influenced by

the hybridization time. The hybridization over 2h does not result in equilibrium. This effect can be due to the steric hindrance of the triblock tail, which blocks the two added ODNs to form a linkage between two triblock molecules. In comparison to the first hybridization experiment the degree of polymerization is lower. This might also be because of the steric hindrance.

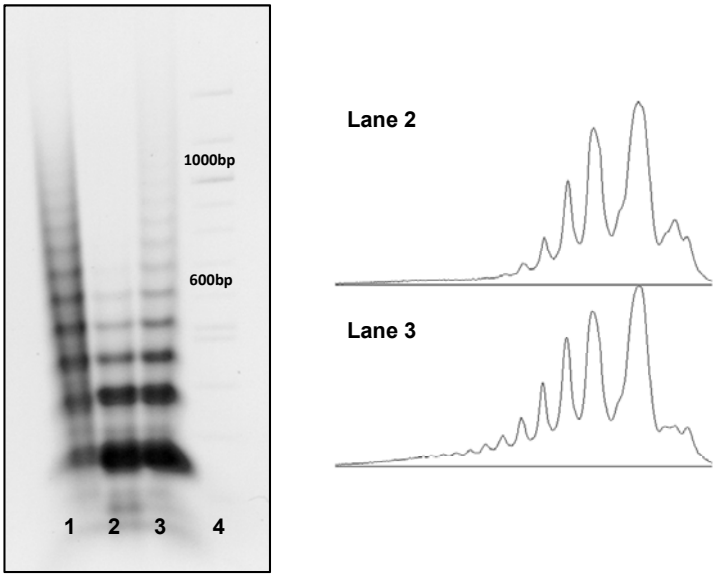

Figure 6.7 Agarose gel electrophoresis (3%) and gel intensity profiles of the hybridization of ODN-di-hexapeptide-ODN with T2A and T2B.

The latter two sections showed the synthesis of ODN hexapeptide triblock molecules and their oligomerization by hybridization. The triblock molecules were not obtained by the proposed synthesis approach, because the thiol addition was not successful. Instead the synthesized ODN-hexapeptide conjugates dimerized by disulfide bridging and formed ODN-di-hexapeptide-ODN block copolymers. The next chapter discusses the synthesis of ODN-ELP-ODN triblock copolymers based on a slightly modified approach.

6.3 Synthesis ODN-ELP-ODN triblock copolymers

The synthetic approach for ODN-ELP-ODN triblock copolymers involves first the synthesis of the ODN-ELP diblock by activated ester chemistry (Chapter 5.4) and its isolation by salt precipitation. The second oligonucleotide is functionalized with SMCC and combined with the ODN-ELP diblock copolymer (Figure 6.8) in solution.

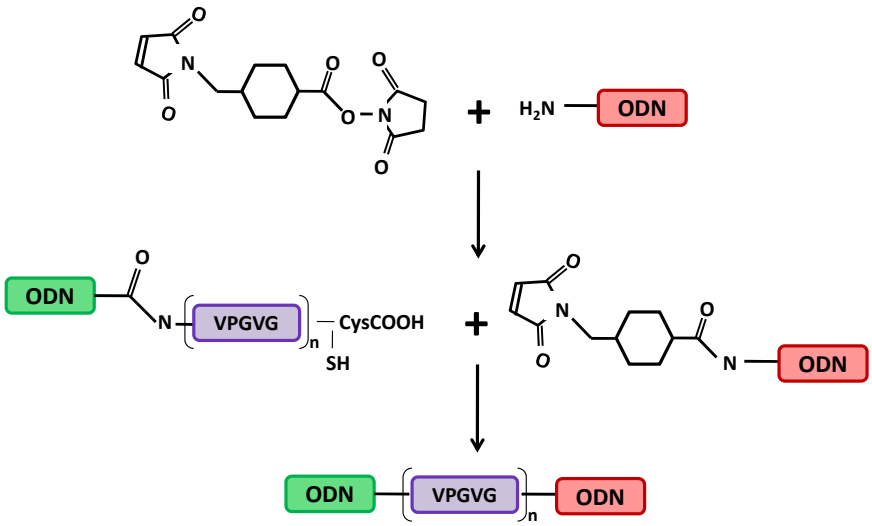

Figure 6.8 Reaction schematic for the synthesis of ODN-ELP-ODN triblock copolymers.

This synthesis approach was tested by using two oligonucleotides with the same base sequence of 23 bases (S2). The ODN-ELP diblock was synthesized using the described protocol in Chapter 5.4.2. The maleimide functionalization was performed as shown in Chapter 5.2.3 The diblock was purified by salt precipitation and incubated with reducing agent prior to the addition of the maleimide oligonucleotide, which was performed in degassed PBS buffer (0.01M phosphate, 0.015M NaCl) at pH=7.3 with a 20x excess of the maleimide compound. The results of this reaction are presented in Fig 6.9.

Lane 1 in Figure 6.9 contains the ELP E4-40 with reducing agent. In lane 2 the same peptide was analyzed without adding reducing agent. It is clearly demonstrated that the peptide in solution forms dimers by disulfide bridging. The molecular weight of the monomeric ELP4-40 is M_w=16800g/mol. Lane 5 contains the purified diblock ODN23-E440 after salt precipitation. In lane 5 the reaction mixture of the triblock synthesis shows an additional intense band of M_w ~ 35 000g/mol. The expected molecular weight of the triblock ODN23-E440-ODN23 is 31 000g/mol.

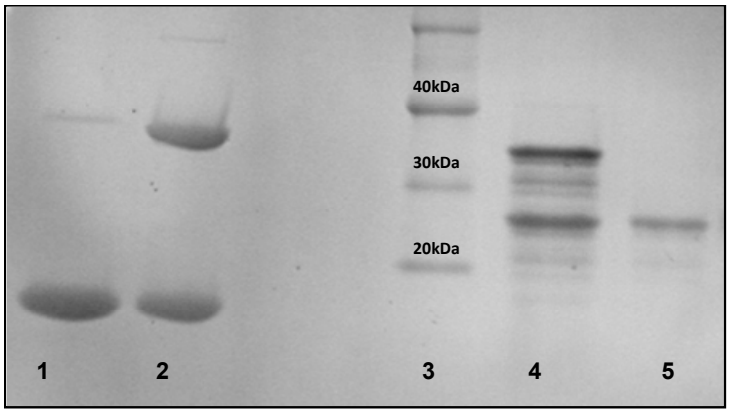

Figure 6.9 Gradient (10-20%) SDS-PAGE of the ODN23-ELP-ODN23 triblock synthesis stained by EtBr. Lane 1: reduced E4-40; Lane 2: non-reduced E4-40; Lane 3: peptide marker (Roti-mark); Lane 4: reaction mixture triblock synthesis; Lane 5: purified diblock ODN23-E440.

As described in Chapter 4.2 the electrophoretic mobility for ELPs is usually smaller than expected, which may explain the deviation of the triblock migration from the expected electrophoretic mobility compared to the marker lanes. The additional faint bands between the triblock and the diblock bands are surprising, because the reaction mixture contains only the diblock, the maleimide functionalized ODN and unmodified ODN. The first two components are monodisperse and yield a monodisperse conjugate with a defined mass. The unmodified ODN2 has no reactive group to interfere with the conjugation reaction. Hence, only a conjugate with a defined molecular weight, resulting in one band in the electrophoretic analysis, should be formed. One possible explanation of the additional bands might be the interference of the negatively charged oligonucleotide with the formation of SDS-micelles. In SDS-PAGE a constant weight ratio of SDS to the peptide (1.4g/1g) is assumed. This results in a constant net charge per unit length of the peptide. The intrinsic charges of the peptide are superimposed by the SDS charges (Chapter 2.4.1). The high charge density of the oligonucleotides therefore may influence the micelle formation. The observation of multiple band occurs rarely. Figure 6.12 shows a SDS-PAGE gel with the expected band pattern. The yield of the triblock synthesis is ~50% by gel intensities. The isolation and purification of the ODN23-ELP-ODN23 triblock is discussed in Chapter 6.4.

The triblock synthesis was also tested by conjugating an ODN46-ELP, a diblock carrying an oligonucleotide with 46 bases, with a 23mer. The diblock was not purified by dialysis prior to the conjugation reaction. The diblock solution (obtained after the solid support cleavage) was concentrated and incubated with 50mM TCEP reducing agent for 1h followed by the isolation of the diblock by salt precipitation. The conjugation reaction was performed with 10x excess of the maleimide ODN23 in degassed 10mM PBS buffer (pH=7.3) for 2 days under

argon at room temperature. The gel analysis for this conjugation reaction is shown in Figure 6.10. The sample shows four bands. The fastest migration is achieved by the unconjugated maleimide functionalized ODN23 with the band at the lower exclusion limit at the bottom of the gel. The following band with a migration around 400bp compared to the marker in lane 2 corresponds to the unreacted diblock ODN46-E4-40. The triblock ODN46-E4-40-ODN23 exhibits an electrophoretic mobility comparable to 500bp. A very weak band (indicated with an arrow) around 1000bp additionally occurs for the oxidized diblock. In this conjugation approx. 12% of the diblock reacted analyzed by gel intensities. Compared to the synthesis of the ODN23-E4-40-ODN23 the yield is decreased by 38%. The oligonucleotide length seems to have a big influence on the coupling efficiency. The synthesis of a ODN46-E4-40-ODN46 was also tested, but for this reaction no triblock formation was observed so far.

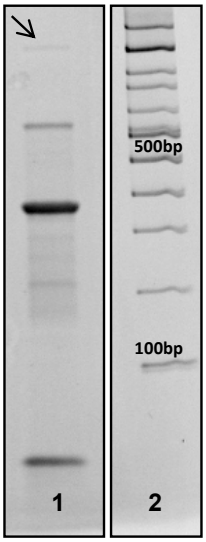

Figure 6.10 Gradient (10-20%) SDS-PAGE of the ODN46-E4-40-ODN23 triblock synthesis stained by EtBr. Lane 1: reaction mixture triblock synthesis; Lane 2: 100bp DNA marker

In cooperation with Jasmin Bühler, different reaction conditions for the triblock synthesis were tested. First results showed that an equimolar coupling is not possible at all. This approach was tested at different pH values and ionic strengths of the buffer (10mM up to 100mM) as well as at different temperatures (room temperature or T=37°C). The increased temperature showed a slight increase in yield for the synthesis of ODN23-ELP-ODN23 triblock copolymers performed with an excess of the maleimide ODN. The conjugation reaction was also tested in the presence of the reducing agent TCEP. This non-thiol containing reducing agent does not need to be removed prior to the addition reaction according to many conjugation protocols.[78] The test reaction containing 10mM TCEP showed no triblock formation. The inhibition of thiol addition to maleimides has been

observed by Getz et al.[81] and Tyagarajan et al.[82] Therefore the presence of any reducing agent in the reaction mixture is not advisable. This observation led to the analysis of the elution behavior of TCEP and DTT, an alternative reducing agent, in gel filtration. Usually the diblock copolymer is reduced with TCEP prior to the conjugation reaction. To remove the reducing agent, the diblock solutions were applied to a Sephadex gel filtration column. These columns are usually used for desalting or buffer exchange. The molecules penetrate the pores of the gel resin depending on their size. Large molecules (M_w > 1000 g/mol) are excluded from the pores and elute first. Smaller molecules are retarded due to the penetration of the matrix. The elution profiles of TCEP (M_w=287 g/mol) and DTT (M_w=154 g/mol) were analyzed by applying a 10mM solution of the reducing agent to a NAP5-column (Sephadex™ G-25 resin, GE healthcare.) According to the standard protocol, 0.5ml sample solution were applied. Large molecules (DNA) are expected to elute within V_{elu}= 1ml. The smaller contaminants (salt) are supposed to elute after the first milliliter. The collected fractions (V=0.1ml) were combined with DTNB, Ellman's reagent. All fractions were subjected to UV analysis measuring the absorbance at 412nm, the absorption maximum of the reduced DTNB (see Chapter. 5.4.1).

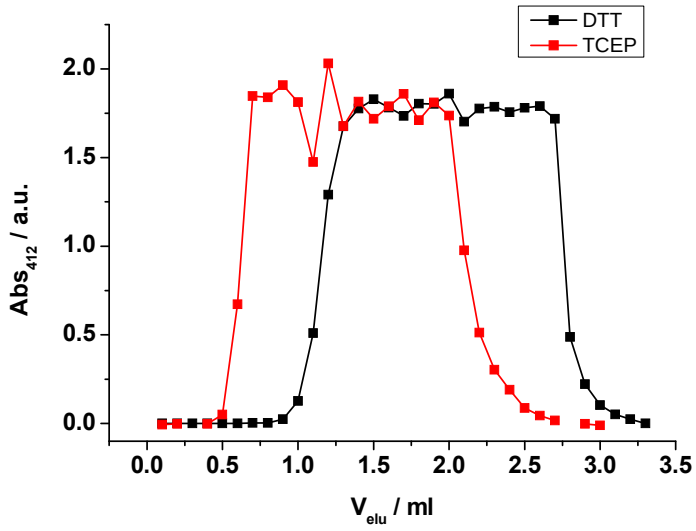

Figure 6.11 Elution profil of DTT (black) and TCEP (red) on a NAP5-column (Sephadex G-25 resin). The fractions were assayed by using Ellman's reagent to monitor the free reducing agent. The absorbance was recorded at λ=412nm. The sample solutions were applied to a column equilibrated with PBS buffer (10mM) and fractions of 0.1ml were collected.

The elution profiles show that the TCEP elutes already in the void volume (up to V_{elu}= 1ml) of the column, where only the large molecules are expected. The DTT elution shows the expected behavior and is mainly found in the fractions after the void volume. The last two fractions of the void volume (0.9ml and 1.0ml) contain a minor fraction of DTT. The

anomalous elution behavior of TCEP was already observed by de Shafer et al.[156] Hence, the complete removal of the reducing agent by gel filtration is not successful. The absence of reducing agent though has to be guaranteed by all means to avoid any inhibition of the conjugation reaction. In the synthesis of the ODN46-E440-ODN23 (Figure 6.7) the reducing agent was removed by the salt precipitation of the diblock component. This method could be an alternative to gel filtration procedures.

6.4 Isolation of ODN23-ELP-ODN23 triblocks by adsorption onto gold nano spheres

The synthesis of the ODN-ELP-ODN triblock copolymers resulted in a 1:1 mixture of triblock and diblock as shown above. The two compounds both carry the same ODN sequences. Hence, a purification by sequence specific hybridization can not be employed. The salt precipitation is also not applicable, because both compounds contain the same thermosensitive ELP block. The triblock and the diblock copolymer differ only in their molecular weight and in their end groups. The difference in molecular weight is not significant enough to use any size dependent purification like dialysis or ultrafiltration. Concerning the end groups, the diblock still contains the free thiol group which is covalently linked in the triblock molecule. The free thiol residue can be used to adsorb the diblock onto gold nano spheres by exploiting the high affinity of sulfur to gold.

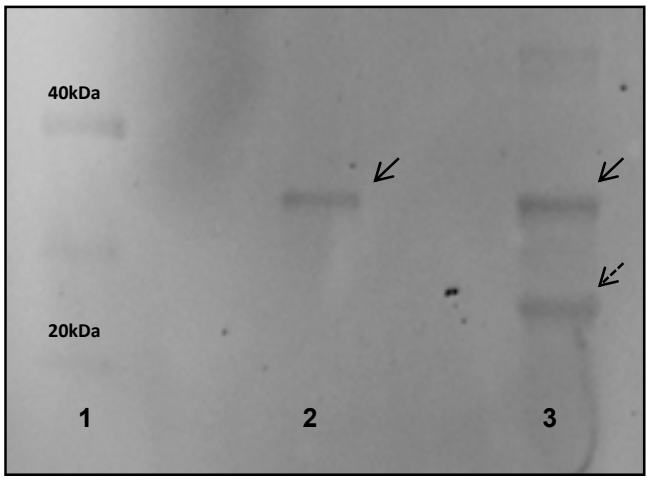

Figure 6.12 Gradient (10-20%) SDS-PAGE of the ODN46-ELP-ODN23 triblock purification with gold nano particles, stained by EtBr. Lane 1: peptide marker (Roti mark 10-100kDa); Lane 2: purified ODN23-E440-ODN23 triblock copolymer; Lane 3: ODN23-E440-ODN23 di/triblock copolymer mixture after first incubation with gold nano particles.

In cooperation with Inga Zins (Group of Prof. Sönnichsen, University of Mainz), who synthesized citrate stabilized gold nano spheres with a radius of 20nm, the purification of the triblocks by adsorption onto gold nano spheres was tested. For the experiment a sample of the triblock reaction mixture was incubated with a highly concentrated gold particle solution over night. After the incubation the gold nano particles were separated from the supernatant by centrifugation.

In Figure 6.12 the SDS-PAGE analysis after the incubation of the triblock-diblock mixture is presented. The picture shows that after a first incubation step (lane 3) still a mixture of the two components is present in the sample. A second incubation with an increased amount of

gold nanospheres led to the desired result: only the triblock molecule is detected. The diblock copolymers completely adsorbed onto the nano particles. The change of the surface coating of the gold particles was investigated by agarose gel electrophoresis shown in Figure 6.13.

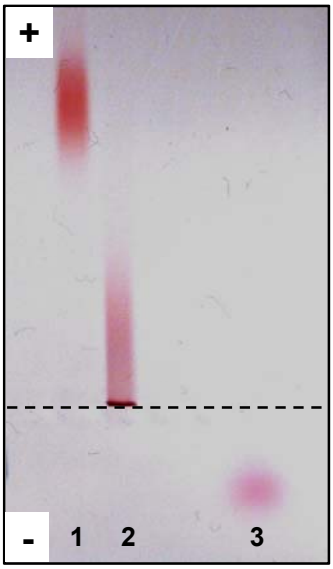

Figure 6.13 Horizontal agarose (0.2%) gel electrophoresis of gold nanoparticles. Lane 1: gold nano spheres incubated with ODN23-E440/ODN23-E440-ODN23 mixture; Lane 2: citrate stabilized gold nano spheres (d=20nm); Lane 3: vitamin B12.

The investigation of gold nanoparticles by gel electrophoresis yields information on their surface charges. The analysis is performed by using a low concentrated and horizontal agarose gel, where the samples are applied in the middle of the gel (dashed line in Figure 6.13). The migration direction of the samples shows if the particle surfaces are negatively or positively charged. The migration velocity gives information on the charge density of the particles. In Figure 6.13 lane 3 contains Vitamin B12, which migrates with the net electro osmotic flow. In lane 2 citrate stabilized gold nanospheres with a diameter of 20nm were applied. The citrate layer results in a negative surface charge of the particles, which migrate to the anode. In lane 1 a sample of gold nanospheres after the incubation with the diblock/triblock mixture is shown. The migration behavior changes strongly. The adsorption of the ODN23-E440 diblock leads to a highly negative surface charge because of the negatively charged phosphate groups of the oligonucleotide.

The gold adsorption experiment showed that a purification of the triblock by selective adsorption onto gold nano particles is successful. It is an easy and fast method. One major draw back of this method is the amount of gold particles needed. The application of this method for a larger scale purification is therefore not worthwhile. At the moment the

purification by preparative GPC is investigated as an alternative method for the separation of the diblock and triblock copolymers. Furthermore, the selective hybridization as purification method is applicable, if the two ODN sequences of the ODN-ELP-ODN triblock are different (ODN1, ODN2). The triblock molecule can be selectively hybridized to a solid support bound oligonucleotide complementary to ODN2. The remaining diblock, which only carries ODN1, is washed off and the triblock isolated by denaturation.

6.5 Summary

The synthesis of ODN-ELP-ODN triblock copolymers was performed successfully with oligonucleotides of 23 bases. The increase of the oligonucleotide length resulted in a decreased yield of triblock copolymers. The reaction conditions were varied in the means of reactant concentration, reducing agent, temperature, ionic strength and pH of the buffer. The triblock synthesis is neither successful at an equimolar ratio of the reactant nor in presence of reducing agent. Hence, the removal of the reducing agent seems to be a crucial condition for a successful synthesis. The elimination of reducing agent by gel column chromatography is not complete, which was proved by UV analysis of the elution behavior for TCEP and DTT. A potential new strategy is the salt precipitation of the diblock after the reduction, but this could also lead to an undefined aggregation as discussed in Chapter 5.4.3. The reaction conditions and the up scaling for the triblock copolymers therefore have to be optimized, which is the aim of the ongoing diploma thesis of J. Bühler.

7 Conclusions and Outlook

In this work, the synthesis of monodisperse oligonucleotide-Elastin-like polypeptide (ODN-ELP) diblock and triblock copolymers was demonstrated successfully. The oligonucleotide building blocks were obtained from standard solid phase synthesis and functionalized with different linkers. The ELP building blocks were synthesized by genetic engineering yielding well defined and monodisperse polypeptides. Their sequences were designed to carry two reactive endgroups: a free amino group at the N-terminus and a free thiol group of a cysteine residue at the C-terminus. The polypeptide repeat unit (Val-Pro-Gly-Val-Gly) itself carries only hydrophobic amino acids. An important characteristic of the ELPs is their temperature senstive behavior (LCST). ODN-ELP diblock copolymers were obtained by two different synthetic approaches. One approach involved the functionalization of an amino oligonucleotide with a sulfhydryl reactive linker carrying a maleimide residue. The conjugation results from the reaction of the maleimide functionality of the ODN with the free thiol group of the polypeptide. The second approach includes the reaction of an activated ester oligonucleotide bound to a solid support with the N-terminal amino group of the ELP block. Both reactions were demostrated to yield monodisperse blockcopolymers characterized by PAGE and dynamic light scattering. Further, the two orthogonal approaches were combined to yield ODN-ELP-ODN triblock copolymers.

The potential to use the synthesized blockcoplymers in molecular assemblies was demonstrated by self-assembling an ODN-ELP four-arm star due to the hybridization of complementary ODN strands. The ODN sequences were designed to build up a four-arm DNA junction. The DNA junction with 23 basepairs per arm itself was investigated in means of thermal stability and hybridization efficiency prior to the hybridization of the ODN –ELP blockcopoylmers. The measurements revealed the successful construction of a stable four-arm DNA junction. The junction showed single structure formation and quantitative rehybridization. Additionally, a second junction was constructed and hybridized in parallel with the first one. The hybridization was specific for each junction itself as designed, and no interfering interaction have been detected. Furthermore, the linear self-assembly of ODN conjugates was analyzed by the hybridization of ODN-dihexapeptide-ODN conjugates.

In summary, the synthesis of new biocompatible blockcopolmyers was achieved. They are:

a) monodisperse
b) designable
c) functionalisable
d) able to self-assemble
e) thermosensitive.

The genetic engineering of the ELP building block and the solid-phase synthesis of the ODN block ensure the monodispersity. Both blocks are designable in sequence. The ODN sequence can be chosen to be compatible with molecular self-assembly to create multi-responsive ODN-ELP superstuctures. It can also be chosen to be immune active for future use in biomedical applications. The ODN sequence can easily be modified by internal or endgroup functionalities, e.g. fluorescent dyes, provided by the solid-phase synthesis. The ELP sequence can be designed to carry additional and perfectly located functional groups and defined endgroups as well. Therefore, the synthesis of ELP-ODN-ELP triblock copolymers using a similar approach is straight forward. The ELP sequence also determines the LCST behavior of the polypeptide block. By using ELP blocks differing in their repeat unit sequence, a sequential temperature dependent aggregation can be envisioned. As mentioned before, the self-assembly of the ODN-ELP diblock copolymers can be due to the chosen DNA sequence, but the thermal aggregation of the ELP block can also lead to molecular assemblies like micelles. Both described assembly processes are thermally reversible. The double stranded DNA in molecular self-assemblies though can be chemically crosslinked, for example by psoralen, in need to get thermal stable structures also.

The formation of defined supramolecluar self-assemblies using the described monodisperse ODN-ELP block coplymers is possible. The diblock hybridization demonstrated the defined assembly into a four-arm star. The design of the independent DNA junctions and their defined hybridization opened a new strategy to form nano networks by sequential self-assembly. However, the chosen purification procedure by salt precipitation probably introduced the unexpected problem of irreversible aggregation of the diblock copolymers. The aggregation leads not only to problems in the further purification. It prevents as well the defined hybridization of the diblock copolymers and inhibits possibly the conjugation reaction to form the ODN-ELP-ODN triblock copolymer. This aggregation behavior is not understood and can therefore not be explained so far. The interplay between disulfid bridging, hydrophobic and electrostatic interactions as well as the influence of the ionic

strength of the solvent is still unclear. These interactions though have to be analyzed and controlled to ensure the self-assembling into defined superstructures later on. Especially, if the thermally induced aggregation of the ELP block is to be exploited with respect to the network formation, the molecular parameters relevant to the ELP collapse should be well understood. The investigation of the inter- and intramolecular interactions of the ODN and ELP block are therefore essential to achieve the network formation.

The present work is a basic approach to multi-responsive and multi-functional monodisperse blockcopolymers. Their applications are manifold. The formation of a four-arm star by hybridization of complementary ODN-ELP diblock copolymers demonstrated their application for DNA self-assembly. Extending this approach to the ODN-ELP-ODN triblock copolymers provides the opportunity to build up controlled network structures (see Chapter 1). Especially in biomedical research the use of monodisperse systems may facilitate the understanding of the complex structure-property relationship in physiological processes. The opportunity to combine the discussed synthetic approaches with the coupling of drugs to the ODN-ELP blockcopolymers envisions the design of tri- or even multifunctional blockcoplymers. The ODN block might also be applicable for immune recognition. The ELP could enhance the cellular uptake and increase the stability of the ODN and the drug by encapsulation.

8 Materials and Methods

The materials and methods section is based on the outline of the Chapters 3-6. For example, the experimental details concerning the results discussed in Chapter 3 can be found in Chapter 8.1. At the end of this section the more general methods, like gel electrophoresis, and materials used are described. All reaction conditions are summarized in the Appendix 9.2.

8.1 DNA four-arm junctions

8.1.1 Junction sequences

The following ODN sequences were designed by using the SEQUIN program except the sequences of junction J1, which were are taken from literature. All ODNs were purchased from Biomers.net GmbH (Ulm, Germany). Prior to the hybridization all strands were purified by gel extraction.

Junction J1

K2S1: 5'-CGC AAT CCT GAG CAC G-3'

K2S2: 5′-GCC ATA GTG GAT TGC G-3′

K2S3: 5′-GCA TTC GGA CTA TGG C-3′

K2S4: 5′-CGT GCT CAC CGA ATG C-3′

Junction K3

K3S1: 5′-CGG TAG TAC AAC GCT CGC AAT CCT GAG CAC GTT CGA TAC TCC GTG GTT TAC TGT GAC TTG TCC TAA GAC AT-3′

K3S2: 5′-GAG ATG ACC AGG TAT GCC ATA GTG GAT TGC GAG CGT TGT ACT ACC GTT TAC TGT GAC TTG TCC TAA GAC AT-3′

K3S3: 5′-TGA TCG TTA CGA CAC GCA TTC GGA CTA TGG CAT ACC TGG TCA TCT CTT TAC TGT GAC TTG TCC TAA GAC AT-3′

K3S4: 5′-CCA CGG AGT ATC GAA CGT GCT CAC CGA ATG CGT GTC GTA ACG ATC ATT TAC TGT GAC TTG TCC TAA GAC AT-3′

Junction K4

K4S1: 5'-CGG TAG TAC AAC GCT CGC AAT CCT GAG CAC GTT CGA TAC TCC GTG G-3′

K4S2: 5'-GAG ATG ACC AGG TAT GCC ATA GTG GAT TGC GAG CGT TGT ACT ACC G-3′

K4S3: 5'-TGA TCG TTA CGA CAC GCA TTC GGA CTA TGG CAT ACC TGG TCA TCT C -3'

K4S4: 5'-CCA CGG AGT ATC GAA CGT GCT CAC CGA ATG CGT GTC GTA ACG ATC A -3'

Junction K5

K5S1: 5'-CGA GAC TGA CTC GAC GGT TAG CTC CTA AGC AAC ATC A GC AGT TCA C-3'

K5S2: 5'-CAC CTT ACT GTA GAG TTG ACG CCA GCT AAC CGT CGA GTC AGT CTC G-3'

K5S3: 5'-CGG ATG CAC ATG CTA TCT GCC GAG GCG TCA ACT CTA CAG TAA GGT G-3'

K5S4: 5'-GTG AAC TGC TGA TGT TGC TTA GGT CGG CAG ATA GCA TGT GCA TCC G-3'

Junction K6

K6S1: 5'-GCA AGT GAC AAT GTA ATC GCT GTG GCT CTT TCG CGT ACC AAT TCT C-3'

K6S2: 5'-CCA TTA GAA CAC TGG AAT CAT GGA CAG CGA TTA CAT TGT CAC TTG C-3'

K6S3: 5'-CGA AGC CGT ATA GAC GTA GCG CAC CAT GAT TCC AGT GTT CTA ATG G-3'

K6S4: 5'-GAG AAT TGG TAC GCG AAA GAG CCT GCG CTA CGT CTA TAC GGC TTC G-3'

8.1.2 Gel extraction protocol

The purchased oligonucleotides were subject to a denaturating PAGE (15%) analysis. Per well 17µg oligonucleotide in 10µl loading buffer were applied (15 wells per gel: m_{total}(ODN) =250µg). After the gel analysis and staining with ethidium bromide (EtBr) the main oligonucleotide band was cut out and the crushed gel pieces were suspended in ~2ml elution buffer (500mM NH_4OAc, 10mM $Mg(OAc)_2$, 2 mM EDTA) over night. The supernatant was isolated and the gel pieces were washed twice with 0.1ml elution buffer. The combined solutions were extracted with n-butanol till the aqueous phase was concentrated to a total volume of 0.2ml. Then 2ml ethanol (100%) were added and the sample was stored at T=-20°C over night to precipitate the oligonucleotide. After centrifugation at 11000rpm for 20min, the supernatant was discarded and 2ml cold ethanol (70%) were added carefully to the pellet. The sample was centrifuged again under the same conditions and the supernatant was discarded. The pellet was dried using an Eppendorf Concentrator and dissolved in 2ml Milli-Q water. The ODN concentration was determined by UV absorption at 260nm.

8.1.3 Hybridization protocol

The chosen strands were mixed in an equimolar ratio with a total DNA concentration of c=0.1-0.4µg/µl in TAE/Mg buffer (40 mM Tris acetate, 1 mM EDTA, 12.5 mM Magnesium acetate, pH=8.3) and gradually annealed using the following temperature programs (Table 8.1) if not indicated otherwise. The annealing was performed in a thermocycler type Primus

25 advanced (Peqlab Biotechnologie GmbH, Erlangen, Germany). The hybridization was usually analyzed by native PAGE.

Table 8.1: Temperature programs used for the hybridization of DNA four-arm junctions

Hyb90		**Hyb90nig**	
lid heat 110°C		lid heat 110°C	
90°C	5 min	90°C	5 min
65°C	20 min	85°C to 65°C	1 h at every 5°C
lid heat off		lid heat off	
55°C	20 min	60°C to 20°C	1 h at every 5°C
45°C	20 min	store at 8°C	
37°C	30 min		
23°C	30 min		
store at 8°C			

8.1.4 Determination of the junction melting point

The thermal transition profiles of the DNA four-arm junctions K3 and K4 were recorded by monitoring the UV absorption at 260nm versus the temperature. The measurements were performed using a Carry 100Bio UV-VIS Spectrophotometer (Varian, Inc) and an external thermostat (Haake C25P Phoenix II, Thermo Scientific). An equimolar mixture (0.11 µM per strand) of the junction strands in 1mM $MgCl_2$ solution was measured in a final volume of V= 3ml. The heating and cooling rate was 1°C per minute. The applied heating ramp is presented in Table 8.2. All samples were measured in three consecutive temperature cycles. The absorption was recorded in intervals of 1s.

Table 8.2: Temperature ramp used for the thermal UV analysis of DNA four-arm junctions

temperature ramp	
20°C	20 min
20°C-90°C	70 min
90°C	20 min
90°C-20°C	70 min
20°C	20min

The temperature calibration was performed by measuring the temperature inside the cuvette filled with water. The data were analyzed by determining the fraction of single stranded DNA using equation 2.8 (Chapter 2).

8.2 Genetic engineering and expression of ELPs

All experiments concerning the genetic engineering and the expression of Elastin-like Polypeptides (ELPs) were performed in the lab of Prof. Chilkoti (Duke University, North Carolina, USA).

8.2.1 Materials

E. coli strains

The strain TOP10 *E. coli* (Invitrogen Corporation, Carlsbad, CA) was used for all cloning experiments. The cells are chemically competent and provide a stable replication of high-copy number plasmids. They have no promoter for protein expression.

BLR(DE3) cells (Novagen, Madison, WI) were used for the protein expression. DE3 strains carry the RNA polymerase gene of the T7 phage. Therefore they activate the T7 promoter of the pET vector. The expression of the polymerase is usually controlled by the lac promoter, which is activated by isopropyl-1-thio-β-D-galactopyranoside (IPTG), but the overexpression of most ELPs does not require the addition of IPTG. In some cases the addition can increase the overall yield. No IPTG was used in the protein expressions reported, here.

Plasmids

Two different plasmids were used. Both are based on the pET24a(+) expression vector (for sequence see Appendix 9.3.1). They were modified to produce specific leading and trailing sequences in the peptide. They both carry a kanamycin resistance gene.

- The JMD2 vector (for sequence see Appendix 9.3.3) was used for the modified RDL method. The clones for ELP-26 were synthesized in this vector. It carries an encoded tyrosine at the peptide C-terminus.
- The SF1 vector (for sequence see Appendix 9.3.2) was used for all peptide expression. It was modified to produce a phenylalanine-cysteine termination of each polypeptide.

Enzymes and Media

All enzymes were purchased from NEB (New England Biolabs). The restriction enzymes and their restriction sites are listed in Table 4.1 (Chapter 4).

TB media

Terrific Broth (TB) Dry containing 12g/l tryptone, 24g/l yeast extract, 4g/l proprietary carbon source, 12.54g/l dipotassium phosphate and 2.31g/l monopotassium phosphate was used for all cloning and expression cultures. For the preparation of 1l media 55g TB Dry is dissolved in DI water and autoclaved.

LB media

Luria Bertani (LB) broth media containing 10g/l Tryptone, 10g/l sodium chloride and 5g/l yeast extract was used for the recovery of the cells after transformation.

Plasmid Isolation

For the plasmid isolation the Miniprep Kit QIAprep Spin (Qiagen, Valencia, CA) was used according to the standard procedure.

Gel extraction

For the agarose gel extraction the gel extraction Kit QIAquick (Qiagen, Valencia, CA) was used according to the standard procedure.

Buffers

TAE buffer (50x): 18.6g EDTA in 75ml dest. water (adjust pH to 8.0 and fill up to 100ml), 242g Tris base in 750ml dest. water and 57.1ml glacial acetic acid were combined and filled up to a volume of 1l.

SDS-Tris-Glycine buffer (10x): 30g Tris base, 144g Glycine and 10g SDS were combined and filled up with dest. water to 1l.

PBS buffer (1x): One tablet PBS-buffer (Calbiochem) was dissolved in 1l dest. water. This resulted in a buffer containing 10mM Phosphate buffer, 140mM NaCl, 2.7mM KCl at a pH of 7.4.

8.2.2 Molecular Cloning Protocols

The ELP encoding genes were constructed using the recursive directional ligation method (see Chapter 2.2.2). The ELP 4 gene library with oligomers of 20, 30, 60, 120 and 240 was already produced in the JMD2 vector by the new RDL method by J. McDaniel. Therefore, only a transfer had to be done of the oligomeric inserts into the new vector SF1. The oligomer that encodes 10 repeat units was also synthesized by ligating the corresponding synthetic

oligonucleotides (for sequence see Appendix 9.3.2) into the SF1 vector. By concatemerization, the self-ligation of a DNA monomer with cohesive ends, an additional oligomer encoding 40 repeat units was produced.

The ELP26 library was already built up to inserts of 40 repeat units. The clones encoding 80 and 160 repeat units were synthesized by the new RDL method in the JMD2 vector. The inserts were transferred into the SF1 vector. In the following part the standard protocols for the vector linearization, the insert preparation and the following ligation are presented.

Vector Linearization (VectorPrep)

15µl Plasmid solution were combined with 9µl Neb2-Puffer, 65.5µl water and 0.5µl BseR1 enzyme solution. The mixture was incubated at 37°C over night. Then 1µl calf intestinal alkaline phosphatase (CIP) was added and the solution was incubated for 1 hour at 37°C. The plasmid isolation and purification was done by standard MiniPrep protocols.

Insert Preparation (InsertPrep)

For the preparation of an insert 40µl of plasmid DNA solution were combined with 9µl Neb2 buffer, 39µl water and 1µl of the chosen enzymes.

- For the standard RDL procedure 1µl BSeR1 and 1µl Acu1 were used.
- For the modified RDL method one aliquot of DNA and buffer was combined with 35µl water, 2µl Acu1 and 4µl Brl1. To the second aliquot 2µl of BSeR1 instead of Acu1 was added.

In all cases the mixtures were incubated for 3h at 37°C. The inserts were purified by gel extraction. 90µl of the insert prep were combined with 18µl loading buffer. The samples were run on a 1 % agarose gel at 4°C for around 10min. The insert bands were cut out and purified with a standard gel extraction kit. The samples were either ligated immediately or stored frozen at -20°C.

Ligation

To a volume of 5µl VectorPrep 10µl InsertPrep solution, 4µl Ligase buffer and 1µl Ligase were added. The mixture was incubated for 1h at room temperature. The transformation into competent cells followed immediately.

A volume of 5µl ligation mix was cooled down in an ice bath. Then 125µl of Top10-cells were added to the ligation mix. The mixture was kept 10min on ice, then 45sec at 42°C and again 2min on ice. The cells were incubated at 37°C for 1h after the addition of 100µl LB media. After the incubation the cell mixture was spread on a media plate and the cells were cultured at 37°C over night (~ 18h). On the following day 10 cell colonies of each ligation were picked and grown up in 4ml cultures (4ml TB media containing 4µl Kanamycin) over night at 37°C. The plasmid purification was done by standard MiniPrep protocols. The plasmid modification was analyzed by a diagnostic digest. The growth of small 4ml cultures was skipped, if a small insert was ligated (up to 80mers). Selected colonies of these ligations were screened immediately by colony PCR (cPCR).

Colony PCR (cPCR) for insert screening

The cells are picked and added to 12.5µl Master mix (Taq DNA polymerase, standard Taq reaction buffer and dNTPs). The PCR was carried out with the following cycle:

2min at 95°C (1x)

40sec at 95°C
40sec at 55°C
2min at 72°C
} 35 cycles

hold at 4°C

The elongation period at 72°C was altered depending on the insert length.

Diagnostic Digest for insert screening

10µl DNA were incubated with 2µl BSA, 2µl NEB 3 buffer, 5µl water and 0.5µl XbaI and 0.5µl BamH1 for at least 1h at 37°C. The mixture was then combined with 2µl loading dye and applied to a 1% agarose gel or analyzed by automated chip electrophoresis.

8.2.3 Expression Protocols

Cell growth

First a 50ml starter culture with TB media and 50µl Kanamycin was inoculated with cells from a DMSO stock. The cells were grown up over night (~18h) at 37°C with shaking. The following day the cultures were centrifuged at 3000rpm for 10min and the pellet was

resuspended in 1 to 2ml 1x PBS buffer. The cells were then added to 6 (12)x 1l TB media containing 1ml Kanamycin solution and were incubated at 37°C with shaking for 24h.

Peptide isolation

The grown up cells were harvested by centrifugation in 1l centrifuge tubes at 3000rpm at 4°C for 15min. The pellets were resuspended in 10ml PBS and transferred to a 250ml centrifuge tube. Each 1l tube was washed again with 10ml PBS and the solutions were combined. The isolated cells were then sonicated on ice in three cycles of 3min each (10sec on/20sec off, power ~8.5). After sonication 2ml PEI per liter culture were added and the mixture was centrifuged at 4°C at 11000rpm for 10min. The supernatant containing the desired peptide was than transferred to a new tube.

Peptide purification by inverse transition cycling (ITC)

The temperature of the supernatant was increased to 37°C and/or NaCl powder (2-3M) was added. The turbid solution was then centrifuged at 40°C at 11000rpm for 10min (Hot spin 1). The supernatant was discarded and the pellet was resuspended in cold 1x PBS buffer by repeatedly pipetting up and down. The solution was centrifuged at 13 000rpm at 4°C for 10min (Cold spin 1) to remove any insoluble matter. The pellet was discarded and the supernatant was heated up again. Then 2-3M NaCl solution were added until precipitation occurs. The mixture was centrifuged again at 40°C at 11000rpm for 10min (Hot spin 2) and the supernatant was discarded. The pellet was resuspended in 1x PBS buffer and reducing agent TCEP (5-20mM) was added. The cycle of hot and cold spins was repeated until no impurities can be detected by SDS-PAGE.

8.2.4 Characterization methods

All characterization experiments described in the next section were performed in the lab of Prof. Chilkoti (Duke University, North Carolina). Only the light scattering measurements were carried out at the University of Mainz.

Horizontal agarose gel electrophoresis

A 1% agarose gel was prepared by dissolving 0.5g Agarose (OmniPur, EMD Chemicals) in 50ml TAE buffer (1x) and heating the mixture up in the microwave for 1min. Before casting the gel 5µl Sybr Safe were added and the gel solidified in 30min. A volume of 10µl sample was combined with 2µl loading dye and applied to the gel. The running conditions were 20-30min at constant voltage of 130V.

For a gel extraction the same procedure was applied, but low melting temperature agarose (Ultra pure Aqua Por, National diagnostics) was used and were run at 4°C.

Automated Chip Electrophoresis

The automated chip electrophoresis was performed with the Experion system (Bio-Rad, Laboratories Inc., Hercules, CA) using the standard protocol.

Vertical polyacrylamide gel electrophoresis (SDS-PAGE)

The SDS-PAGE was performed in a Mini-Protean cell (Bio-Rad) using precast gels with a gradient of 4-20%. The running buffer was 1x SDS running buffer. The conditions were chosen according to the standard procedure by Bio-Rad. The gels were stained with copper staining (0.5M $CuCl_2$).

UV spectroscopy

The concentration of DNA solutions was determined with a NanoDrop instrument (Thermo scientific).

The cloud point measurements of the ELPs were performed on a Cary100 equipped with a multi cell holder and temperature probe accessory. The absorption at 350nm was monitored as a function of temperature in the range from 15°C to 60°C. The heating rate was 1°C per minute. The cooling rate was 10°C per minute. The data intervals were 0.33°C for the heating ramp and 1°C for the cooling ramp. The cloud points were usually measured for five different peptide concentrations from 10µM to 100µM.

Dynamic light scattering

The dynamic light scattering measurements were performed with a He-Ne laser (λ=632.8nm, 21mW) (JDS Uniphase). The instrument is equipped with a goniometer SP-86#060 (ALV9) with an Avalanche photodiode and an ALV-3000 digital correlator. The measurements were done at 20°C at a scattering angle of 30°. The ELP samples were dissolved in 20mM NaCl solution at a concentration of 5mg/ml. The solutions were filtered with an anotop filter (20nm, d=13mm, Whatman) and an additional GHP filter (0.2µm, Pall) applied in series into dust-free Suprasil cuvettes (20mm diameter, Hellma, Mülheim, Germany).

8.3 Diblock copolymer synthesis

In advance of the diblock copolymer synthesis, the modification of ODNs by different hetero bifunctional linkers was tested. The basic protocols are given in the following sections. Additionally, all reaction conditions are summarized in the Appendix 9.2.1. The reactions were tested with an oligonucleotide ODN23 of 23 bases (S2) prior to the use of the junction sequences of 46 bases (Chapter 8.1.1).

8.3.1 ODN sequence S2 (ODN23)

The ODN was purchase from Biomers.net GmbH with 5'-amino or 5' thiol functionalization as well as with the succinimidyl linker (see Chapter 2.1.2). In the latter case, the ODN was still bound to the solid support, a CPG with a pore size of 2000Å.

S2 (or ODN23): 5'-gtc ctc gcc tag tgt ttc att ga-3'

8.3.2 Thiol addition to Acrydite™ ODNs

Acrydite™ functionalized ODNs carry a methacrylate group at the 5'-end. They were purchased from IDT (Integrated DNA Technologies) with the base sequence S2 (23 bases). The thiol addition to the Acrydite™ ODNs was test with different thiol components and under various conditions (Chapter 5.1). The given protocol is an example of the reaction with thiol-PEO. The conditions for all other conjugation reactions described are summarized in the Appendix 9.2.1.

Conjugation of thiol-PEO to Acrydite™ ODN

A solution of 0.71ml thiol-PEO (m-dPEG®6-thio, M_w=356g/mol, QuantaBiodesign, c=10mg/ml, 1000x excess) in PBS buffer (0.1M phosphate, 0.15M NaCl, 1mM EDTA) was combined with 0.1ml Acrydite™ ODN (sequence S2, c=1.45mg/ml) and incubated at RT over night. The reaction was analyzed by denat. PAGE without any further purification.

8.3.3 Linker modification of amino functionalized ODNs

The results of the following linker modifications are discussed in Chapter 5.2.

BMPS linker

The amino functionalized oligonucleotide (10µl, c=10ug/µl) was diluted with 1ml PBS buffer (0.01M phosphate, 0.015M NaCl,pH=7.3, degassed) and 125µl BMPS in dry DMF (c=4.1mg/ml, 100x excess) were added (under Argon). After 4h incubation at RT the mixture was applied to a gel filtration column (NAP 25, Sephadex G-25) and eluted in 3ml PBS buffer

(ph=7.2, 10mM phosphate) in fraction of 1ml. The DNA concentration of each fraction was determined by UV absorption.

Sulfo-SMCC linker

The amino functionalized oligonucleotide (10µl, c=10ug/µl) was diluted with 1ml 10mM PBS buffer (pH=7.3, degassed) and 125µl sulfo-SMCC in dry DMF (c=6.7mg/ml, 140x excess) were added (under Argon). After 4h incubation at RT the mixture was applied to a gel filtration column (NAP 25, Sephadex G-25) and eluted in 3ml PBS buffer (ph=7.3, 10mM phosphate) in fraction of 1ml. The DNA concentration of each fraction was determined by UV absorption.

SMCC linker

The SMCC functionalization was tested under various conditions. The following procedure is the optimized version resulting in the highest yield of functionalized oligonucleotide. The conditions for the additionally discussed reactions in Chapter 4 are given in Appendix 9.2.1.

An amount of 500ug amino functionalized oligonucleotide (50µl, c=10ug/µl) was diluted with 1ml 10mM PBS buffer (pH=7.3, degassed) and 300µl SMCC in dry DMF (c=10mg/ml) were added (under Argon). After 2h incubation at RT again 300µl SMCC were added. The mixture was incubated for another 2h. Then the solution was applied to a gel filtration column (NAP 25, Sephadex G-25) and eluted in 3ml PBS buffer (ph=7.3, 10mM) in fraction of 1ml. The DNA concentration of each fraction was determined by UV absorption.

8.3.4 HPLC measurements of linker functionalization

The HPLC measurements were performed using a RP-C18- column (LiCrospher™, 100RP-18, particle size 5um, 250x4mm, MZ-Analysentechnik, Mainz, Germany). The setup was equipped with a gradient pump (Hitachi, model L-7100), degasser (ERC-3114) column thermostat (Jetstream 2Plus), a UV detector (Lambda Max Model 481, Waters) and a light scattering detector (PL-ELS 2100 Ice, Polymer Laboratories). For the recording and analysis of the data the Millenium 2.15 software was used.

Usually a sample volume of 20µl was injected (c=0.1-0.5mg/ml). The measurements were performed with a flow rate of 0.45ml/min (p~63bar) at T=25°C. The gradient elution started at 100% of the eluent A (triethylammonium acetate (TEAA), 0.1M, pH=7) and ended after 30 min with an eluent content of 60% eluent B (acetonitril). For the kinetics of the SMCC functionalization 15µl crude reaction mixture were diluted with 15µl TEAA buffer for the

injection. The reaction was monitored by measuring every 60min starting 10min after the addition of SMCC to the ODN.

Sequences used in HPLC measurements

ODN23 (S2NH2): 5'-GTC CTC GCC TAG TGT TTC ATT GA-3'
ODN30 (30NH2): 5'-CGG TAG TAC AAC GCT CGC AAT CCT GAG CAC -3'
ODN38 (38NH2): 5'-CGG TAG TAC AAC GCT CGC AAT CCT GAG CAC GTT CGA TA -3'
ODN46 (K4S1): 5'-CGG TAG TAC AAC GCT CGC AAT CCT GAG CAC GTT CGA TAC TCC GTG G-3' (with and without amino linker)
Poly(46dT): 5'-TTT TTT TTT TTT TTT TTT TTT TTT TTT TTT TTT TTT TTT TTT TTT TTT T-3'

8.3.5 Thiol conjugation to maleimide functionalized ODNs

Different thiol containing components were tested in the addition reaction to SMCC functionalization ODNs. The conditions for the SMCC modifications are given in the Appendix 9.2.1. The procedure followed the optimized protocol for the SMCC functionalization in Chapter 8.3.2

Addition of thiol-PEO

A solution of SMCC modified oligonucleotide (c (DNA) = 0.4mg/ml, V=0.05ml, sequence S2) in degassed 0.1M PBS buffer (pH=7.3) was combined with 0.1ml thiol-PEO (c=1mg/ml m-dPEG®6-thio, M_w=356g/mol, QuantaBiodesign,) in the same buffer. The mixture was incubated for 2 days at RT under argon. The reaction was analyzed by denat. PAGE without any further purification.

Addition of a thiol-ODN

A solution of SMCC modified oligonucleotide (c (DNA) = 0.17mg/ml, V=0.05ml, sequence S2) in degassed 0.1M PBS buffer (pH=7.3) was combined with 0.05ml thiol-ODN (sequence S2 with 5'-thiol modification, c= 0.2mg/ml, 1.2x excess) in the same buffer. The mixture was incubated over night at RT under argon. The reaction was analyzed by denat. PAGE without any further purification.

Addition of a hexapeptide

A solution of SMCC modified oligonucleotide (c (DNA) = 43 µg/ml, V=2ml, sequence S2) in degassed 0.1M PBS buffer (pH=7.3) was combined with 0.25ml hexapeptide Val-Pro-Gly-Val-Gly-Cys (PANAtecs GmbH, M_w=531.64 g/mol, c= 8mg/ml, 285x excess) in the same buffer. The mixture was incubated over night at RT under argon. The reaction was analyzed by denat. PAGE without any further purification.

8.3.6 ODN-ELP diblock copolymer synthesis by thiol coupling

The synthesis of ODN-ELP diblock copolymers by thiol coupling was performed using different ELP and ODN components. The ODN sequences used are given in Chapter 9.3.4. For the peptide block the ELPs of the E4 library were used (E4-20, E4-30, E4-40, E4-60 and E4-120). The following protocols are an example for the synthesis of ODN46-E4-40 diblock copolymers.

Reduction of the ELP component

The ELP E4-40 (m=10mg) was reduced by the addition of 300µl TCEP solution (c=100mM) and incubation for 1h at 15°C. Then 0.2ml saturated NaCl solution were added and the mixture was heated to 50°C to precipitate the peptide completely. After centrifugation for 10min at 11 000rpm the supernatant was discarded and the peptide pellet was resolubilized in PBS buffer (0.01M phosphate, 0.015M NaCl, pH=7.2). The reduced ELP was used immediately in the thiol conjugation.

Conjugation of reduced ELP and SMCC-ODN

A solution of SMCC modified oligonucleotide (c (DNA) = 0.25 µg/ml, V=1ml, sequence K4S1) in degassed PBS buffer (0.01M phosphate, 0.015M NaCl, pH=7.2) was combined with 0.25ml reduced E4-40 in the same buffer. The mixture was incubated over night at RT under argon in the dark. An aliquot of the reaction was analyzed by denat. PAGE without any further purification. The mixture was incubated additional 24h at T=30°C.

Purification of ELP-ODN conjugates

For the separation of the diblock from remaining unreacted DNA, the diblock and remaining ELP was coprecipitated by addition of saturated sodium chloride solution to a final concentration of 2M salt and heating to 50°C for 5min. The aggregated diblock/ELP mixture was separated from solution by centrifugation (30min at 4000rpm). The resulting pellet was resolubilized in Milli-Q water. The purification grade was analyzed by denat. PAGE (15%) and the precipitation was repeated, if unreacted ODN was not removed completely.

For the separation of the diblock from the unreacted ELP, the pellet solution was applied to DNA binding spin columns (QIAquick nucleotide removal kit, Qiagen) using the standard protocol. The samples were eluted in 50µl dest. water (pH=7.8). The DNA concentration of the sample was determined by UV. The samples were analyzed by SDS-PAGE and denat. PAGE.

8.3.7 ODN-ELP diblock copolymer diblock synthesis by NHS chemistry

The following protocols describe the synthesis of an ODN-E4-40 diblock copolymer by activated ester chemistry as an example. The synthesis of diblock copolymers with other peptide components (E4-20, E4-30, E4-60 or E4-120) or oligonucleotides proceeded identically.

TNB protection of free thiol residues

A solution of 64mg DTNB in 20ml PBS (0.1M phosphate, 0.15M NaCl, pH=8) was combined with 200mg E4-40 in 20ml of the same buffer. The mixture was incubated for 1h at RT on a shaker. The solution was dialyzed against Milli-Q water (regenerated cellulose, MWCO 1000, Spectrum Laboratories) over 2 days. The peptide was precipitated by addition of sodium chloride to a final concentration of 2M salt. The aggregated peptide was separated from solution by centrifugation (30min at 4000rpm). The resulting pellet was resolubilized in 22.5ml Milli-Q water to a final peptide concentration of c (peptide) =10mg/ml estimated by UV analysis (calibration curve Appendix 9.1.2).

Conjugation of NHS-ODN (solid-support bound) to TNB protected ELPs

The oligonucleotide bound to the solid support (10-15mg) was treated with ELP E4-40TNB (0.42ml, c= 10mg/ml) and 0.51ml PBS buffer (0.1M phosphate, 0.15M NaCl, pH= 7.3) under argon overnight. The solid support was washed three times with 0.5ml Milli-Q water. For the cleavage of the TNB-protecting group the solid support was incubated with 0.1M TCEP solution (0.1ml 0.5M TCEP+0.4ml H2O) for 15min at RT. The solid support was washed again three times with 0.5ml Milli-Q water.

Cleavage off the solid-support

The DNA was cleaved off the solid support by the addition of 0.7ml concentrated Ammonia (28%ig). The mixture was incubated at 47°C over night. The supernatant was removed and the solid support was washed with Milli-Q water (3x 0.5ml). The supernatant was combined with the washing solutions and concentrated to 1ml. The DNA concentration was determined by UV absorption. The reaction result was monitored by denat. gel electrophoresis (15%).

Purification of ODN-ELP diblock copolymers

For further purification the crude reaction mixture was dialyzed (cellulose ester membrane, MWCO 10000, Float-A-Lyzer, Spectrum) against Milli-Q water for 3 days to remove

impurities. For the separation of the diblock from remaining unreacted DNA the diblock was precipitated by addition of saturated sodium chloride solution to a final concentration of 2M salt and heating to 50°C for 5min. The aggregated diblock was separated from solution by centrifugation (30min at 4000rpm). The resulting pellet was resolubilized in Milli-Q water. The purification grade was analyzed by denat. PAGE (15%) and the precipitation was repeated, if unreacted ODN was not removed completely.

8.3.8 DLS measurements of ODN-ELP diblock copolymers

Dynamic light scattering measurements were performed at T=20°C with an ALV-SP86 goniometer, an Uniphase HeNe laser (25 mW output power at 632.8 nm wave length), an ALV/High QE APD avalanche diode fiberoptic detection system and an ALV-3000 correlator. Only one concentration per sample was investigated in the extremely dilute regime 0.15 g/L < c < 0.5 g/L, which is very close if not equal to the infinite dilution limit. All solutions were filtered through anotop 0.02um Filter (Whatman) followed by GHP 0.2um Filter (Pall) into dust-free Suprasil cuvettes (20 mm diameter, Hellma, Mülheim).

The oligonucleotide and diblock copolymer samples (cODN46, ELP4-40, ssODN46-E4-40, dsODN46-ELP4-40) were measured in 32mM NaCl solution. The dsODN46-ELP4-40 sample was prepared by adding the complementary strand cODN46 (sequence K4S3k) in 32mM NaCl solution to the diblock copolymer ODN46-ELP4-40 (sequence K4S3) till an equimolar mixture was obtained. This sample was measured at T=20°C and at T=55°C.

Oligonucleotide sequence cODN46 (K4S3k)

K4S3k: 5'- GAG ATG ACC AGG TAT GCC ATA GTC CGA ATG CGT GTC GTA ACG ATC A -3'

8.3.9 Self-assembly of ODN-E4-40 diblock copolymers

The hybridization was performed as described in section 8.1.3. The hybridization was analyzed by 1.7% agarose gel electrophoresis.

8.4 Triblock copolymer synthesis

The triblock synthesis was tested first with the conjugation of a hexapeptide to two ODNs. Then the synthesis of ODN-ELP-ODN conjugates were performed under various conditions. The basic protocols are given in the following sections. Additionally, all reaction conditions are summarized in the Appendix 9.2.1.

8.4.1 Synthesis of ODN-hexapeptide-ODN conjugates

NHS coupling of ODN23 and the hexapeptide

The oligonucleotide ODN23 (23b, sequence S2, see Chapter 8.3) bound to the solid support (5mg) was treated with 0.5ml hexapeptide solution (c=37.2mg/ml) in PBS buffer (0.1M phosphate, 0.15M NaCl, pH=7.2). The mixture was incubated for 6h on a shaker at room temperature (RT). The supernatant was removed and the solid-support was washed three times with 1ml Milli-Q water and incubated with 1ml 0.05M TCEP solution for 15min. The solid-support was washed again three times with 1ml Milli-Q water.

SMCC functionalization of ODN23

An amount of 250ug amino functionalized ODN23 (25µl, c=10g/l, 23b, sequence S2, Chapter 8.3.1) was diluted with 2ml 10x PBS buffer (0.1M phosphate, 0.15M NaCl, pH=7.2) and 0.3ml SMCC in dry DMF (c=10mg/ml) were added. The reaction was incubated for 4h at RT on a shaker and purified by gel filtration using a NAP25 column (Sephadex G-25, GE healthcare). The sample was eluted with Milli-Q water (V_{total}=3.5ml) in fractions of 1ml (3x) and 0.5ml (1x). The DNA concentration of each fraction was determined by UV absorption. The thiol coupling followed immediately. Prior to the thiol coupling reaction 0.11ml 10xPBS buffer were added to each collected fraction resulting in a buffer concentration of 0.01M phosphate and 0.015M NaCl at pH=7.2.

Thiol coupling of ODN23-hexapeptide conjugate to SMCC functionalized ODN

After the reducing step with TCEP the oligonucleotide-hexapeptide conjugate bound to the solid-support was immediately treated with 2ml solution of a SMCC modified ODN23 (sequence S2) in PBS buffer (0.01M phosphate, 0.015M NaCl, pH=7.2). The mixture was incubated over night on a shaker at RT. Then the supernatant was removed and the solid-support was washed three times with 1ml Milli-Q water and the oligonucleotide was cleaved off the solid-support according to the standard procedure given in Chapter 8.3.4. The reaction was analyzed by denat. PAGE.

8.4.2 Self-assembly of ODN-dihexapeptide-ODN conjugates

Hybridization procedure

The hybridization was performed as described in section 8.1.3. The hybridization was analyzed by 1.7% agarose gel electrophoresis.

ODN sequences

All ODNs were purchased from Biomers.net GmbH (Ulm, Germany). Prior to the hybridization all strands were purified by gel extraction (see Chapter 8.1.2).

T2A: 5´-TCA ATG AAA CAC TAG GCG AGG ACG CAC AGA TCG CAG CAC GCT CTT GAT AGA TGC TGT ATC-3´

T2B: 5´-TCA ATG AAA CAC TAG GCG AGG ACG ATA CAG CAT CTA TCA AGA GCG TGC TGC GAT CTG TGC-3´

PD1: 5‘ GAT ACA GCA TCT ATC AAG AGC GTG CTG CGA TCT GTG C TC AAT GAA ACA CTA GGC GAG GAC 3‘

PD2: 5-‘GCA CAG ATC GCA GCA CGC TCT TGA TAG ATG CTG TAT CTC AAT GAA ACA CTA GGC GAG GAC-3‘

8.4.3 Synthesis of ODN23-E4-40-ODN23 triblock copolymers

NHS coupling of ODN23 and E4-40TNB

The oligonucleotide ODN23 (23b, sequence S2, Chapter 8.3.1) bound to the solid support (12mg) was treated with 0.6ml TNB protected E4-40 solution (c=8mg/ml, for TNB protection protocol see Chapter 8.3.4) in degassed PBS buffer (0.058M phosphate, 0.087M NaCl, pH=7.3). The mixture was incubated under argon over night at RT. The supernatant was removed and the solid-support was washed three times with 0.5ml Milli-Q water. The oligonucleotide conjugate was cleaved off the solid-support according to the standard procedure given in Chapter 8.3.4. The ODN-ELP diblock copolymer was isolated by salt precipitation (see Chapter 8.3.4). The reaction and purification process were analyzed by denat. PAGE.

SMCC functionalization of ODN23

An amount of 400µg amino functionalized ODN23 (23b, sequence S2, Chapter 8.3.1) was functionalized with SMCC according to the optimized procedure given in Chapter 8.3.1. The freshly prepared and purified SMCC-ODN23 was used immediately.

Thiol coupling of ODN23-E4-40 conjugate to SMCC functionalized ODN

A solution of V=65µl of the purified ODN23-E4-40 (c=1.4µg/µl) was incubated with V=1ml TCEP solution (20mM) for 1h on a shaker. The reducing agent was removed by gel filtration using a NAP5 column (Sephadex G-25, GE healthcare). The sample was eluted with 1ml 1x PBS buffer (0.01M phosphate, 0.015M NaCl, pH=7.3) in fractions of 0.25ml. After the reducing step with TCEP the ODN-E4-40 conjugate (V=0.5ml, fraction 2+3) was combined with 2ml solution of a SMCC modified ODN23 (sequence S2) in PBS buffer (0.01M phosphate, 0.015M NaCl, pH=7.2). The mixture was incubated in the dark for seven days under argon and at RT. After the second day the temperature was raised to T=37°C. Aliquots of the reaction were analyzed after the first day, the second day and after seven days by denat. PAGE and SDS-PAGE.

The isolation of the triblock copolymer by salt precipitation was not successful. Therefore the adsorption of the unreacted diblock copolymer onto gold nano spheres was tested.

Purification of ODN-E4-40-ODN by adsorption onto gold nano spheres

An aqueous mixture of diblock and triblock copolymer (V=0.1ml, c (DNA) =0.2µg/µl) was first incubated for 30min with 20µl TCEP solution (0.5M). The excess of reducing agent was removed by gel filtration (NAP5 column, Sephadex G-25, GE healthcare). The sample was eluted with Milli-Q water. 1ml of the eluted sample (m (DNA) ~10µg) was added to a pellet of citrate stabilized gold nano spheres (d=20nm, c~ 10^{11}particels/ml, 1ml standard solution, centrifuged) . The mixture was shaken over night at RT and then centrifuged at 10 000rpm for 10min. The supernatant was separated and subject to SDS-PAGE. The pellet was resuspended and analyzed by horizontal 0.2% agarose gel electrophoresis. The supernatant was incubated a second time with the 10fold amount of gold nano spheres (d=20nm, c~ 10^{11}particels/ml, 10ml standard solution, centrifuged) under the same conditions.

8.4.4 Synthesis of ODN46-E4-40-ODN23 triblock copolymers

NHS coupling of ODN23 and the hexapeptide

An ODN46-E4-40 conjugate (sequence K4S3, 46b) was prepared according to the optimized procedure given in Chapter 8.4.3. The diblock conjugation was analyzed by denat. PAGE prior to the thiol coupling. For the following coupling reaction the diblock copolymer was not purified by salt precipitation or dialysis. The reaction mixture after cleavage off the solid support and removal of the ammonia was used in this case.

SMCC functionalization of ODN23

An amino functionalized ODN23 (23b, sequence S2, see Chapter 8.3) was functionalized with SMCC according to the optimized procedure given in Chapter 8.3.3. The freshly prepared and purified SMCC-ODN23 was used immediately.

Thiol coupling of ODN23-hexapeptide conjugate to SMCC functionalized ODN

The unpurified ODN46-E4-40 (V=50µl, c (DNA) ~0.5µg/µl) was incubated with 50µl TCEP solution (0.5M) for 1h at 15°C. After adding 0.1ml saturated NaCl solution the mixture was centrifuged at 11000rpm for 10min and the supernatant was discarded. The pellet was resuspended in 0.1ml degassed PBS buffer (0.01M phosphate, 0.015M NaCl, pH 7.3). The reduced ODN-E4-40 conjugate was immediately combined with V=1ml of SMCC modified ODN23 (c=0.23µg/µl) in degassed PBS buffer (0.01M phosphate, 0.015M NaCl, pH=7.2). The mixture was incubated for two days in the dark under argon at RT. The reaction was analyzed by denat. PAGE and SDS-PAGE.

8.5 Materials

Chemicals:

Ammonium hydroxide solution (28%), ethidium bromide (10mg/ml), TCEP solution (0.5M), 5,5'-(dithiobis-(2-nitrobenzoic acid)(DTNB), urea (for electrophoresis), butanol (for molecular biology), ethanol (absolute puriss.), acetonitril (HPLC grade) formamide, triethylamine and TAE buffer (10x concentrated) were obtained from Sigma-Aldrich. Sodium Chloride (NaCl), sodium dodecyl sulfate (SDS, ultra pure), glycine, tetramethylethylendiamine (TEMED), tris(hydroxymethyl)aminomethane (Tris), tris(hydroxymethyl)aminomethane hydrochloride (Tris·HCl), D(+)-succrose, ammonium peroxydisulfate (APS), Agarose (High Resolution, ROTI®GAROSE) and Acrylamide/Bisacrylamide 40% (Rotiphorese 40, 19:1) were purchased in molecular biology grade from Roth. Glycerol (anhydrous), ammonium acetate and ethylenediamine tetraacetate (EDTA) disodium salt came in molecular biology grade from Fluka. The linkers BMPS, sulfo-SMCC, SMCC and premixed PBS buffer (BupH phosphate buffered saline, 10x concentrated, 0.1M phosphate, 0.15M NaCl) were purchase from Pierce (Thermo Scientific). 3',3",5',5"-tetrabromophenolsulfonphthalein sodium salt (bromphenol blue, BPB), glacial acetic acid were obtained from Merck. DMF (extra dry, over molecular sieves) was purchased from Acros Organics. GelRed came from Biotium (Bio Trend Chemikalien GmbH). Water was purified by a Milli-Q filter system.

8.6 General Methods

8.6.1 Purification by gel filtration

Gel filtration columns NAP-5 or NAP-25 (Sephadex™ G-25, GE healthcare) were used according to the standard protocol. The column was first equilibrated with 30ml of the desired buffer. The sample was applied and allowed to enter the gel bed completely. The elution buffer (V=1ml or V=3.5ml) was loaded onto the column and fractions of V= 0.2ml or V=1.ml were collected. The DNA concentration of each fraction was determined by UV.

8.6.2 UV Spectroscopy

All DNA absorption spectra were monitored using a Carry 100Bio UV-VIS Spectrophotometer (Varian, Inc). The concentrations of DNA solutions were determined by measuring the absorption Abs_{260nm} at λ=260nm using the Carry 100Bio Spectrophotometer or an Eppendorf Biophotometer (Eppendorf). The concentration was estimated by multiplying the absorption Abs_{260nm} with 37µg/ml for ssDNA or with 47µg/ml for dsDNA.

8.6.3 DNA Polyacrylamide Gel Electrophoresis (DNA PAGE)

The DNA PAGE analysis was performed using the PerfectBlue Twin L vertical double gel system (200x200x0.8mm, Peqlab, Germany). The gels were always freshly prepared. After the electrophoresis the gels were stained either with GelRed or with Ethidium Bromide (EtBr). The gels were documented by using the E-Box 1000/20M gel imaging system (Peqlab, Germany). The E-Capt software (Vilber Lourmat) was used to analyze the gel pictures. Gel intensities were determined by the Scion Image software (Scion Corporation).

Denaturating conditions

Gels under denaturating conditions were prepared by diluting the 40% Acrylamide/Bisacrylamide (n:n=19:1) stock solution with 10x TBE containing 50% w/v urea and Milli-Q water to the desired gel concentration (10-20%). The polymerization was initiated by adding 1% v/v APS solution (10%w/v in Milli-.Q) and 0.1% v/v TEMED. The samples (m (DNA) =1µg) were diluted with denat. loading buffer (90% formamide, 10mM NaOH, 1mM EDTA, 0.1% w/v bromphenol blue) and denaturated by incubation at T=90°C for 2-4min. The electrophoresis was performed in 1x TBE running buffer (0.1M Tris-borate, 2mM EDTA, pH=8.3) at T=50°C at a constant voltage of U=600V.

Native conditions

Gels under denaturating conditions were prepared by diluting the 40% Acrylamide/Bisacrylamide (n:n=19:1) stock solution with 10x TAE/$Mg(OAc)_2$ (400 mM Tris acetate, 10 mM EDTA, 125 mM Magnesium acetate, pH=8.3)and Milli-Q water to the desired gel concentration (8-15%). The polymerization was initiated by adding 1% v/v APS solution (10%w/v in Milli-.Q) and 0.1% v/v TEMED. The samples (m (DNA) =1µg) were diluted with native loading buffer (30% sucrose in 1x TAE/ $Mg(OAc)_2$). The electrophoresis was performed in 1x TAE/$Mg(OAc)_2$ running buffer (40mM TAE, 12.5mM $Mg(OAc)_2$,) at the desired temperature (T=4-50°C) and at constant voltage of U=250V.

Gel staining

The GelRed staining solution was prepared by diluting 65µl GelRed stock solution (10 000x in DMSO with 250ml Milli-Q water. The gels were incubated in the staining solution for 15min in the dark.

The EtBr staining solution was prepared by diluting 250µl ethidium bromide stock solution (10mg/ml) with 500ml Milli-Q water. The gels were incubated in the staining solution for 5min and then rinsed in Milli-Q water for 10min.

8.6.4 Native Agarose Gel Electrophoresis

The analysis of the hybridization experiments was done by native agarose gel electrophoresis using the vertical single gel GENterphorese system (70x66x2mm, GENterprise Genomics, Germany). The gels contained 1.7% High Resolution Agarose (ROTI AGAROSE, Carl Roth, Germany) in 1x TBE puffer which was also used as running buffer. 2µl of sample were combined with 2µl tracking dye (0.05% w/v bromphenol blue, 40% w/v sucrose, 0.5% w/v SDS, 0.1M EDTA, pH=8, Sigma-Aldrich). The gels were run at constant current of 85mA for 1h and stained with EtBr (Chapter 8.5.3).

8.6.5 SDS Polyacrylamide Gel Electrophoresis

The SDS-PAGE was performed in an XCell Surelock Mini-Cell (Invitrogen) using precast Tris-Glycine gels with a gradient of 4-20% or 10-20%. The gels were run in a 1x SDS running buffer (0.025M Tris, 0.192 Glycine, 0.1% w/v SDS). The conditions were chosen according to the standard procedure by Invitrogen. Usually the gel were run at constant voltage of U=125V for 1h 30min. The samples (c_{final}=0.1-0.3µg/µl) were diluted with 2.5µl loading buffer (100mM Tris-HCl, pH=6.8, 4%w/v SDS, 24% v/v glycerol, 0.4mM bromphenol blue) and Milli-Q water to a final volume of 10 µl. The gels were stained first with EtBr and second with silver staining (SilverQuest Kit, Invitrogen) using the standard fast protocol.

9 Appendix

9.1 Additional data

9.1.1 UV melting curve of junction K3

In Figure 9.1 the melting profils of junction K4 and K3 are shown. In comparsion, the melting curve of K4 is more prononced than the one of K3. The early rise in absorption ofr K3 is due to the melting of the single stranded dangling ends.

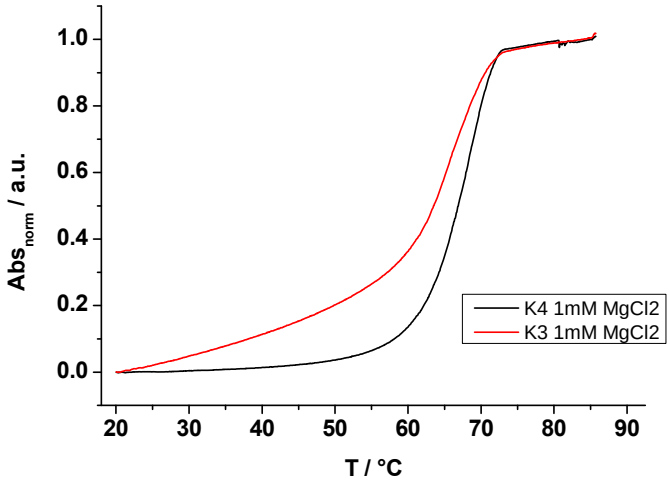

Figure 9.1 Normalized melting profil of junction K4 and K3 measured in 1mM $MgCl_2$ solution.

9.1.2 Peptide concentration determination

The ELP concentration was estimated by measuring the absorption at λ=230nm. Figure 9.1 shows the calibration curve. It was obtained by measuring the absorption A_{230} for E4-40 samples of known concentration. The linear fit was used to determine the peptide concentration of E4-40 solution with unknown concentration.

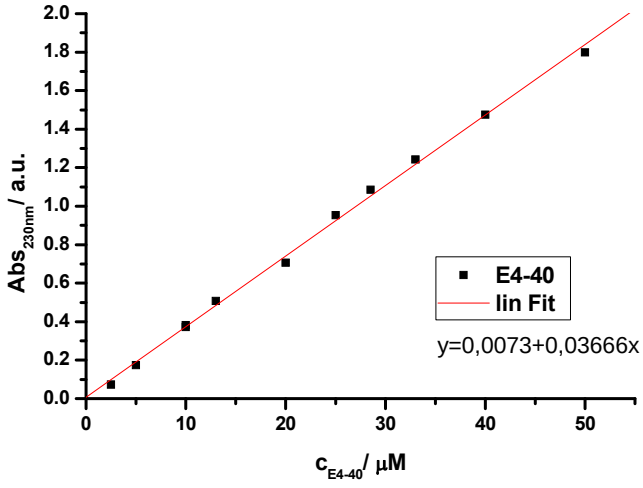

Figure 9.2 Plot of the absorption at 230nm versus the ELP E4-40 concentration in µM.

9.1.3 ODN-hexapeptide conjugation

In Figure 6.3 the gel analysis of the reduced ODN-hexapeptide conjugate after step 3 (see Chapter 6.1.

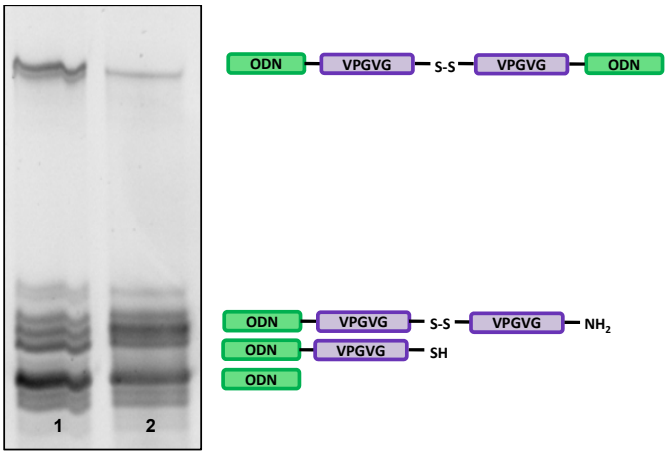

Figure 6.3 Denat. PAGE (20%) of the ODN-hexapeptide conjugation reaction. Lane 1: non-reduced sample of the reaction after step 3; Lane 2: reduced sample of the reaction after step 3.

9.2 Reaction Conditions

Each table contains the detailed reaction conditions for the results discussed in Chapter 5 and 6. The figure number corresponding to the discussed reaction result is given in each table.

9.2.1 Conditions for Reactions described in Chapter 5

Table 9.1 Conditions for thiol addition of thio-PEG to Acrydite™ ODNs

Fig 5.2	A		B
c (thio-PEG)	0.03M (1000x excess) in buffer	**c (thio-PEG)**	0.03M (1000x excess) in buffer
V (thio-PEG) / ml	0.71	**V (thio-PEG) / ml**	0.18
n (Acrydite)	~ 0.02umol	**n (Acrydite)**	~ 0.005umol
V(Acrydite) / ml	0.10	**V(Acrydite) / ml**	0.025
buffer	PBS-E	**buffer**	PBS-E
ionic strength	0.1M Phosphate, 0.15M NaCl, 1mM EDTA	**ionic strength**	0.1M Phosphate, 0.15M NaCl, 1mM EDTA
pH	7.5	**pH**	6.7, 7.5 or 8.3
reaction time / h	25h	**reaction time / h**	19h
temperature / °C	RT or 40°C	**temperature / °C**	40°C

Table 9.2 Conditions for BPMS and sulfo-SMCC modification of amino ODNs

Fig 5.7	BPMS		sulfo-SMCC
c (linker)	10mM (100x excess) in DMF	**c (linker)**	15.5mM (100x excess)
V (linker) / ul	90.0	**V (linker) / ul**	125.0
n (ODN)	0.014umol	**n (ODN)**	0.035umol
V (buffer) / ml	0.8	**V (buffer) / ml**	1.1
buffer	PBS	**buffer**	PBS
ionic strength	0.1M Phosphate, 0.15M NaCl	**ionic strength**	0.1M Phosphate, 0.15M NaCl
pH	7.0	**pH**	7.0
reaction time / h	4	**reaction time / h**	4

Table 9.3 Conditions for SMCC modification of amino ODNs in solution

Fig 5.9	A		B
c (SMCC)	13mM (100x excess) in DMF	**c (SMCC)**	1.5mM (50x excess) in DMF
V(SMCC) / ml	0.23	**V(SMCC) / ml**	1.0
n (ODN)	0.0375umol	**n (ODN)**	0.035umol
V (buffer) / ml	2.0	**V (buffer) / ml**	1.0
buffer	PBS	**buffer**	PBS
ionic strength	0.1M Phosphate, 0.15M NaCl	**ionic strength**	0.1M Phosphate, 0.15M NaCl
pH	7.2	**pH**	7.3
reaction time / h	4	**reaction time / h**	3

Table 9.4 Conditions for SMCC modification of solid support bound amino ODNs

Fig 5.10	A		B
c (SMCC)	30mM (500x excess) in DMF	**c (SMCC)**	7.5mM (45x excess) in DMF
V(SMCC) / ml	1.0	**V(SMCC) / ml**	0.5
n (ODN)	0.056umol (CPG)	**n (ODN)**	0.083umol
m (CPG) / mg	10.0	**V (buffer) / ml**	1.0
buffer	DMF	**buffer**	PBS
ionic strength	-	**ionic strength**	0.01M Phosphate, 0.015M NaCl
pH	-	**pH**	7.3
reaction time / h	over night	**reaction time / h**	4

Table 9.5 Conditions for thiol addition of thio-PEG to SMCC-ODNs

Fig. 5.15	step 1		step 2
c (SMCC)	1.5mM (50x excess) in DMF	c (thio-PEG)	12mM (100x excess) in buffer
V(SMCC) / ml	1.0	V(thio-PEG) / ml	0.1
n (ODN)	0.035umol	n (ODN-SMCC)	0.0027umol
V (buffer) / ml	1.0	V (ODN-SMCC) / ml	0.43
buffer	PBS	buffer	PBS
ionic strength	0.1M Phosphate, 0.15M NaCl	ionic strength	0.1M Phosphate, 0.15M NaCl
pH	7.3	pH	7.3
reaction time / h	3	reaction time / h	3

Table 9.6 Conditions for thiol addition of thio-ODN to SMCC-ODNs

Fig 5.17	step 1		step 2
c (SMCC)	1.5mM (50x excess) in DMF	n (SH-ODN)	0.0014 umol (1.3x excess) in water
V(SMCC) / ml	1.0	V(SH-ODN) / ml	0.1
n (ODN)	0.035umol	n (ODN-SMCC)	0.0011 umol in buffer
V (buffer) / ml	1.0	V (ODN-SMCC) / ml	0.42
buffer	PBS	buffer	PBS
ionic strength	0.1M Phosphate, 0.15M NaCl	ionic strength	0.1M Phosphate, 0.15M NaCl
pH	7.3	pH	7.3
reaction time / h	3	reaction time / h	over night

Table 9.7 Conditions for thiol addition of a hexapeptide to SMCC-ODNs

Fig 5.19	step 1		step 2
c (SMCC)	9.5mM (50x excess) in DMF	n (Hexapeptide)	3.8 umol (290x excess) in buffer
V(SMCC) / ml	0.3	V(Hexapeptide) / ml	0.3
n (ODN)	0.042umol	n (ODN-SMCC)	0.013 umol in buffer
V (buffer) / ml	0.6	V (ODN-SMCC) / ml	2.00
buffer	PBS	buffer	PBS
ionic strength	0.1M Phosphate, 0.15M NaCl	ionic strength	0.1M Phosphate, 0.15M NaCl
pH	7.3	pH	7.3
reaction time / h	4	reaction time / h	over night

Table 9.8 Conditions for thiol addition of ELP to SMCC-ODNs

Fig 5.21	step 1		step 2
c (SMCC)	30mM (250-500x excess) in DMF	c (ELP)	0.6-0.8 uM (4.3-11x excess) in buffer
V(SMCC) / ml	0.6	V(ELP) / ml	0.25
n (ODN)	0.035-0.07 umol	n (ODN-SMCC)	0.018-0.035 umol in buffer
V (buffer) / ml	1.0	V (ODN-SMCC) / ml	1.00
buffer	PBS	buffer	PBS
ionic strength	0.01M Phosphate, 0.015M NaCl	ionic strength	0.01M Phosphate, 0.015M NaCl
pH	7.3	pH	7.3
reaction time / h	4	reaction time / h	over night

Table 9.9 Conditions for TNB protection of ELP.

Fig. 5.27	
c (DTNB)	8.2mM (14x excess) in buffer (E4-120 60x excess)
V(DTNB) / ml	5.0
n (ELP)	3 umol (E4-120 0.7umol) in buffer
V (buffer) / ml	5ml
buffer	PBS-E
ionic strength	0.1M Phosphate, 0.15M NaCl, 1mM EDTA
pH	78.0
reaction time / min	15

Table 9.10 Conditions for reaction of TNB-protected E4-40 with NHS ODNs bound to solid support.

Fig. 5.29	A		B
c (E4-40-TNB)	0.3mM (4.3x excess) in buffer	c (E4-40-TNB)	0.6mM (6x excess) in buffer
V(E4-40-TNB) / ml	0.6	V(E4-40-TNB) / ml	1.0
n (ODN)	~ 0.067umol (CPG)	n (ODN)	~ 0.1umol (CPG)
m (CPG) / mg	12.0	m (CPG) / mg	20.0
buffer	PBS	buffer	PBS
ionic strength	0.58M Phosphate, 0.87M NaCl	ionic strength	0.50M Phosphate, 0.3M NaCl
pH	7.3	pH	7.3
reaction time / h	over night	reaction time / h	over night

Table 9.11 Conditions of TNB protected ELP with NHS ODNs

Fig. 5.32	
c (ELP-TNB)	0.09-0.5mM (1.7-10x excess) in buffer
V(ELP-TNB) / ml	0.7
n (ODN)	~ 0.038-0.05umol (CPG)
m (CPG) / mg	7.5-10
buffer	PBS
ionic strength	0.55M Phosphate, 0.83M NaCl
pH	7.3
reaction time / h	over night

9.2.2 Conditions for Reactions described in Chapter 6

Table 9.7 Conditions for synthesis of ODN23-hexapeptide-ODN23 conjugates

Fig. 6.2	step 1		step 2		step 3
c (hexapeptide)	70mM (100x excess) in buffer	c (SMCC)	13.4mM (100excess) in DMF	n (diblock)	~ 0.015umol (CPG)
V (hexapeptide) / ml	0.5	V(SMCC) / ml	0.2	m (CPG) / mg	<5.0
n (ODN)	~ 0.03umol (CPG)	n (ODN)	0.035umol	n (SMCC-ODN)	~ 0.016umol in buffer
m (CPG) / mg	5.0	V (buffer) / ml	2.0	V (buffer) / ml	1.8
buffer	PBS	buffer	PBS	buffer	PBS
ionic strength	0.1M Phosphate, 0.15M NaCl	ionic strength	0.1M Phosphate, 0.15M NaCl	ionic strength	0.01M Phosphate, 0.015M NaCl
pH	7.2	pH	7.2	pH	7.2
reaction time / h	6	reaction time / h	4	reaction time / h	over night

Table 9.7 Conditions for the synthesis of ODN23-E4-40-ODN23 conjugates

Fig. 6.9	**step 1**		**step 2**		**step 3**
c (E4-40-TNB)	0.3mM (4.3x excess)	**c (SMCC)**	7.5mM (100excess) in DMF	**n (diblock)**	~ 0.0073umol in buffer
V(E4-40-TNB) / ml	0.6	**V(SMCC) / ml**	0.7	**V(SMCC) / ml**	0.5
n (ODN)	~ 0.067umol (CPG)	**n (ODN)**	0.056umol	**n (SMCC-ODN)**	~ 0.039umol (5x excess) in buffer
m (CPG) / mg	12.0	**V (buffer) / ml**	1ml	**V(SMCC-ODN) / ml**	2ml
buffer	PBS	**buffer**	PBS	**buffer**	PBS
ionic strength	0.58M Phosphate, 0.87M NaCl	**ionic strength**	0.01M Phosphate, 0.015M NaCl	**ionic strength**	0.01M Phosphate, 0.015M NaCl
pH	7.3	**pH**	7.3	**pH**	7.3
reaction time / h	8	**reaction time / h**	4	**reaction time / h**	over night

9.3 Plasmid Sequences

9.3.1 peT 24a(+) plasmid (New England Biolabs, NEB)

```
BASE COUNT     1260 a      1374 c      1422 g      1254 t
ORIGIN
        1 atccggatat agttcctcct ttcagcaaaa aacccctcaa gacccgttta gaggccccaa
       61 ggggttatgc tagttattgc tcagcggtgg cagcagccaa ctcagcttcc tttcgggctt
      121 tgttagcagc cggatctcag tggtggtggt ggtggtgctc gagtgcggcc gcaagcttgt
      181 cgacggagct cgaattcgga tccgcgaccc atttgctgtc caccagtcat gctagccata
      241 tgtatatctc cttcttaaag ttaaacaaaa ttatttctag aggggaattg ttatccgctc
      301 acaattcccc tatagtgagt cgtattaatt tcgcgggatc gagatctcga tcctctacgc
      361 cggacgcatc gtggccggca tcaccggcgc cacaggtgcg gttgctggcg cctatatcgc
      421 cgacatcacc gatggggaag atcgggctcg ccacttcggg ctcatgagcg cttgtttcgg
      481 cgtgggtatg gtggcaggcc ccgtggccgg gggactgttg ggcgccatct ccttgcatgc
      541 accattcctt gcggcggcgg tgctcaacgg cctcaaccta ctactgggct gcttcctaat
      601 gcaggagtcg cataagggag agcgtcgaga tcccggacac catcgaatgg cgcaaaacct
      661 ttcgcggtat ggcatgatag cgcccggaag agagtcaatt cagggtggtg aatgtgaaac
      721 cagtaacgtt atacgatgtc gcagagtatg ccggtgtctc ttatcagacc gtttcccgcg
      781 tggtgaacca ggccagccac gtttctgcga aaacgcggga aaaagtggaa gcggcgatgg
      841 cggagctgaa ttacattccc aaccgcgtgg cacaacaact ggcgggcaaa cagtcgttgc
      901 tgattggcgt tgccacctcc agtctggccc tgcacgcgcc gtcgcaaatt gtcgcggcga
      961 ttaaatctcg cgccgatcaa ctgggtgcca gcgtggtggt gtcgatggta gaacgaagcg
     1021 gcgtcgaagc ctgtaaagcg gcggtgcaca atcttctcgc gcaacgcgtc agtgggctga
     1081 tcattaacta tccgctggat gaccaggatg ccattgctgt ggaagctgcc tgcactaatg
     1141 ttccggcgtt atttcttgat gtctctgacc agacacccat caacagtatt attttctccc
     1201 atgaagacgg tacgcgactg ggcgtggagc atctggtcgc attgggtcac cagcaaatcg
     1261 cgctgttagc gggcccatta agttctgtct cggcgcgtct gcgtctggct ggctggcata
     1321 aatatctcac tcgcaatcaa attcagccga tagcggaacg ggaaggcgac tggagtgcca
     1381 tgtccggttt tcaacaaacc atgcaaatgc tgaatgaggg catcgttccc actgcgatgc
     1441 tggttgccaa cgatcagatg gcgctgggcg caatgcgcgc cattaccgag tccgggctgc
     1501 gcgttggtgc ggatatctcg gtagtgggat acgacgatac cgaagacagc tcatgttata
     1561 tcccgccgtt aaccaccatc aaacaggatt ttcgcctgct ggggcaaacc agcgtggacc
     1621 gcttgctgca actctctcag ggccaggcgg tgaagggcaa tcagctgttg cccgtctcac
     1681 tggtgaaaag aaaaaccacc ctggcgccca atacgcaaac cgcctctccc cgcgcgttgg
     1741 ccgattcatt aatgcagctg gcacgacagg tttcccgact ggaaagcggg cagtgagcgc
     1801 aacgcaatta atgtaagtta gctcactcat taggcaccgg gatctcgacc gatgcccttg
     1861 agagccttca acccagtcag ctccttccgg tgggcgcggg gcatgactat cgtcgccgca
     1921 cttatgactg tcttctttat catgcaactc gtaggacagg tgccggcagc gctctgggtc
     1981 attttcggcg aggaccgctt tcgctggagc gcgacgatga tcggcctgtc gcttgcggta
     2041 ttcggaatct tgcacgccct cgctcaagcc ttcgtcactg gtcccgccac caaacgtttc
     2101 ggcgagaagc aggccattat cgccggcatg gcggccccac gggtgcgcat gatcgtgctc
     2161 ctgtcgttga ggacccggct aggctggcgg ggttgcctta ctggttagca gaatgaatca
     2221 ccgatacgcg agcgaacgtg aagcgactgc tgctgcaaaa cgtctgcgac ctgagcaaca
     2281 acatgaatgg tcttcggttt ccgtgtttcg taaagtctgg aaacgcggaa gtcagcgccc
     2341 tgcaccatta tgttccggat ctgcatcgca ggatgctgct ggctaccctg tggaacacct
     2401 acatctgtat taacgaagcg ctggcattga ccctgagtga tttttctctg gtcccgccgc
     2461 atccataccg ccagttgttt accctcacaa cgttccagta accgggcatg ttcatcatca
     2521 gtaacccgta tcgtgagcat cctctctcgt ttcatcggta tcattacccc catgaacaga
     2581 aatccccctt acacggaggc atcagtgacc aaacaggaaa aaaccgccct taacatggcc
     2641 cgctttatca gaagccagac attaacgctt ctggagaaac tcaacgagct ggacgcggat
     2701 gaacaggcag acatctgtga atcgcttcac gaccacgctg atgagcttta ccgcagctgc
     2761 ctcgcgcgtt tcggtgatga cggtgaaaac ctctgacaca tgcagctccc ggagacggtc
     2821 acagcttgtc tgtaagcgga tgccgggagc agacaagccc gtcagggcgc gtcagcgggt
     2881 gttggcgggt gtcggggcgc agccatgacc cagtcacgta gcgatagcgg agtgtatact
     2941 ggcttaacta tgcggcatca gagcagattg tactgagagt gcaccatata tgcggtgtga
     3001 aataccgcac agatgcgtaa ggagaaaata ccgcatcagg cgctcttccg cttcctcgct
     3061 cactgactcg ctgcgctcgg tcgttcggct gcggcgagcg gtatcagctc actcaaaggc
     3121 ggtaatacgg ttatccacag aatcagggga taacgcagga aagaacatgt gagcaaaagg
     3181 ccagcaaaag gccaggaacc gtaaaaaggc cgcgttgctg gcgtttttcc ataggctccg
     3241 ccccccctgac gagcatcaca aaaatcgacg ctcaagtcag aggtggcgaa acccgacagg
     3301 actataaaga taccaggcgt ttcccccctgg aagctccctc gtgcgctctc ctgttccgac
```

```
3361 cctgccgctt accggatacc tgtccgcctt tctcccttcg ggaagcgtgg cgctttctca
3421 tagctcacgc tgtaggtatc tcagttcggt gtaggtcgtt cgctccaagc tgggctgtgt
3481 gcacgaaccc cccgttcagc ccgaccgctg cgccttatcc ggtaactatc gtcttgagtc
3541 caacccggta agacacgact tatcgccact ggcagcagcc actggtaaca ggattagcag
3601 agcgaggtat gtaggcggtg ctacagagtt cttgaagtgg tggcctaact acggctacac
3661 tagaaggaca gtatttggta tctgcgctct gctgaagcca gttaccttcg gaaaaagagt
3721 tggtagctct tgatccggca aacaaaccac cgctggtagc ggtggttttt ttgtttgcaa
3781 gcagcagatt acgcgcagaa aaaaaggatc tcaagaagat cctttgatct tttctacggg
3841 gtctgacgct cagtggaacg aaaactcacg ttaagggatt ttggtcatga acaataaaac
3901 tgtctgctta cataaacagt aatacaaggg gtgttatgag ccatattcaa cgggaaacgt
3961 cttgctctag gccgcgatta aattccaaca tggatgctga tttatatggg tataaatggg
4021 ctcgcgataa tgtcgggcaa tcaggtgcga caatctatcg attgtatggg aagcccgatg
4081 cgccagagtt gtttctgaaa catggcaaag gtagcgttgc caatgatgtt acagatgaga
4141 tggtcagact aaactggctg acggaattta tgcctcttcc gaccatcaag cattttatcc
4201 gtactcctga tgatgcatgg ttactcacca ctgcgatccc cgggaaaaca gcattccagg
4261 tattagaaga atatcctgat tcaggtgaaa atattgttga tgcgctggca gtgttcctgc
4321 gccggttgca ttcgattcct gtttgtaatt gtccttttaa cagcgatcgc gtatttcgtc
4381 tcgctcaggc gcaatcacga atgaataacg gtttggttga tgcgagtgat tttgatgacg
4441 agcgtaatgg ctggcctgtt gaacaagtct ggaaagaaat gcataaactt ttgccattct
4501 caccggattc agtcgtcact catggtgatt tctcacttga taaccttatt tttgacgagg
4561 ggaaattaat aggttgtatt gatgttggac gagtcggaat cgcagaccga taccaggatc
4621 ttgccatcct atggaactgc ctcggtgagt tttctccttc attacagaaa cggctttttc
4681 aaaaatatgg tattgataat cctgatatga ataaattgca gtttcatttg atgctcgatg
4741 agtttttcta gaattaatt catgagcgga tacatatttg aatgtattta gaaaaataaa
4801 caaatagggg ttccgcgcac atttccccga aaagtgccac ctgaaattgt aaacgttaat
4861 attttgttaa aattcgcgtt aaatttttgt taaatcagct catttttaa ccaataggcc
4921 gaaatcggca aaatccctta taaatcaaaa gaatagaccg agatagggtt gagtgttgtt
4981 ccagtttgga acaagagtcc actattaaag aacgtggact ccaacgtcaa agggcgaaaa
5041 accgtctatc agggcgatgg cccactacgt gaaccatcac cctaatcaag ttttttgggg
5101 tcgaggtgcc gtaaagcact aaatcggaac cctaaaggga gcccccgatt tagagcttga
5161 cggggaaagc cggcgaacgt ggcgagaaag gaagggaaga aagcgaaagg agcgggcgct
5221 agggcgctgg caagtgtagc ggtcacgctg cgcgtaacca ccacacccgc cgcgcttaat
5281 gcgccgctac agggcgcgtc ccattcgcca
```

9.3.2 Design SF1 vector

New Ult vector cloning and expression vector designed by J. McDaniel and A. MacKay

- Protocol: cut pET-24a T7 promoter plasmid with NdeI and BamHI

```
NDEI
|
    M   G    BSEI   BSEI       G    F   C  stop
 t atg gg|c gGAGGAG CTCCTCtg  gg|c TTC TGC tga taa g|
    ac|cc g cCTCCTC GAGGAGac |cc g AAG ACG act att c CTAG|
                                                 BamHI
```

ULT_SF1_f: forward(38 nucleotides):

5′-tat ggg cgG AGG AGC TCC TCt ggg cTT CTG Ctg ata ag-3′

ULT_SF1_r: reverse (40 nucleotides):

5′-GAT Cct tat caG CAG AAg ccc aGA GGA GCT CCT Ccg ccc a-3′

9.3.3 JMD2 vector

Cloning and expression vector for new RDL strategy designed by J. McDaniel and A. MacKay.

- Protocol: cut pET-24a T7 promoter plasmid with XbaI and BamHI

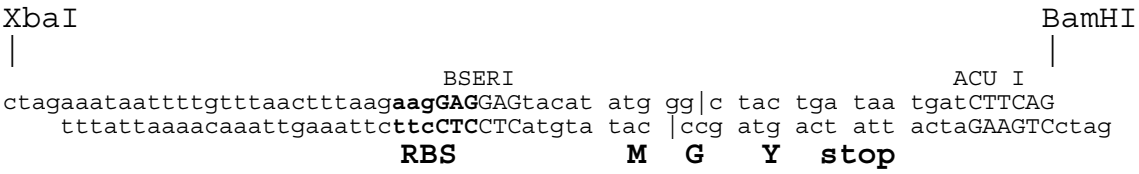

forward(66 nucleotides):
5′-cta gaa ata att ttg ttt aac ttt aag aag GAG GAG tac ata tgg gct act gat aat gat CTT CAG-3′

reverse (5′ to 3′) (66 nucleotides):

5′-gat cCT GAA Gat cat tat cag tag ccc ata tgt aCT CCT Cct tct taa agt taa aca aaa tta ttt-3‘

9.4 ELP 4: 5 pentamer vector

ELP pentamer sequence with the guest residues V. The amino acid sequence is encoded by:

v p g v g

gtt cca ggt gcg ggc

For an ELP4-5 pentamer insert the following oligonucleotide sequences have to be ligated into the vector. The polypeptides expressed by this vector have the amino acid sequence MG[VGVPG]$_n$Y (with Y= amino acid encoded in the terminating sequence).

Forward (75 nucleotides)

5′-C**GT G**GG TGT TCC GGG C**GT A**GG TGT CCC AGG T**GT G**GG CGT ACC GGG C**GT T**GG TGT TCC TGG T**GT C**GG CGT GCC GGG-3′

Reverse (75 nucleotides)

5′-CGG CAC GCC GAC ACC AGG AAC ACC AAC GCC CGG TAC GCC CAC ACC TGG GAC ACC TAC GCC CGG AAC ACC CAC GCC-3′

9.5 Abbreviations

A	adenine
AFM	atomic force microscopy
BMPS	N-[ß-Maleimidopropyloxy]succinimide ester
bp	base pair
C	cytosine
CPG	controlled pore glass (solid support for ODN synthesis)
Cys	cysteine
DLS	dynamic light scattering
DMT	dimethoxytrityl
DNA	deoxyribonucleic acid
ds	double stranded
DTT	dithiothreitol
DX	DNA double crossover
EDC	1-ethyl-3-(3-dimethylaminopropyl) carbodiimide)
EDTA	ethylendiamine tetraacetate
ELP(s)	Elastin-like polypeptide(s)
EtBr	ethidium bromide
FRET	fluorescence resonance energy transfer
G	guanine
GE	gel electrophoresis
Gly, G	glycine
HPLC	high-performance liquid chromatography
Hyb90, Hyb90nig	temperature controlled hybridization programs
IDT	Integrated DNA technologies
IP	ion pair
IP-RP HPLC	ion pair-reversed phase high performance liquid chromatography
ITC	inverse transition cycling
LCST	lower criticl solution temperature
MBS	m-Maleimidobenzoyl-N-hydroxysuccinimide ester

mRNA	messenger ribonucleic acid
MWCO	molecular weight cutoff
NHS	N-hydroxysuccinimide
NMR	nuclear magnetic resonance
NP	normal phase
OD	optical density
ODN	oligodeoxynucleotide, oligonucleotide
ODN-ELP	oligonucleotide-Elastin-like-polypeptide block copolymer
OPC	oligonucleotide-peptide conjugate
PAGE	polyacrylamide gel electrophoresis
PBS	phosphate buffered saline
PCR	polymerase chain reaction
PEI	polyethylenimine
PEO	polyethylene oxide
Phe	phenylalanine
PLGA	poly(D,L-lactic-co-glycolic acid)
PLL	poly(L-lysine)
PO, POC	peptide-oligonucleotide conjugate
PPO	polypropylene oxide
Pro, P	proline
RDL	recursive directional ligation
RP	reversed phase
rpm	rounds per minute
RT	room temperature
SDS	sodium dodecyl sulfate
SLS	static light scattering
SMCC	succinimidyl 4-[N-maleimidomethyl]cyclohexane-1-carboxylate
ss	single stranded
sulfo-NHS	N-hydroxysulfosuccinimide
sulfo-SMCC	sulfosuccinimidyl 4-[N-maleimidomethyl]cyclohexane-1-carboxylate

T	thymine
TAE	tris acetate-EDTA
TCEP	tris(2-carboxyethyl)phosphine
TEAA	triethylammonium acetate
Tris	tris(hydroxymethyl)aminomethane
Tyr, Y	tyrosine
UV	ultraviolet
Val, V	valine
Vis	visible

References

[1] C. Boyer, V. Bulmus, T. P. Davis, V. Ladmiral, J. Q. Liu, S. Perrier, *Chemical Reviews* 2009, *109*, 5402.
[2] L. Hartmann, H. G. Borner, *Advanced Materials* 2009, *21*, 3425.
[3] C. K. Ober, S. Z. D. Cheng, P. T. Hammond, M. Muthukumar, E. Reichmanis, K. L. Wooley, T. P. Lodge, *Macromolecules* 2009, *42*, 465.
[4] G. M. Whitesides, B. Grzybowski, *Science* 2002, *295*, 2418.
[5] M. Putz, K. Kremer, R. Everaers, *Physical Review Letters* 2000, *84*, 298.
[6] P. J. R. Flory, Jr, J.; , *Journal of Chemical Physics* 1943, *11*, 521.
[7] P. J. Flory, *Principles of polymer chemistry*, 13. print. ed., Cornell Univ. Press, Ithaca 1986.
[8] P.-G. d. Gennes, *Scaling concepts in polymer physics*, Cornell Univ. Press, Ithaca, 1979.
[9] F. Miescher, *Hoppe-Seyler's medizinisch-chem. Untersuchungen* 1871, 441.
[10] O. T. Avery, C. M. MacLeod, M. M., *Journal of Experimental Medicine* 1944, *79*, 137.
[11] R. E. Franklin, R. G. Gosling, *Nature* 1953, *171*, 740.
[12] J. D. Watson, F. H. C. Crick, *Nature* 1953, *171*, 737.
[13] S. Neidle, *Principles of nucleic acid structure*, 1. ed., Elsevier Acad. Press, Amsterdam, 2008.
[14] W. Saenger, *Principles of nucleic acid structure*, 2., corr. print.. ed., Springer, New York, 1988.
[15] R. R. Sinden, *DNA structure and function*, Academic Press, San Diego, 1994.
[16] R. L. Ornstein, R. Rein, D. L. Breen, R. D. Macelroy, *Biopolymers* 1978, *17*, 2341.
[17] J. Graw, *Genetik* 4. ed., Springer, Berlin, 2006.
[18] N. Theodorakopoulos, *Lecture* 2003.
[19] J. SantaLucia, *Proceedings of the National Academy of Science of the United States of America* 1998, *95*, 1460.
[20] M. Zuker, *Nucleic Acids Research* 2003, *31*, 3406.
[21] I. D.T (Integrated DNA Technologies), *Oligoanalyzer Online Tool*, http://eu.idtdna.com/ANALYZER/Applications/OligoAnalyzer/Default.aspx.
[22] L. Stryer, *Biochemie*, 4. Aufl. 1996, 1. korr. Nachdr.. ed., Spektrum, Akad. Verl., Heidelberg, 1999.
[23] R. B. Merrifield, *Journal of the American Chemical Society* 1963, *85*, 2149.
[24] C. B. Reese, *Organic & Biomolecular Chemistry* 2005, *3*, 3851.
[25] Biomers.net GmbH, *Technical Informations: Synthesis of Oligonucleotides* http://www.biomers.net/en/index/Technical_Information/Synthesis.html.
[26] N. J. Greco, Y. Z. Tor, *NATURE PROTOCOLS* 2007, *2*, 305.
[27] E. J. Devor, M. A. Behlke, *Technical Bulletin: Oligonucleotide Yield, Resuspension and Storage, 2005, IDT (Integrated DNA Technologies),* http://eu.idtdna.com/Support/Technical/TechnicalBulletinPDF/Oligonucleotide_Yield_Resuspension_and_Storage.pdf.
[28] Biomers.net GmbH, *Technical Informations: Purification PAGE* http://www.biomers.net/en/index/Technical_Information/Purification/Page.html

[29] IDT (Integrated DNA technologies), *Attachement Chemistry/ Linker Modifications* http://eu.idtdna.com/catalog/Modifications/ModificationHome.aspx .
[30] Glenresearch, *The Glen Report* 2002, *15*, 10.
[31] R. Holliday, *Genetical Research* 1964, *5*, 282.
[32] N. C. Seeman, *Journal of theoretical biology* 1982, *99*, 237.
[33] N. C. Seeman, N. R. Kallenbach, *Biophysical journal* 1983, *44*, 201.
[34] N. C. Seeman, *Journal of Biomolecular Structure & Dynamics* 1990, *8*, 573.
[35] J. P. Cooper, P. J. Hagerman, *Journal of molecular biology* 1987, *198*, 711.
[36] D. R. Duckett, A. I. Murchie, S. Diekmann, K. E. von, B. Kemper, D. M. Lilley, *Cell* 1988, *55*, 79.
[37] T. Shida, H. Iwasaki, H. Shinagawa, Y. Kyogoku, *Journal of Biochemistry* 1996, *119*, 653.
[38] J. Liu, A. C. Declais, D. M. Lilley, *Journal of molecular biology* 2004, *343*, 851.
[39] D. M. Lilley, *Quarterly reviews of biophysics* 2008, *41*, 1.
[40] A. I. Murchie, R. M. Clegg, K. E. von, D. R. Duckett, S. Diekmann, D. M. Lilley, *Nature* 1989, *341*, 763.
[41] G. Vamosi, R. M. Clegg, *The journal of physical chemistry* 2008, *112*, 13136.
[42] F. J. J. Overmars, C. Altona, *Journal of Molecular Biology* 1997, *273*, 519.
[43] J. A. Pikkemaat, H. Vandenelst, J. H. Vanboom, C. Altona, *Biochemistry* 1994, *33*, 14896.
[44] M. Ortiz-Lombardia, A. Gonzalez, R. Eritja, J. Aymami, F. Azorin, M. Coll, *Nature Structural Biology* 1999, *6*, 913.
[45] D. M. Lilley, *Quarterly reviews of biophysics* 2000, *33*, 109.
[46] N. C. Seeman, *Nature* 2003, *421*, 427.
[47] J. H. Chen, N. C. Seeman, *Nature* 1991, *350*, 631.
[48] X. J. Li, X. P. Yang, J. Qi, N. C. Seeman, *Journal of the American Chemical Society* 1996, *118*, 6131.
[49] E. Winfree, F. R. Liu, L. A. Wenzler, N. C. Seeman, *Nature* 1998, *394*, 539.
[50] C. Lin, Y. Liu, H. Yan, *Biochemistry* 2009, *48*, 1663.
[51] P. W. K. Rothemund, *Nature* 2006, *440*, 297.
[52] Y. G. Ke, J. Sharma, M. H. Liu, K. Jahn, Y. Liu, H. Yan, *Nano Letters* 2009, *9*, 2445.
[53] H. Dietz, S. M. Douglas, W. M. Shih, *Science* 2009, *325*, 725.
[54] L. Debelle, A. M. Tamburro, *International Journal of Biochemistry & Cell Biology* 1999, *31*, 261.
[55] A. Pepe, B. Bochiechio, A. M. Tamburro, *Nanomedicine* 2007, *2*, 203.
[56] A. M. Tamburro, *Nanomedicine* 2009, *4*, 469.
[57] D. W. Urry, T. M. Parker, *Journal of Muscle Research and Cell Motility* 2002, *23*, 543.
[58] B. Li, D. O. V. Alonso, B. J. Bennion, V. Daggett, *Journal of the American Chemical Society* 2001, *123*, 11991.
[59] A. M. Tamburro, V. Guantieri, L. Pandolfo, A. Scopa, *Biopolymers* 1990, *29*, 855.
[60] B. Li, D. O. V. Alonso, V. Daggett, *Journal of Molecular Biology* 2001, *305*, 581.
[61] B. Li, V. Daggett, *Journal of Muscle Redearch and Cell Motility* 2002, *23*, 561.
[62] T. A. Brown, *Genomes*, 3. ed., Garland Science, New York 2007.
[63] D. E. Meyer, A. Chilkoti, *Biomacromolecules* 2002, *3*, 357.
[64] D. E. Meyer, A. Chilkoti, *Nature Biotechnology* 1999, *17*, 1112.
[65] J. A. MacKay, M. N. Chen, J. R. McDaniel, W. G. Liu, A. J. Simnick, A. Chilkoti, *Nature Materials* 2009, *8*, 993.
[66] D. W. Urry, *Journal of Protein Chemistry* 1988, *7*, 1.
[67] D. W. Urry, *Journal of Physical Chemistry B* 1997, *101*, 11007.
[68] D. E. Meyer, A. Chilkoti, *Biomacromolecules* 2004, *5*, 846.
[69] D. W. Urry, C. H. Luan, T. M. Parker, D. C. Gowda, K. U. Prasad, M. C. Reid, A. Safavy, *Journal of the American Chemical Society* 1991, *113*, 4346.

[70] M. R. Dreher, A. J. Simnick, K. Fischer, R. J. Smith, A. Patel, M. Schmidt, A. Chilkoti, *Journal of the American Chemical Society* 2008, *130*, 687.
[71] J. C. Rodriguez-Cabello, L. Martin, M. Alonso, F. J. Arias, A. M. Testera, *Polymer* 2009, *50*, 5159.
[72] D. Chow, M. L. Nunalee, D. W. Lim, A. J. Simnick, A. Chilkoti, *Materials Science & Engineering R-Reports* 2008, *62*, 125.
[73] H. Betre, L. A. Setton, D. E. Meyer, A. Chilkoti, *Biomacromolecules* 2002, *3*, 910.
[74] R. M. Schweller, P. E. Constantinou, N. W. Frankel, P. Narayan, M. R. Diehl, *Bioconjugate Chemistry* 2008, *19*, 2304.
[75] Y. T. Wu, J. D. Liao, J. I. Lin, C. C. Lu, *Bioconjugate Chemistry* 2007, *18*, 1897.
[76] A. Dondoni, *Angewandte Chemie-International Edition* 2008, *47*, 8995.
[77] D. A. Stetsenko, M. J. Gait, *Journal of Organic Chemistry* 2000, *65*, 4900.
[78] G. T. Hermanson, *Bioconjugate techniques*, Acad. Press, San Diego CA, 1996.
[79] A. J. Lomant, G. Fairbanks, *Journal of Molecular Biology* 1976, *104*, 243.
[80] J. March, *Advanced organic chemistry : reactions, mechanisms, and structure*, 4. ed., Wiley, New York, 1992.
[81] E. B. Getz, M. Xiao, T. Chakrabarty, R. Cooke, P. R. Selvin, *Analytical Biochemistry* 1999, *273*, 73.
[82] K. Tyagarajan, E. Pretzer, J. E. Wiktorowicz, *Electrophoresis* 2003, *24*, 2348.
[83] S. Akhtar, M. D. Hughes, A. Khan, M. Bibby, M. Hussain, Q. Nawaz, J. Double, P. Sayyed, *Advanced Drug Delivery Reviews* 2000, *44*, 3.
[84] N. Venkatesan, B. H. Kim, *Chemical Reviews* 2006, *106*, 3712.
[85] T. S. Zatsepin, J. J. Turner, T. S. Oretskaya, M. J. Gait, *Current Pharmaceutical Design* 2005, *11*, 3639.
[86] J. J. Schwartz, S. G. Zhang, *Current Opinion in Molecular Therapeutics* 2000, *2*, 162.
[87] F. Kukolka, B. K. Muller, S. Paternoster, A. Arndt, C. M. Niemeyer, C. Brauchle, D. C. Lamb, *Small* 2006, *2*, 1083.
[88] B. P. Duckworth, Y. Chen, J. W. Wollack, Y. Sham, J. D. Mueller, T. A. Taton, M. D. Distefano, *Angewandte Chemie-International Edition* 2007, *46*, 8819.
[89] F. E. Alemdaroglu, A. Herrmann, *Organic & Biomolecular Chemistry* 2007, *5*, 1311.
[90] J. H. Jeong, T. G. Park, *Bioconjugate Chemistry* 2001, *12*, 917.
[91] M. Oishi, S. Sasaki, Y. Nagasaki, K. Kataoka, *Biomacromolecules* 2003, *4*, 1426.
[92] M. Oishi, F. Nagatsugi, S. Sasaki, Y. Nagasaki, K. Kataoka, *Chembiochem* 2005, *6*, 718.
[93] F. E. Alemdaroglu, K. Ding, R. Berger, A. Herrmann, *Angewandte Chemie-International Edition* 2006, *45*, 4206.
[94] J. Xu, E. A. Fogleman, S. L. Craig, *Macromolecules* 2004, *37*, 1863.
[95] A. Tiselius, *Transactions of the Faraday Society* 1937, *33*, 524.
[96] H. V. Thorne, *Journal of Molecular Biology* 1967, *24*, 203.
[97] A. E. Barron, H. W. Blanch, *Separation and Purification Methods* 1995, *24*, 1.
[98] B. G. Johansson, *Scandinavian Journal of Clinical & Labratory Investigation* 1972, *29*, 7.
[99] S. H. Chiou, S. H. Wu, *Analytica Chimica Acta* 1999, *383*, 47.
[100] F. Lottspeich, *Bioanalytik*, 2. ed., Spektrum Akad. Verl., Heidelberg, 2006.
[101] Y. Xu, *The Chemical Educator* 1996, *1*, 1.
[102] J. L. Viovy, J. Lesec, *Advances in Polymer Science: Separation of Macromolecules in Gels: Permeation Chromatography and Electrophoresis, Vol. 114*, Springer, Berlin, 1994.
[103] P. W. Atkins, J. Paula, *Atkins' Physical chemistry*, 7 ed., Oxford Univ. Press, Oxford, 2002.
[104] M. D. Dutton, R. J. Varhol, D. G. Dixon, *Analytical Biochemistry* 1995, *230*, 353.
[105] D. B. Davies, S. F. Baranovsky, A. N. VEselkov, *Journal of the Chemical Society-Faraday Transactions* 1997, *93*, 1559.
[106] C. R. Cantor, M. M. Warshaw, H. Shapiro, *Biopolymers* 1970, *9*, 1059.

[107] M. M. Warshaw, I. Tinoco, *Journal of Molecular Biology* 1966, *20*, 29.
[108] M. J. Cavaluzzi, P. N. Borer, *Nucleic Acids Research* 2004, *32*, e13.
[109] Marky/Breslauer, *Biopolymers* 1987, *26*, 1601.
[110] L. Wartell, R. M., A. S. Benight, *Physics Reports- Review Section of Physics Letters* 1985, *126*, 67.
[111] N. R. Markham, M. Zuker, *Nucleic Acids Research* 2005, *33*, W577.
[112] D. T. Gjerde, C. P. Hanna, D. Hornby, *DNA Chromatography*, Wiley-VCH, Weinheim, 2002.
[113] U. Birsner, U. Gilles, P. Nielsen, G. K. McMaster, *Journal of Chromatography* 1987, *402*, 381.
[114] M. Gilar, E. S. P. Bouvier, *Journal of Chromatography A* 2000, *890*, 167.
[115] M. Gilar, K. J. Fountain, Y. Budman, U. D. Neue, K. R. Yardley, P. D. Rainville, R. J. Russell, J. C. Gebler, *Journal of Chromatography A* 2002, *958*, 167.
[116] A. Bartha, *Journal of Chromatography A* 1994, 255.
[117] F. Gritti, G. Guiochon, *Journal of Chromatography A* 2005, *1099*, 1.
[118] W. Brown, *Dynamic light scattering: The method and some applications, Vol. 49*, Clarendon Press, Oxford, 1993.
[119] W. Schärtl, *Light scattering from polymer solutions and nanoparticle dispersions*, Springer, Berlin, 2007.
[120] N. Heimann, Dissertation thesis, Johannes Gutenberg Universität (Mainz), 2008.
[121] N. R. Kallenbach, R. I. Ma, N. C. Seeman, *Nature* 1983, *305*, 829.
[122] H. Yamakawa, M. Fujii, *Macromolecules* 1973, *6*, 407.
[123] H. Yamakawa, M. Fujii, *Macromolecules* 1974, *7*, 649.
[124] O. Kratky, G. Porod, *Recueil Des Travaux Chimiques Des Pays-Bas-Journal of the Royal Netherlands Chemical Society* 1949, *68*, 1106.
[125] M. Schmidt, *Macromolecules* 1984, *17*, 553.
[126] D. Voet, J. G. Voet, *Biochemie*, 1. korr. Nachdr. der 1. Aufl.. ed., VCH, Weinheim, 1994.
[127] A. Valiaev, D. W. Lim, S. Schmidler, R. L. Clark, A. Chilkoti, S. Zauscher, *Journal of the American Chemical Society* 2008, *130*, 10939.
[128] A. Janshoff, M. Neitzert, Y. Oberdorfer, H. Fuchs, *Angewandte Chemie-International Edition* 2000, *39*, 3213.
[129] S. Kobayashi, C. Ogawa, *Chemistry- A European Journal* 2006, *12*, 5954.
[130] P. F. Xiao, L. Cheng, Y. Wan, B. L. Sun, Z. Z. Chen, S. Y. Zhang, C. Z. Zhang, G. H. Zhou, Z. H. Lu, *Electrophoresis* 2006, *27*, 3904.
[131] R. D. C. Mitra, Geroge M.; , *Nucleic Acids Research* 1999, *27*, e34.
[132] E. J. B. Devor, M. A.;, *IDT, Integrated DNA Technologies* 2005.
[133] A. W. Yem, D. E. Epps, W. R. Mathews, D. M. Guido, K. A. Richard, N. D. Staite, M. R. Deibel, *Journal of Biological Chemistry* 1992, *267*, 3122.
[134] D. E. Epps, A. W. Yem, J. F. Fisher, J. E. Mcgee, J. W. Paslay, M. R. Deibel, *Journal of Biological Chemistry* 1992, *267*, 3129.
[135] J. K. A. Kamal, L. Zhao, A. H. Zewail, *Proceedings of the National Academy of Sciences of the United States of America* 2004, *101*, 13411.
[136] R. E. Hibbs, T. T. Talley, P. Taylor, *Journal of Biological Chemistry* 2004, *279*, 28483.
[137] E. J. M. Tournier, J. Wallach, P. Blond, *Analytica Chimica Acta* 1998, *361*, 33.
[138] K. C. Wood, S. M. Azarin, W. Arap, R. Pasqualini, R. Langer, P. T. Hammond, *Bioconjugate Chemistry* 2008, *19*, 403.
[139] J. G. Harrison, S. Balasubramanian, *Nucleic Acids Research* 1998, *26*, 3136.
[140] C. H. Tung, M. J. Rudolph, S. Stein, *Bioconjugate Chemistry* 1991, *2*, 464.
[141] M. A. Zanta, P. Belguise-Valladier, J. P. Behr, *Proceedings of the National Academy of Sciences of the United States of America* 1999, *96*, 91.

[142] P. Seibel, J. Trappe, G. Villani, T. Klopstock, S. Papa, H. Reichmann, *Nucleic Acids Research* 1995, *23*, 10.
[143] M. Lovrinovic, C. M. Niemeyer, *Chembiochem* 2007, *8*, 61.
[144] C. F. Brewer, J. P. Riehm, *Analytical Biochemistry* 1967, *18*, 248.
[145] K. A. Melzak, C. S. Sherwood, R. F. B. Turner, C. A. Haynes, *Journal of Colloid and Interface Science* 1996, *181*, 635.
[146] QIAGEN, *QIAquick Spin column handbook, 2008* http://www1.qiagen.com/Products/DnaCleanup/GelPcrSiCleanupSystems/QIAquickNucleotideRemovalKit.aspx#Tabs=t2 .
[147] F. Kukolka, C. M. Niemeyer, *Organic & Biomolecular Chemistry* 2004, *2*, 2203.
[148] C. Minard-Basquin, C. Chaix, C. Pichot, B. Mandrand, *Bioconjugate Chemistry* 2000, *11*, 795.
[149] N. Kanayama, H. Shibata, A. Kimura, D. Miyamoto, T. Takarada, M. Maeda, *Biomacromolecules* 2009, *10*, 805.
[150] K. M. Millea, I. S. Krull, *Journal of Liquid Chromatography & Related Technologies* 2003, *26*, 2195.
[151] S. Howorka, Z. Siwy, *Chemical Society Reviews* 2009, *38*, 2360.
[152] L. Song, M. R. Hobaugh, C. Shustak, S. Cheley, H. Bayley, J. E. Gouaux, *Science* 1996, *274*, 1859.
[153] A. V. Lebedev, D. Combs, R. I. Hogrefe, *Bioconjugate Chemistry* 2007, *18*, 1530.
[154] T. W. Greene, P. G. M. Wuts, *Protective groups in organic synthesis*, 2. ed.. ed., Wiley, New York, 1991.
[155] M. Durand, J. C. Maurizot, H. N. Borazan, C. Helene, *Biochemistry* 1975, *14*, 563.
[156] Shafer, J. K. Inman, A. Lees, *Analytical Biochemistry* 2000, *282*, 161.